

A NONLINEAR DIFFUSION THEORY MODEL FOR
XENON-INDUCED FLUX OSCILLATIONS,

by

John David Teachman

Dissertation submitted to the Graduate Faculty of the
Virginia Polytechnic Institute and State University
in partial fulfillment of the requirements for the degree of
DOCTOR OF PHILOSOPHY

in

Nuclear Science and Engineering

APPROVED:

R. J. Omega, Chairman

A. Robeson

T. F. Parkinson

H. A. Kurstedt

W. C. Thomas

July, 1981

Blacksburg, Virginia

Acknowledgments

I wish to express my appreciation to the members (both past and present) of my committee for their patience and help on this work. These include _____, Dr. H. A. Kurstedt, Dr. T. F. Parkinson, Dr. A. Robeson,

_____, and Dr. W. C. Thomas. I extend my special thanks to my advisor, Dr. Ronald J. Onega, without whom this work would not have been possible.

Finally, to all the people who gave me moral support, especially my mother, I thank you.

Table of Contents

	<u>Page</u>
Acknowledgments	ii
List of Figures	iv
List of Tables	vi
 <u>Chapter</u>	
I Xenon Oscillations - an Introduction	1
II The Direct and Adjoint Systems	22
III The Nonlinear Systems of Equations	38
IV Computational Methods - the XORA Program	54
V Numerical Results	62
VI Conclusions - Recommendations	95
References	100
 <u>Appendix</u>	
A Quantities Involving the Adjoint Flux	105
B Basis Expansion Parameters	111
C Logic Flow Diagram for XORA	114
D Sample XORA Input	122
E Partial XORA Listing	124
F XORA Output for Sample Input	156
VITA	166

List of Figures

<u>Figure</u>	<u>Page</u>
1.1.1 Reactivity due to Xe^{135} Buildup Following Shutdown	3
1.1.2 Energy Dependence of Xe^{135} Absorption Cross Section	4
1.1.3 Equilibrium Xenon Poisoning During Reactor Operation	6
1.2.1 Partial Fission-Decay Chain for Isobar 135	8
1.2.2 Xenon Oscillations	10
1.3.1 Comparison of Period of Oscillation of a Linearized Xenon Oscillation Model with a Similar Nonlinear Model	14
1.4.1 Development Flow of the Residual Xenon Oscillation Model	21
2.1.1 Reactor Geometric Model	24
2.1.2 Typical Reactor Region	25
3.3.1 Euler's Approximation to the Time Derivative	47
3.3.2 The Second Order Approximation for the Time Derivative	49
4.1.1 Major Logic Sections in XORA	56
5.4.1 Comparison of Three- and One-Energy Group Model Flux Oscillations	84
5.4.2 Comparison of Flux Oscillations due to Alternative Three-Group Energy Structures	85
5.4.3 Model Response Exhibiting Limit Cycle	89

List of Figures (Continued)

<u>Figure</u>	<u>Page</u>
5.5.1 One-Group Linear Model Flux Response	90
5.5.2 Three-Group Linear Model Flux Response	91
5.5.3 Low Flux level, Linear & Nonlinear Models Showing Period Difference	93
C.1.1 INPUT Logic Flow Section	115
C.1.2 INITIALIZAION Logic Flow Section	116
C.1.3 DIRECT Logic Flow Section	117
C.1.4 ADJOINT Logic Flow Section	119
C.1.5 PERTURB Logic Flow Section	121

List of Tables

<u>Table</u>		<u>Page</u>
1.1.1	Selected Nuclear Properties	5
1.3.1	Xenon Transient Computer Programs	17
2.2.1	Nomenclature	27
5.1.1	The XORA Cases	64
5.1.2	Babcock & Wilcox PWR Reactor Parameters	65
5.1.3	One-Group Parameters - Case A	67
5.1.4	Three-Group Parameters - Case B	68
5.1.5	Three-Group Parameters - Case C	69
5.1.6	Three-Group Parameters - Case D	70
5.2.1	One-Group Equilibrium Results for Data Set A	72
5.2.2	Equilibrium Results for Data Set B	73
5.2.3	Equilibrium Results for Data Set C	74
5.2.4	Equilibrium Results for Data Set D	75
5.3.1	One-Group Adjoint Results for Data Set A	80
5.3.2	Adjoint Results for Data Set C	81
5.3.3	Adjoint Results for Data Sets B and D	82
5.4.1	Computational Times for Selected XORA Cases	87
5.5.1	Parameters for Low Flux Level Case	94

Chapter I

Xenon Oscillations - an Introduction

1.1 The Xenon Problem

Xenon-induced flux oscillations, often referred to simply as xenon oscillations, may be present in some nuclear power plants. The oscillations are actually changes in the spatial neutron flux distribution along with iodine-135 and xenon-135 isotopic spatial changes. The interactions of these changes can lead to an oscillatory effect, and previous experiences with these effects has resulted in extensive investigation of this phenomenon. Hereafter, the use of xenon and iodine will refer to xenon-135 and iodine-135, respectively.

Xenon effects were first noted in the production reactors built at Hanford. These reactors were run at a power level high enough that xenon, which is a major fission product, was detected. It was also noted that xenon had an extraordinarily high thermal neutron absorption cross section [1,2]. The hot spots detected in the Hanford reactors were the initial indications of xenon instability. Finally, conclusive evidence of "flux tilt" oscillations was obtained at Savannah River [2].

Three basic problems can arise due to the presence of xenon in a reactor. One is the continued buildup of xenon, after the reactor shuts down, due to the decay of iodine. The peak concentration of xenon occurs approximately ten hours after shutdown. If the reactor is required to resume operation during this time interval, then enough additional reactivity must be present to overcome the xenon poisoning (neutron absorption by xenon) due to this concentration [3]; see Fig. 1.1.1.

The second problem is that xenon, acting as a poison during reactor operation, absorbs neutrons that would otherwise be available for the chain reaction. Due to the magnitudes of both the thermal absorption cross section and cumulative fission yield of xenon (Table 1.1.1 and Fig. 1.1.2), from 0.7 to 4.8 per cent of the thermal neutrons are absorbed in the xenon for thermal fluxes between 10^{12} and 10^{15} neutrons/cm²-s [3]. An equal amount of excess reactivity must always be present in order to operate the reactor; see Fig. 1.1.3.

The last problem is the xenon-induced flux instabilities occurring when the xenon concentration is perturbed from its equilibrium spatial distribution. These instabilities can lead to damped, undamped, steady, or "limit cycle"

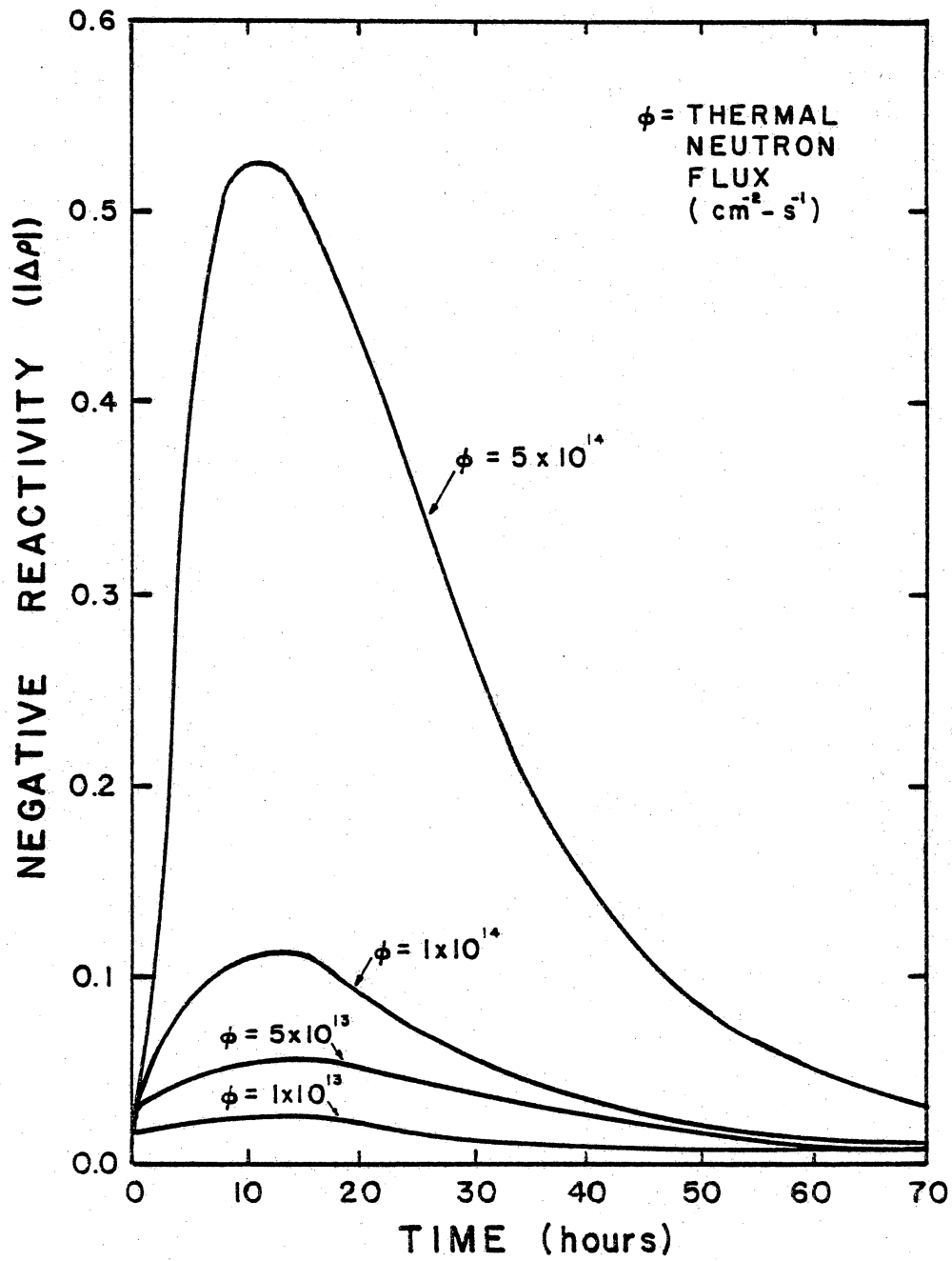


FIGURE I.1.1 Reactivity due to Xe^{135} Buildup Following Shutdown [29]

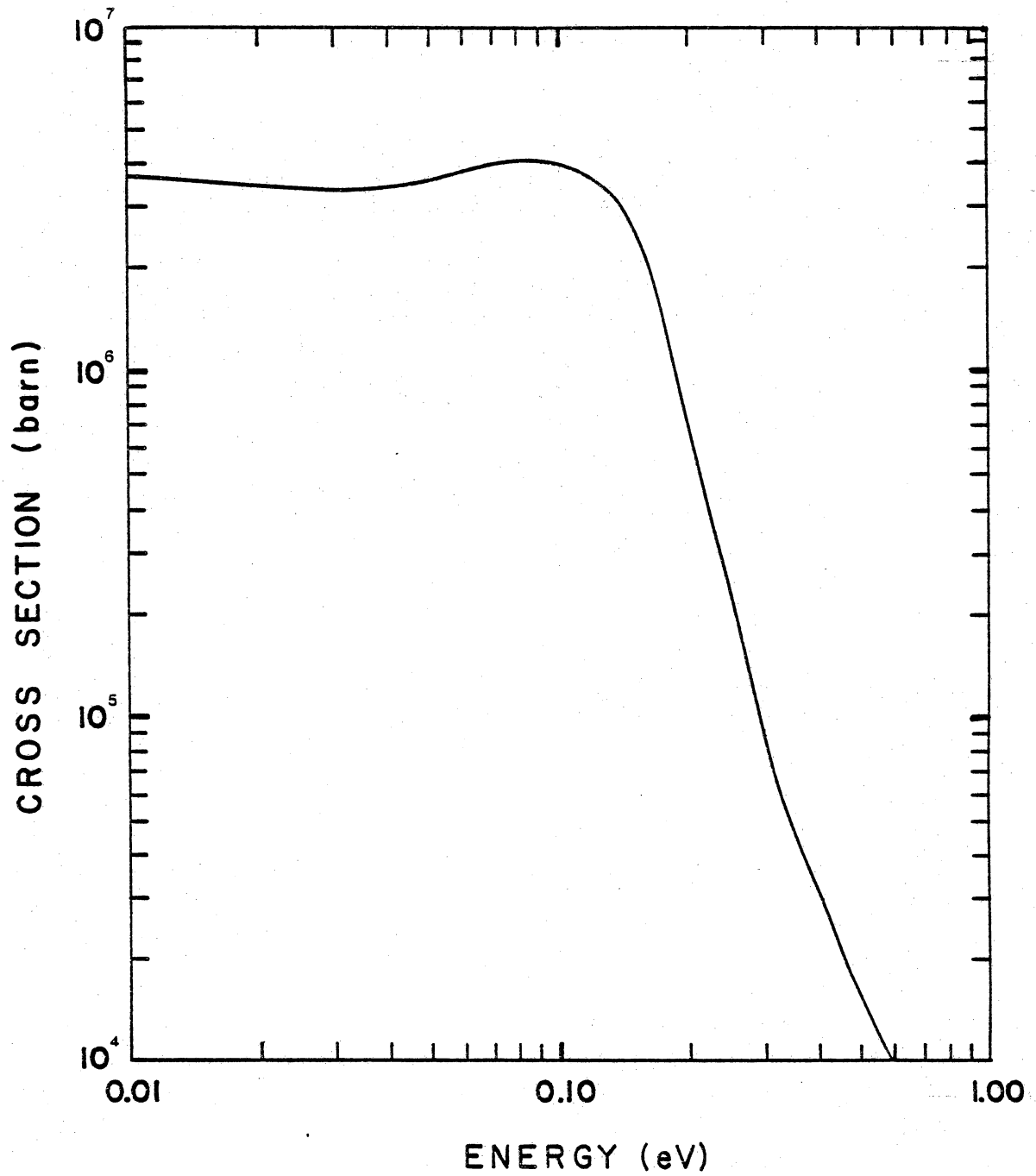


FIGURE 1.1.2 Energy Dependence of Xe^{135} Absorption Cross Section [30]

Table 1.1.1 Selected Nuclear Properties [29,31]

isotope	2200 m/s absorption cross-section (barns)	cumulative ⁽¹⁾ fission yield (%)	half-life
Te ¹³⁵	7	6.1	19.2 s
I ¹³⁵	7	6.1	6.59 hr
Xe ¹³⁵	2.7•10 ⁶	6.4	9.01 hr
Cs ¹³⁵	30	6.4	2.3•10 ⁶ yr
Ba ¹³⁵	1	6.4	stable
U ²³⁵	678	-	7.0•10 ⁸ yr
U ²³⁸	2.7	-	4.5•10 ⁹ yr
Pu ²³⁹	1014	-	24,110 yr
Pu ²⁴⁰	286	-	6,600 yr
Pu ²⁴¹	1375	-	14.3 yr
Pu ²⁴²	30	-	3.87•10 ⁵ yr

(1) Due to U²³⁵ fission

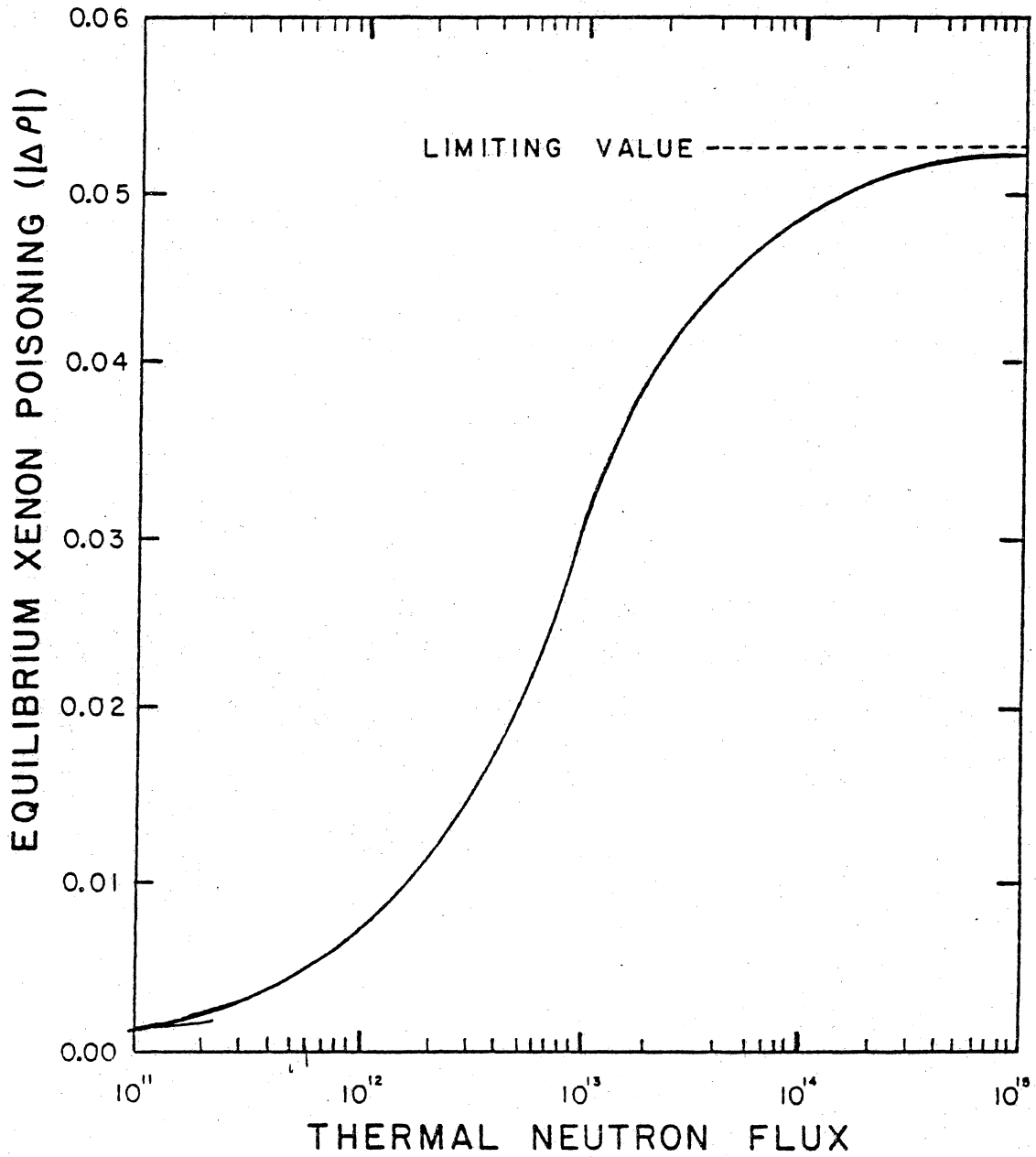


FIGURE I.1.3 Equilibrium Xenon Poisoning
During Reactor Operation

oscillations. The analysis of xenon-induced flux oscillation instabilities is the basis for this work. Specifically a comparison between similar nonlinear and linear models, along with multi- and single-energy group models, is obtained.

1.2 Xenon Induced Flux Oscillations

The flux, iodine, and xenon oscillations that occur in a nuclear reactor are due to the time lags between the production of xenon, its destruction, and the actual fission process. As shown in Fig. 1.2.1, xenon is produced both by direct fission product formation and as the result of iodine decay. Iodine is produced by the decay of tellurium; but the short half-life of tellurium (see Table 1.1.1) allows for its effect to be lumped into the fission product yield of iodine without altering the results.

At an equilibrium state in a commercial power reactor, the majority of xenon is due to iodine decay (about 20 times higher than its fission yield rate). A change in the fissioning rate will have little effect on the xenon production until it causes the decay rate of iodine to change. This iodine decay rate change will lag the fission rate change. Since a large portion of the xenon destruction

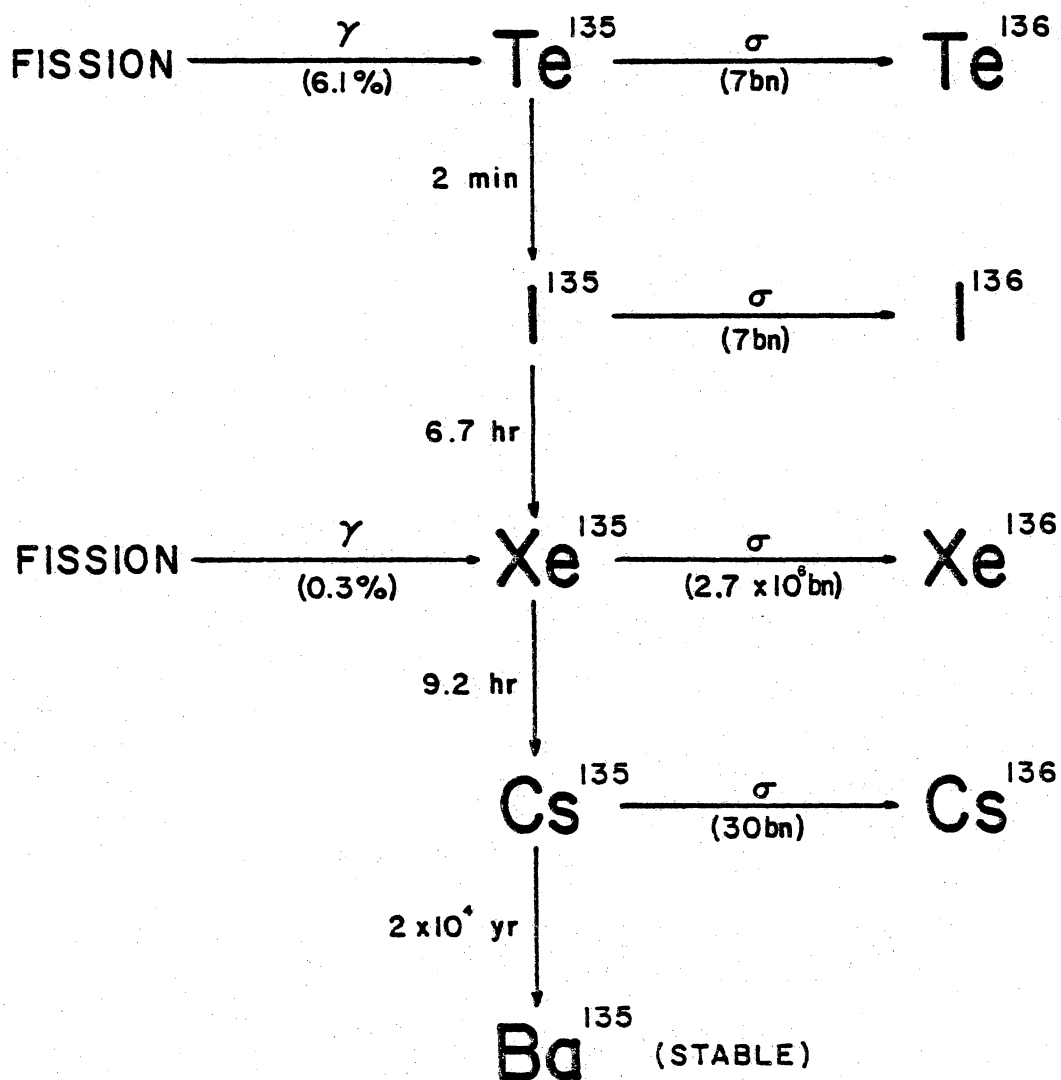


FIGURE 1.2.1 Partial Fission-Decay Chain for Isobar 135

comes from thermal neutron absorption, any change in the flux will immediately affect xenon destruction. This difference between the production and destruction rates of change can lead to the type of instability as described below.

Beginning with an equilibrium state for the flux, iodine, and xenon in a reactor (Fig. 1.2.2a), we perturb the flux to cause it to increase in side one. This can be accomplished by various means, such as by moving a control rod or changing the primary flow distribution in the reactor. Maintaining a constant power output will require the flux in side two to decrease (Fig. 1.2.2b). Iodine, which is produced almost immediately with the fissioning of fuel, will increase in side one and decrease in side two. Since the decay rate of iodine and, therefore, the great majority of xenon production, is due to earlier fissions, the immediate effect on xenon is its destruction by neutron absorption. This absorption rate increases where the flux is greater, causing the xenon to be lowered in side one and thus the xenon is about 180° out of phase with the flux.

The decrease in xenon in side one causes the flux to further increase (Fig. 1.2.2c). When the production rate of xenon, due to iodine decay, finally starts to overtake its

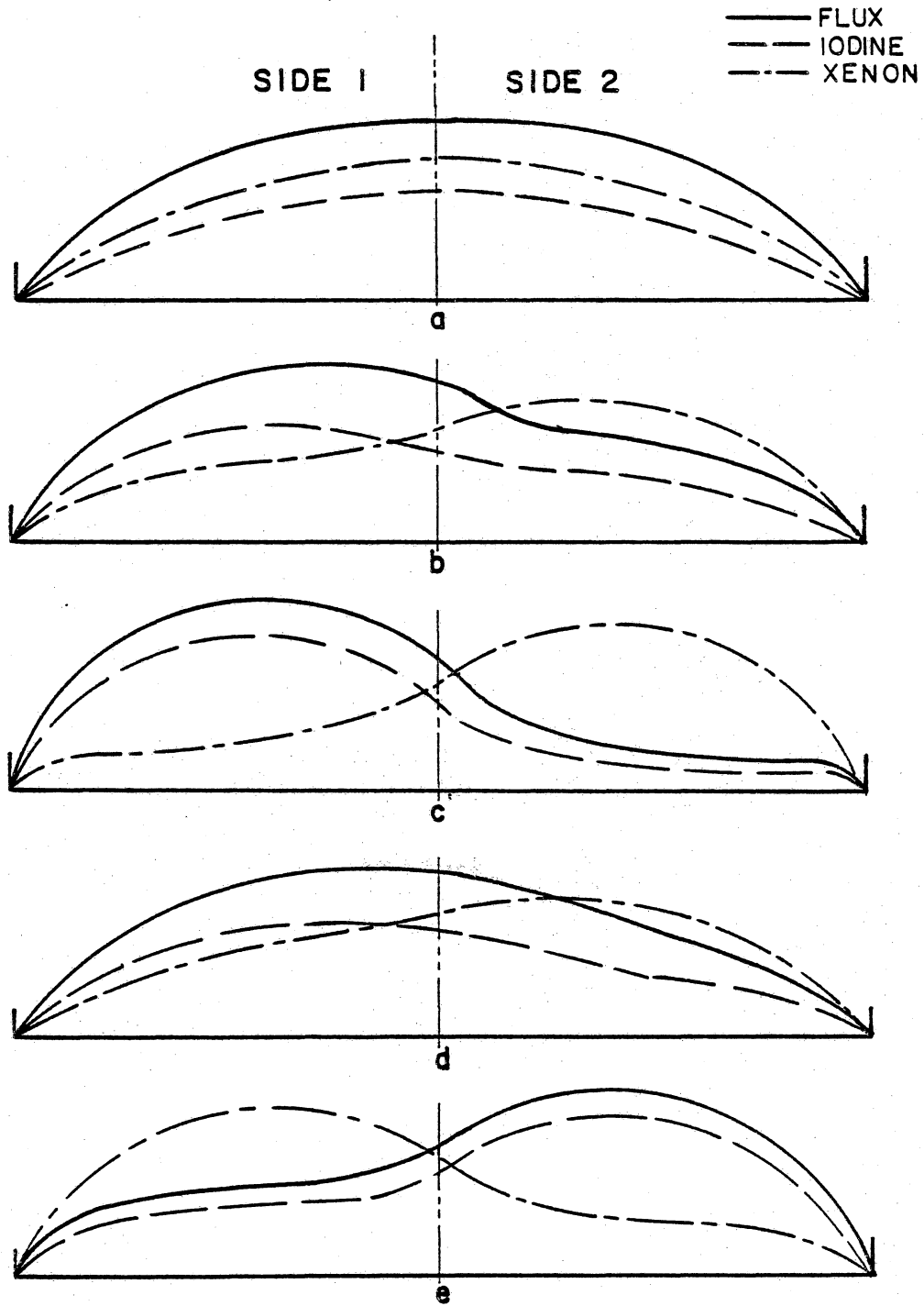


FIGURE 1.2.2 Xenon Oscillations

destruction rate, the flux will start to level off and finally reverse, possibly overshooting the equilibrium point and setting up an oscillatory motion (Figs. 1.2.2d & e).

The initial perturbation in the flux can be due to many reasons, from accidents to planned changes. Accidents that can cause such oscillations to occur range from minor ones like control rod sticking through major ones such as large scale flow blockage in the core.

Planned perturbations in the flux distribution can come from startup, shutdown, and any planned power changes, such as load cycling. The following quotation [4] shows how such load cycling power changes may have to occur on a regular basis.

"U.S. dispatchers generally reckon that when nuclear units generate 20 to 30% of the power in a dispatching area, some daily load cycling and load regulation by these units become necessary."

As other sources of power dwindle, nuclear power will have to increase to fulfill the energy requirements of the nation, ultimately generating more than 20 to 30 per cent. Load cycling will become common, requiring detailed consideration of xenon in order to maintain the stability of the reactor.

Once the xenon-induced flux oscillations are fully known, their problem can be reduced. For example, in load cycling,

prior knowledge of the oscillations can be used to decrease the number of control actions used compared to the number needed if the oscillations are treated after the change in power level has been accomplished. Although not as obvious, knowledge of the oscillations can be used to help "eliminate" the effects of xenon-induced flux oscillations from data and analytical results. This elimination will allow for a better understanding of the other processes taking place in the reactor.

1.3 Previous Approaches of Calculating Xenon Transients

The xenon-induced flux oscillation problem can be described by a system of nonlinear, energy-dependent equations having three-dimensional space and time as independent variables. Most analyses simplify the problem by considering only a few aspects of the complete system. The majority of analyses first linearize the system of equations that describe the xenon problem [2,5,6,7,8,9,10,11,12,13,14].

The nonlinear effects of xenon can have a significant impact on the system, whether the system is stable or not. Although the negative temperature coefficients of reactivity of many power plants tend to make the system more stable,

Chernick [2] has shown that the nonlinearities are important regardless of this parameter. Omega [28] has shown that for flux levels below 5×10^{13} neutrons/cm²-s, the nonlinear and linearized systems can diverge greatly from each other (Fig. 1.3.1). Also the nonlinearities may lead to a limit cycle that bounds the oscillations, and thereby cause the appropriate control actions to be different. Control actions during normal operation are very fast compared to the xenon oscillations; consequently, a nonlinear model would only be required if the situation occurs over a long enough period to allow the oscillations to do some beneficial work. As mentioned earlier, such a situation could be load cycling.

Often, after linearization, the system is considered only in one or two dimensions. Kern [5] has shown that

"The three-dimensional calculation for the xenon oscillations studied resulted in a more stable oscillation than obtained from combined one- and two- dimensional results."

The diffusion of neutrons in three dimensions will cause a decrease in the amount of coupling throughout the reactor, causing this increase in stability. This is because the effect of any change will be spread out in all three dimensions instead of just one dimension thus increasing the area that will be affected. This results in a decrease in

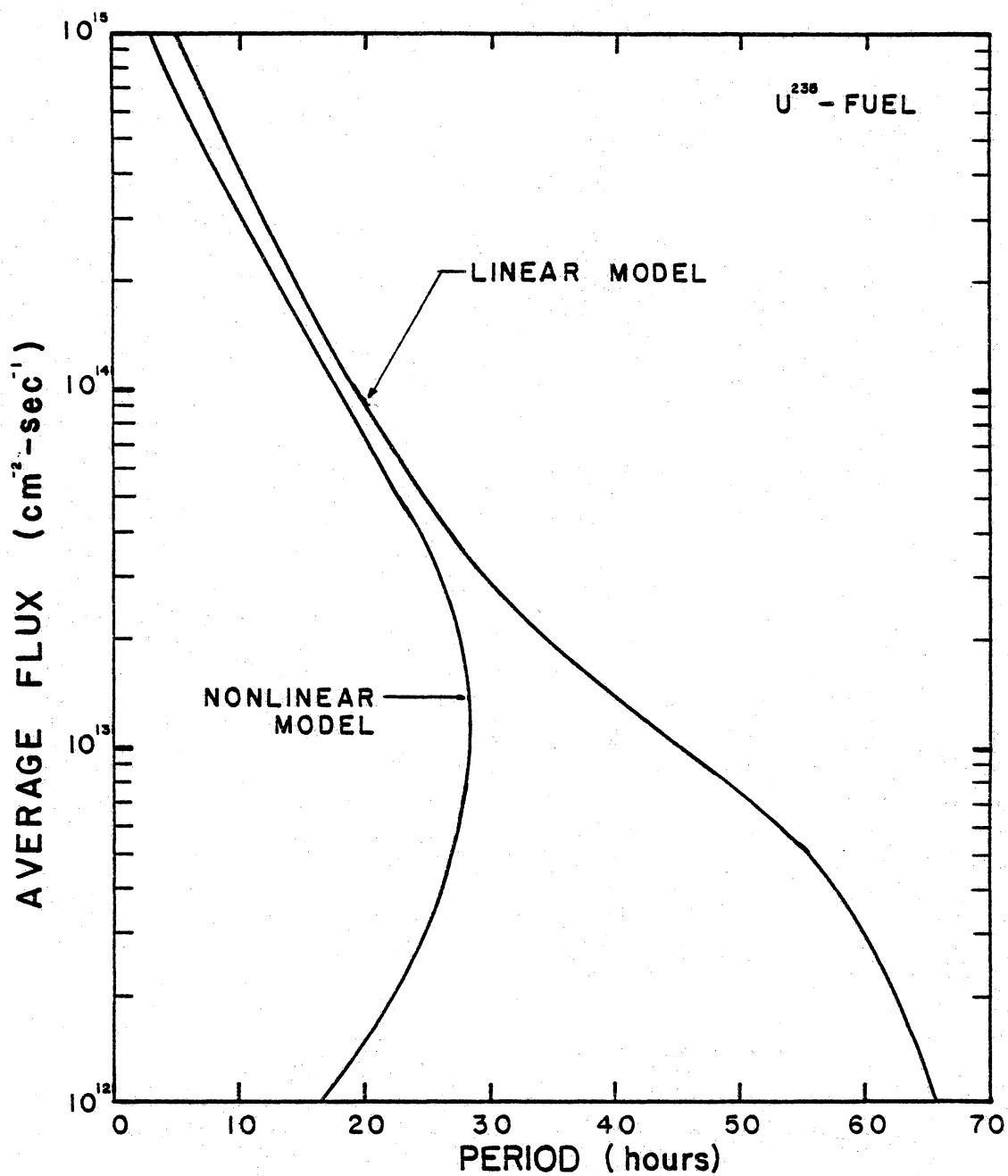


FIGURE 1.3.1 Comparison of Period of Oscillation of a Linearized Xenon Oscillation Model with a Similar Nonlinear Model [28]

the magnitude of the influence of the change in any small area. Also as reactor systems become larger, xenon oscillations can be more localized, thereby reducing any possible symmetry that may be assumed in a one- or two-dimensional calculation.

Kern [5] also states

"The observation that in large power reactors the local fast-to-thermal flux ratio is approximately constant during xenon oscillations led us to the following conclusion: A one-group approximation is sufficient to evaluate xenon oscillations in power reactors provided the fast-to-thermal flux ratio is known everywhere in the core prior to the perturbations ."

The first problem with using a one-group calculation, which is often done, is that the fast-to-thermal flux ratio must first be calculated in order to obtain the proper flux-weighted xenon cross section. Also during accident situations or very large perturbations, the flux ratio can change leading to the necessity of using a multigroup calculation to obtain the required accuracy.

The use of at least two groups is necessary when total power oscillations are of interest. The needed power distributions can be calculated accurately only using a minimum of one fast and one thermal group.

The energy-dependent cross section of xenon can also dictate the use of multiple thermal energy groups. As seen

in Fig. 1.1.2, the cross section of xenon is highly dependent on the neutron energy within the thermal range. This dependency requires the use of multiple thermal energy groups if there is a possible change in the thermal energy flux spectrum.

These reasons indicate that a multigroup, three-dimensional, nonlinear approach should be used; although, in order to have short running times on the computer system used, a one-dimensional model will be used in the numerical calculations. The residual method first described in section 1.4 is one approach to the xenon-induced flux oscillation problem which retains these qualities.

In summary, the basic purpose of this analysis is twofold. First, the significance of the nonlinearities of the system is determined by comparing nonlinear calculations with similar linear calculations. Secondly, the importance of the multigroup calculations is determined by comparing one group with multigroup results. These calculations are performed using a computer code developed from this analysis and given in Appendix E. A list of other computer codes that deal with xenon oscillations and some of their features is given as Table 1.3.1.

Table 1.3.1 Xenon Transient Computer Programs [33]

<u>Name</u>	<u>Source</u>	<u>Remarks</u>
EPRI-NODE	EPRI	1 group, 3 dimensional, PWR nodal code - FLARE type neutronics
HEXBU	TRCF	multigroup, 2 dimensional, PWR nodal and finite element, hex fuel geometry, used only in WWER-440 fuel management, (METHUSELAH II)
NAI-3D	NAI	1 group, 3 dimensional, BWR-PWR, depletion, part of LEAHS
NUFLOW-1	NUS	1 group, 3 dimensional, BWR-PWR, depletion, (FLARE)
NUSIM-3	NUS	1 group, 3 dimensional, BWR-PWR, nodal method
NUTRIX	NUS	1 group, 3 dimensional, BWR-PWR, depletion (FLARE)
XENOLUX	BN	1 group, 3 dimensional, BWR-PWR, depletion, nodal method (TRILUX)

Sources

- BN - Belgonucleaire (Belgium)
- EPRI - Electric Power Research Institute (USA)
- NAI - Nuclear Associates International, Inc. (USA)
- NUS - NUS Corporation (USA)
- TRFU - Technical Research Center of Finland (Finland)

1.4 The Residual Approach

Retaining the nonlinear properties of the xenon-induced flux oscillation problem is accomplished by using a weighted residual approach. The steps used in the particular model developed are stated briefly below.

In any problem it is necessary to first obtain the equations of state that will be used as a basis on which to develop the model. The xenon-induced flux oscillation problem is formulated using the multigroup diffusion equations and the rate equations for the iodine and xenon concentrations. These equations will be referred to as the direct system and are given in Chapter Two. The adjoint system state equations are developed from these direct system equations.

The adjoint system is developed and solved in order to extend the usefulness of the model. Very often the adjoint system is required in order to approximate various quantities. These include the mean prompt generation time, effective delayed neutron fraction, and the effective concentration of delayed neutron precursors. Appendix A contains formal definitions of these and other quantities that require the equilibrium adjoint solution. The two sets of equations, the direct and adjoint systems, are ultimately

expressed in the form of residuals which become zero at the solutions of the systems.

The Galerkin form of a weighted residual scheme is employed. Galerkin's weighted residual is a form of a variational method. Unlike many variational methods, it does not require the simultaneous solution of the direct and adjoint systems and results in a much smaller system of equations. Using the Galerkin method requires that a set of appropriate weighting functions be found for each system. Expanding the adjoint and direct group fluxes and isotopic concentrations as a series of profiles (or basis functions), the Galerkin method requires the profiles to be used as the weighting functions. Taking the inner spatial products of the residuals with all of the weighting functions and setting them to zero results in two sets of nonlinear equations. These will be referred to as the (Galerkin's) direct nonlinear equations and the (Galerkin's) adjoint nonlinear equations for the direct and adjoint systems, respectively.

The adjoint nonlinear equations are solved to obtain the equilibrium adjoint profile coefficients. The direct nonlinear equations, however, are time-dependent. The time derivatives are approximated by a finite difference technique and the system is solved at each finite time step.

At some point during the time-stepping, the xenon-induced flux oscillation is initiated. This is done by perturbing some parameter of the system; for example, the absorption cross section in one region of the reactor. This imbalance from equilibrium causes the group fluxes and isotopic concentrations to change with time, setting up an oscillatory effect. A flow diagram of this residual technique is given in Fig. 1.4.1 and the actual development of the nonlinear model is accomplished in Chapters Two and Three.

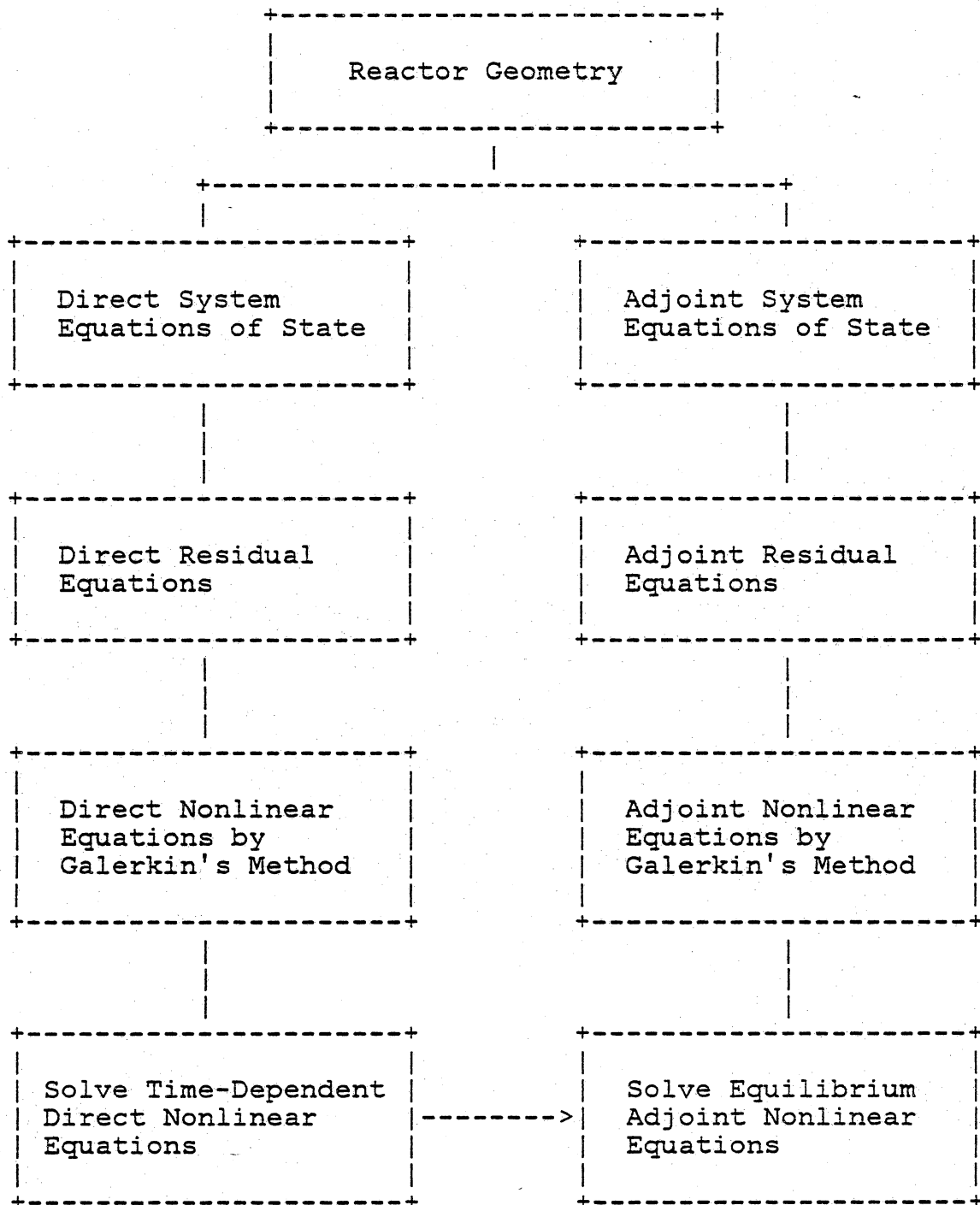


Figure 1.4.1 Development Flow of the Residual Xenon Oscillation Model

Chapter II

The Direct and Adjoint Systems

2.1 Reactor Geometry

Before any model can be developed, it is necessary to consider both the physics and geometry of the system. The actual reactor core is approximated by a right circular cylinder. This cylinder is broken up into homogeneous regions as shown in Fig. 2.1.1. Each region is considered to be a sector of a hollow cylinder with the dimensions indicated in Fig. 2.1.2. Each central section has a zero inner radius. This type of geometry for the reactor requires the use of a cylindrical coordinate system and this influences the choice of finite series and the form of the Laplacian used in the development of the residual system of equations.

The form of the spatial integrals will also be determined by the choice of geometry. To simplify the integrations, each region will be assumed to have constant properties. Any integration over the entire reactor core is the sum of the integrals over each region; and, with constant properties, each integration can be evaluated independently of these properties. Using the diffusion term of the g^{th}

energy group of the multigroup diffusion equations as an example, the spatial integral

$$\int_{\text{core}} \nabla \cdot D_g(\bar{r}) \nabla \phi_g(\bar{r}) d\bar{r} \quad (2.1.1)$$

can be evaluated as

$$\sum_r^R D_g(\bar{r}) \int_r \nabla^2 \phi_g(\bar{r}) d\bar{r} \quad (2.1.2)$$

Thus, for many terms, only a single volume integration needs to be performed. It is then multiplied by the appropriate constants such as the scattering cross sections, absorption cross sections, etc. The result of using constant regional parameters are systems of nonlinear equations, constructed from the nonlinear direct and adjoint residuals developed in Chapter Three, which are easier to evaluate than if the parameters varied within a region. The regional dependence of the reactor properties will thus be assumed and not explicitly declared; for example, D_g will be used instead of $D_g(r)$.

2.2 The Equations of State

The nonlinear system of equations that will be used in solving the time dependent xenon problem is derived from the direct equations of state which describe the reactor core.

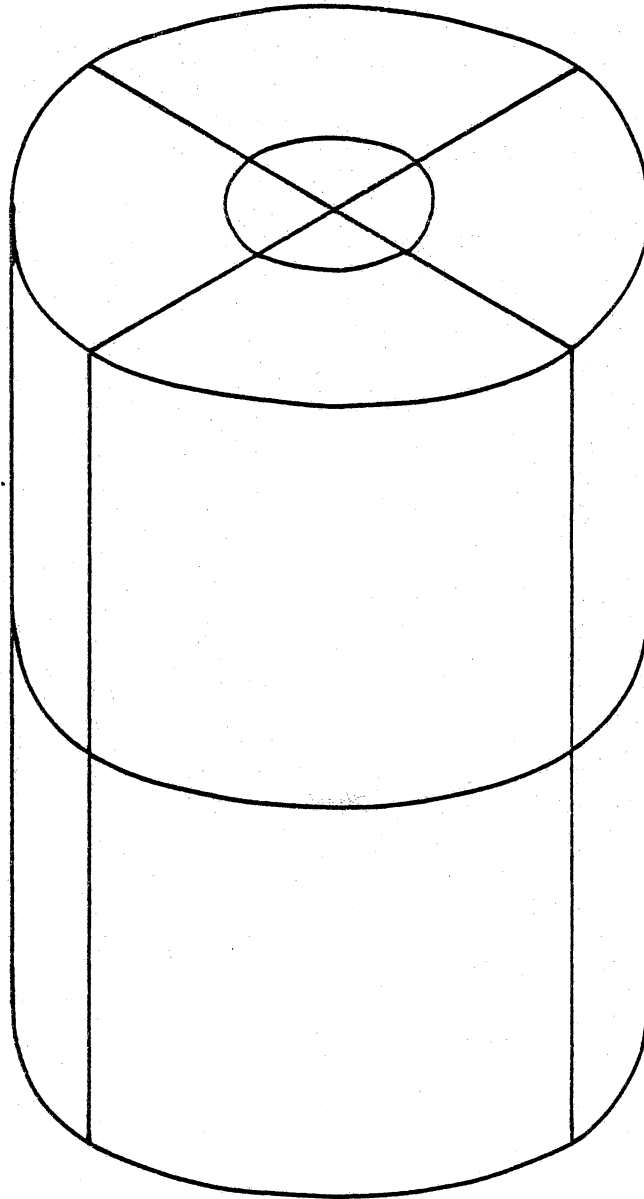


FIGURE 2.1.1 Reactor Geometric Model

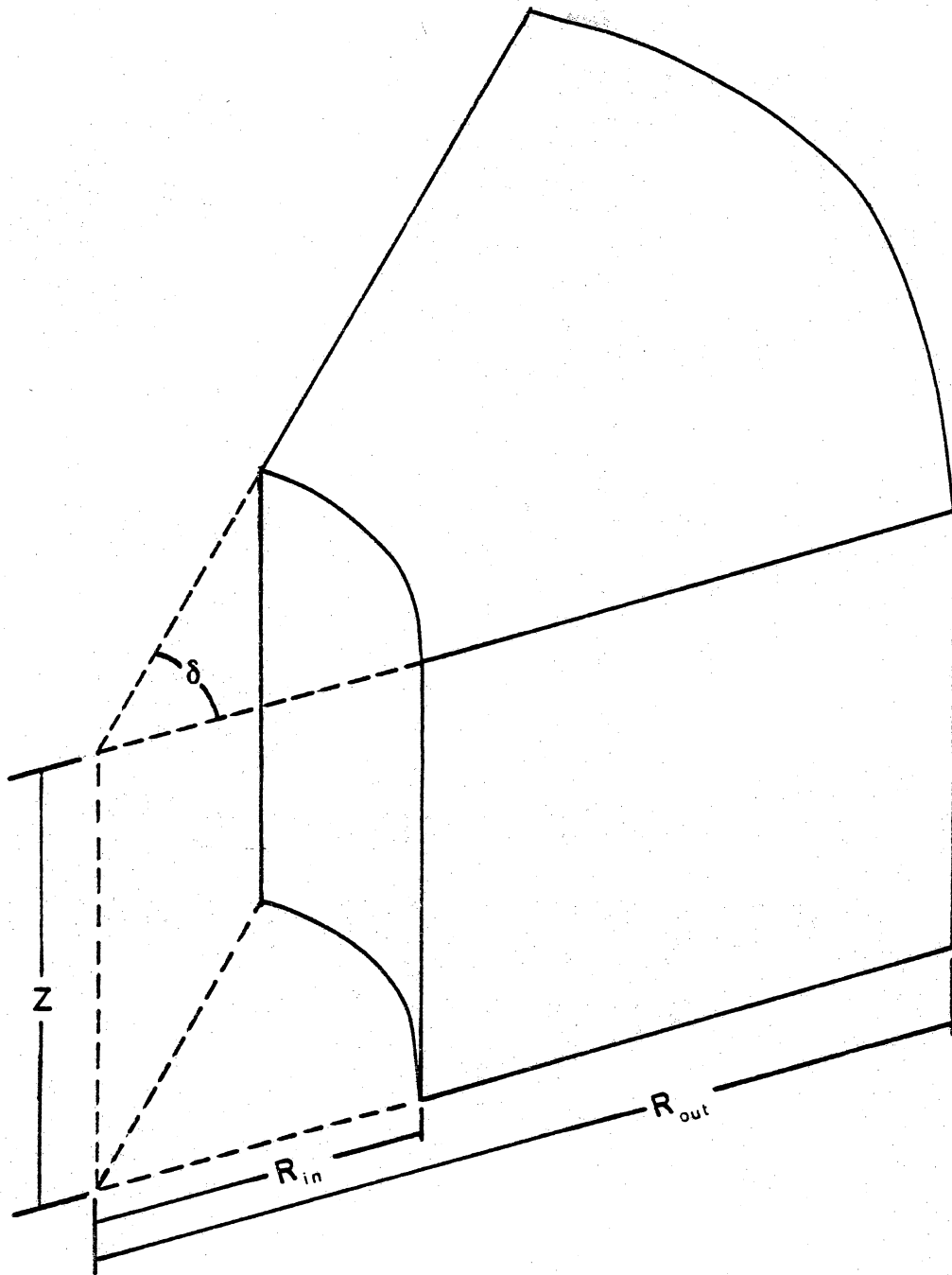


FIGURE 2.1.2 Typical Reactor Region

These state equations consist of the multigroup diffusion equations and the rate equations for the concentrations of iodine and xenon. A similar problem exists for burnup calculations where the rate equations are extended to include the fuel isotopes and any other isotopes of interest; see Chapter Six. This similarity is the reason for the slightly generalized nomenclature in Table 2.2.1 which will be used throughout the mathematical development.

The multigroup diffusion equations, which describe the neutron flux distribution in a reactor, can be written as

$$\begin{aligned}
 -\nabla \cdot D_g \nabla \phi_g + \Sigma_g^a \phi_g - \sum_j^G \Sigma_{g \rightarrow j}^s \phi_j + \sum_j^G \Sigma_{j \rightarrow g}^s \phi_j \\
 + \alpha_g \Sigma_g^a \bar{\phi}_g + \sum_e^E \sigma_g^e \phi_g N^e = \frac{1}{k} \chi_g \sum_j^G \nu_j \Sigma_j^f \phi_j
 \end{aligned}
 \tag{2.2.1}$$

Equation 2.2.1 involves the eigenvalue $1/k$ instead of the time derivative of the flux. Use of the eigenvalue can be done as the flux time rate of change is fast compared to the iodine-xenon dynamics so only time asymptotic flux behavior need be considered. The term $\alpha_g \Sigma_g^a \bar{\phi}_g$ is included to allow for inclusion of prompt temperature feedback in the model.

A generalized rate equation for an isotopic concentration

Table 2.2.1 Nomenclature

Parameters

a_g^n	- basis function coefficient (function n, group g)
D_g	- diffusion coefficient (group g) (cm)
G_c	- thermal power per fission (MWth/fission)
k	- multiplication factor
N^e	- concentration of isotope number "e" (1 = I , 2 = Xe) (cm^{-3})
P_{th}	- reactor thermal power (MWth)
t	- time (seconds)
α_g	- temperature coefficient of reactivity ($\text{cm}^2\text{-s}$)
γ_g^e	- fission product yield (isotope e, group g) (atoms/fission)
χ_g	- fission spectrum yield (group g)
η_g^n	- basis function n (group g)
λ^e	- decay constant (isotope e) (s^{-1})
ν_g	- neutron fission yield (group g fission) (neutrons/fission)
σ_g^e	- microscopic absorption cross section (isotope e, group g) (cm^2)

Table 2.2.1 Nomenclature (continued)

Parameters

Σ_g^a	- macroscopic absorption cross section (group g) (cm^{-1})
Σ_g^f	- macroscopic fission cross section (group g) (cm^{-1})
$\Sigma_{g \rightarrow g'}^s$	- macroscopic scattering cross section (group g into g') (cm^{-1})
ϕ_g	- neutron flux ($\text{cm}^{-2} \text{-s}^{-1}$)

Mathematical

$\int d\bar{r}$	- integration over space
$\int ds$	- integration over surface
\sum_1^N	- summation from 1 to "N"
∇	- gradient
∇^2	- Laplacian
∂_t	- Partial derivative with respect to time
$\langle \rangle$	- "kets" (spatial inner product)
\hat{n}	- unit normal
$\underline{\quad}_t$	- evaluated at t
$\underline{\quad}$	- average over space

Table 2.2.1 Nomenclature (continued)

Mathematical

T	- transpose
t	- adjoint
-	- vector
[]	- matrix
n	- element of [N]
diag[]	- diagonal matrix with elements d_1, d_2, \dots, d_N .
G	- number of energy groups
E	- number of isotopes
P	- number of basis functions
R	- number of regions
N	- all energy group and isotopes

can be written as

$$\frac{d N^e}{d t} = \sum_i^G \gamma_i^e \Sigma_i^f \phi_i + \lambda^e N^e - \lambda^e N^e - \sum_i^G \sigma_i^e \phi_i N^e \quad (2.2.2)$$

where the $\lambda^e N^e$ term is the rate of production due to the decay of the parent isotope. As mentioned in section 1.3, tellurium is lumped into the direct fission yield of iodine, so for iodine, $\lambda^e N^e$ is defined as zero. In practice the multigroup yields of an isotope are not known, so an average yield often is used for all of the groups.

These rate equations for iodine ($e = 1$) and xenon ($e = 2$) along with the multigroup diffusion equations are expressed in matrix form as

$$[R] \underline{\Phi} = [P] \underline{\Phi} \quad (2.2.3)$$

where

$$\underline{\Phi} = \begin{bmatrix} \psi_1 \\ \psi_2 \\ \vdots \\ \psi_G \\ \psi_{N-1} \\ \psi_N \end{bmatrix} = \begin{bmatrix} \phi_1 \\ \phi_2 \\ \vdots \\ \phi_G \\ N^1 \\ N^2 \end{bmatrix}$$

$$(2.2.4)$$

and

$$[P] = \begin{bmatrix} \chi_{1,1} \nu \Sigma_1^f & \chi_{1,2} \nu \Sigma_2^f & \dots & \chi_{1,G} \nu \Sigma_G^f & 0 & 0 \\ \chi_{2,1} \nu \Sigma_1^f & \chi_{2,2} \nu \Sigma_2^f & \dots & \chi_{2,G} \nu \Sigma_G^f & 0 & 0 \\ \vdots & \vdots & & \vdots & \vdots & \vdots \\ \chi_{G,1} \nu \Sigma_1^f & \chi_{G,2} \nu \Sigma_2^f & \dots & \chi_{G,G} \nu \Sigma_G^f & 0 & 0 \\ 0 & 0 & \dots & 0 & 0 & 0 \\ 0 & 0 & \dots & 0 & 0 & 0 \end{bmatrix} \quad (2.2.5)$$

The [R] term can be expressed as

$$[R] = [D] + [S] + [N] + [a] \quad (2.2.6)$$

where

$$[D] = \text{dia} \begin{bmatrix} -\nabla \cdot D_1 \nabla & -\nabla \cdot D_2 \nabla & \dots & & & \\ & -\nabla \cdot D_G \nabla & & -d/dt & -d/dt & \\ & & & & & \end{bmatrix} \quad (2.2.7)$$

$$[S] = \begin{bmatrix} \Sigma_1^r & -\Sigma_{2 \rightarrow 1}^s & \dots & -\Sigma_{G \rightarrow 1}^s & 0 & 0 \\ -\Sigma_{1 \rightarrow 2}^s & \Sigma_2^r & \dots & -\Sigma_{G \rightarrow 2}^s & 0 & 0 \\ \vdots & \vdots & & \vdots & \vdots & \vdots \\ -\Sigma_{1 \rightarrow G}^s & -\Sigma_{2 \rightarrow G}^s & \dots & \Sigma_G^r & 0 & 0 \\ \gamma_1^1 \Sigma_1^f & \gamma_2^1 \Sigma_2^f & \dots & \gamma_G^1 \Sigma_G^f & -\lambda^1 & 0 \\ \gamma_1^2 \Sigma_1^f & \gamma_2^2 \Sigma_2^f & \dots & \gamma_G^2 \Sigma_G^f & \lambda^2 & -\lambda^2 \end{bmatrix} \quad (2.2.8)$$

$$\Sigma_n^r = \Sigma_n^a + \sum_m^G \Sigma_{n \rightarrow m}^s, \quad (2.2.9)$$

$$[N] = \text{dia} \left[\begin{array}{ccc} \sum_e^E \sigma_1^e N^e & \sum_e^E \sigma_2^e N^e & \dots \\ \sum_e^E \sigma_G^e N^e & - \sum_n^G \sigma_n^1 \phi_n & - \sum_n^G \sigma_n^2 \phi_n \end{array} \right], \quad (2.2.10)$$

and

$$[\alpha] = \text{dia} \left[\begin{array}{ccc} \alpha_1 \sum_1^a \bar{\phi}_1 & \alpha_2 \sum_2^a \bar{\phi}_2 & \dots \\ & \alpha_G \sum_G^a \bar{\phi}_G & 0 \quad 0 \end{array} \right]. \quad (2.2.11)$$

Other forms could be chosen for $[N]$, but the use of a diagonal matrix representation simplifies the formulation of the adjoint system of equations.

2.3 The Spatial Adjoint Equations

An adjoint flux for the system of equations corresponding to Eq. 2.2.3 satisfies

$$\left([Ra] \underline{\Phi} \right)^\dagger = \frac{1}{k} \left([Pa] \underline{\Phi} \right)^\dagger. \quad (2.3.1)$$

This can also be written as

$$\underline{\Phi}^\dagger [Ra]^\dagger = \frac{1}{k} \underline{\Phi}^\dagger [Pa]^\dagger \quad (2.3.2)$$

where $[Ra]^\dagger$ is the complex conjugate transpose of the matrix $[Ra]$ and is the adjoint of $[R]$. Also $[Pa]^\dagger$ is similarly defined.

The same nonlinearities found in Eq. 2.2.3 are found in the $[Ra]^\dagger$ term and they remove the uniqueness of the adjoint system. The concept of the "importance function" is no longer valid without a unique adjoint system. As the nonlinearities approach zero, i.e., $\sigma^e \rightarrow 0$, the adjoint system will approach a unique solution, so for nonlinearities, such as those associated with xenon poisoning, using the importance function concept can lead to some insight to the reactor system.

Determination of the adjoint matrices requires the definition of the spatial inner product. Using the "kets" notation to designate integration over the entire reactor volume, the spatial inner product is

$$\langle \underline{\Phi}^\dagger [B]^\dagger, [M] \underline{\Phi} \rangle = \int (\underline{\Phi}^\dagger [B]^\dagger) ([M] \underline{\Phi}) d\bar{r} \quad (2.3.3)$$

where $[B]^\dagger$ and $[M]$ are arbitrary matrices which may contain spatial and time dependence. Using this definition, the adjoints are determined by the relationship

$$\langle \underline{\Phi}^\dagger, [M] \underline{\Phi} \rangle = \langle \underline{\Phi}^\dagger [B]^\dagger, \underline{\Phi} \rangle \quad (2.3.4)$$

and $[B]^\dagger$ is the adjoint operator of $[M]$.

For the linear matrices which contain no differential operators, i.e., [S] and [R],

$$\langle \underline{\Phi}^\dagger, [M] \underline{\Phi} \rangle = \int \sum_i^N \sum_j^N \psi_i^\dagger m_{ij} \psi_j \, d\bar{r} \quad (2.3.5)$$

and

$$\langle \underline{\Phi}^\dagger [B]^\dagger, \underline{\Phi} \rangle = \int \sum_i^N \sum_j^N \psi_i^\dagger b_{ij}^\dagger \psi_j \, d\bar{r} \quad (2.3.6)$$

Equating Eqs. 2.3.5 and 2.3.6 requires that the integrands be equal, i.e.

$$\sum_i^N \sum_j^N \psi_i^\dagger m_{ij} \psi_j = \sum_i^N \sum_j^N \psi_i^\dagger b_{ij}^\dagger \psi_j \quad (2.3.7)$$

with the implication that

$$b_{ij}^\dagger = m_{ji} \quad (2.3.8)$$

Thus,

$$[Pa]^\dagger = [P]^\top \quad (2.3.9)$$

and

$$[Sa]^\dagger = [S]^\top \quad (2.3.10)$$

The remaining matrices are all diagonal. This results in

$$\langle \underline{\Phi}^\dagger, \text{dia}[M] \underline{\Phi} \rangle = \int \sum_i^N \psi_i^\dagger m_i \psi_i \, d\bar{r} \quad (2.3.11)$$

and

$$\langle \underline{\Phi}^\dagger \text{dia}[B]^\dagger, \underline{\Phi} \rangle = \int \sum_i^N \psi_i^\dagger b_i^\dagger \psi_i \, d\bar{r} \quad (2.3.12)$$

Setting like terms of the series expansions in Eqs. 2.3.11 and 2.3.12 equal,

$$\int \psi^\dagger m \psi d\bar{r} = \int \psi b^\dagger \psi^\dagger d\bar{r} \quad (2.3.13)$$

When the diagonal matrices contain no spatial operators, i.e., the $[N]$ and $[a]$ matrices, the integrands in Eq. 2.3.13 must be equal;

$$\psi b^\dagger \psi^\dagger = \psi^\dagger m \psi \quad (2.3.14)$$

This results in

$$b^\dagger = m \quad (2.3.15)$$

as was found in the linear case. For clarity, this result requires that

$$[a a]^\dagger = \text{dia} \left[\begin{array}{cccc} \alpha_1 \sum_1^a \bar{\phi}_1^\dagger & & & \\ & \alpha_2 \sum_2^a \bar{\phi}_2^\dagger & & \dots \\ & & \alpha_G \sum_G^a \bar{\phi}_G^\dagger & \\ & & & 0 \quad 0 \quad] \quad (2.3.16)$$

and

$$[Na]^\dagger = \text{dia} \left[\begin{array}{cccc} \sum_e^E \sigma_1^e N^{e\dagger} & \sum_e^E \sigma_2^e N^{e\dagger} & & \dots \\ & \sum_e^E \sigma_G^e N^{e\dagger} & -\sum_g^G \sigma_g^1 \phi_g^\dagger & -\sum_g^G \sigma_g^2 \phi_g^\dagger \end{array} \right] \quad (2.3.17)$$

The final matrix contains both spatial and time derivatives. The spatial terms of $[D]$ causes Eq. 2.3.13 to

become

$$- \int \psi_n^\dagger \nabla \cdot D_n \nabla \psi_n \, d\bar{r} = \int \psi_n b_n^\dagger \psi_n^\dagger \, d\bar{r} \quad (2.3.18)$$

Integrating the left-hand side of Eq. 2.3.18 by parts twice,

$$\begin{aligned} \int \psi_n^\dagger \nabla \cdot D_n \nabla \psi_n \, d\bar{r} &= \oint \psi_n^\dagger D_n \nabla \psi_n \cdot \hat{n} \, d\bar{s} \\ &\quad - \int \nabla \psi_n^\dagger \cdot D_n \nabla \psi_n \, d\bar{r} \\ &= \oint \psi_n^\dagger D_n \psi_n \cdot \hat{n} \, d\bar{s} \\ &\quad - \oint \psi_n D_n \nabla \psi_n \cdot \hat{n} \, d\bar{s} \\ &\quad + \int \psi_n \nabla \cdot D_n \nabla \psi_n^\dagger \, d\bar{r} \end{aligned} \quad (2.3.19)$$

By requiring that ψ_n^\dagger have the same boundary conditions as ψ_n , that is, zero at the surface of the reactor, the surface integrals in Eq. 2.3.19 vanish. Inserting the remaining term from Eq. 2.3.19 into Eq. 2.3.18,

$$- \int \psi_n \nabla \cdot D_n \nabla \psi_n^\dagger \, d\bar{r} = \int \psi_n b_n^\dagger \psi_n^\dagger \, d\bar{r} \quad (2.3.20)$$

and it is found that

$$b_n^\dagger = -\nabla \cdot D_n \nabla \quad (2.3.21)$$

The time derivatives of [D] are not required as the adjoint system will be solved only for equilibrium conditions.

Now that all of the adjoint terms are defined, it is possible to formulate the adjoint residual mentioned in section 1.4 along with the direct residual.

Chapter III

The Nonlinear Systems of Equations

3.1 The Nonlinear Residuals

The state equations (2.2.3) and the adjoint state equations (2.3.2) (which are nonlinear) are solved using the Galerkin technique. A residual vector \underline{E} is defined using the state equations by

$$\underline{E} = [\underline{R}] \tilde{\underline{\Phi}} - \frac{1}{k} [\underline{P}] \tilde{\underline{\Phi}} \quad (3.1.1)$$

and the corresponding adjoint residual vector \underline{E}^\dagger is

$$\underline{E}^\dagger = \tilde{\underline{\Phi}}^\dagger [\underline{R}a]^\dagger - \frac{1}{k} \tilde{\underline{\Phi}}^\dagger [\underline{P}a]^\dagger \quad (3.1.2)$$

The residuals, \underline{E} and \underline{E}^\dagger are zero when the approximations, $\tilde{\underline{\Phi}}$ and $\tilde{\underline{\Phi}}^\dagger$ used for $\underline{\Phi}$ and $\underline{\Phi}^\dagger$, respectively, approach the true solutions of the state equations.

Applying the Galerkin method of weighted residuals requires formation of the spatial inner products for the residuals \underline{E} and \underline{E}^\dagger with the selected basis functions η_n^i . The resulting (Galerkin) equations are

$$\underline{0} = \int \underline{E}^\dagger * \underline{\eta}^i \, d\bar{r} \quad ; \quad i=1,2 \dots P \quad (3.1.3)$$

for the adjoint system and

$$\underline{Q} = \int \underline{E} * \underline{\eta}^i d\bar{r} \quad (3.1.4)$$

for the direct system. The operator * indicates array multiplication, i.e.,

$$\underline{E} * \underline{\eta}^i = \begin{bmatrix} e_1 \\ e_2 \\ \vdots \\ e_N \end{bmatrix} * \begin{bmatrix} \eta_1^i \\ \eta_2^i \\ \vdots \\ \eta_N^i \end{bmatrix} = \begin{bmatrix} e_1 \eta_1^i \\ e_2 \eta_2^i \\ \vdots \\ e_N \eta_N^i \end{bmatrix} \quad (3.1.5)$$

and the integrations are over the entire reactor core.

3.2 Series Expansions and Boundary Conditions

The nonlinear equations (Eqs. 3.1.3 and 3.1.4) developed in the last section must be set to zero in order to force the residuals (Eqs. 3.1.1 and 3.1.2) to go to zero. Before this can be done, it is necessary to express the group fluxes and isotopic concentrations as functions in both time and space (only space for the equilibrium adjoint system). This is accomplished with finite series expansions that will approximate the true functions and allow the residuals to go toward zero.

These finite series are restricted by the number of dimensions being considered and the geometry of the system as shown in section 2.1. Before these restrictions are imposed, the time and spatial dependencies will be separated for the direct nonlinear system of equations. Galerkin's method requires the approximating series to be of the form

$$\psi_n = \sum_p^P f_n^p(t, \bar{r}) \quad (3.2.1)$$

Separating time-and space results in a time dependent coefficient (to be determined) and a spatial basis function. For the direct system approximation,

$$\psi_n(t, r) = \sum_p^P a_n^p(t) \eta_n^p(\bar{r}) \quad (3.2.2)$$

This time-dependence of the coefficients will be found by applying a finite difference technique in the time domain.

Now that the form of the expansions has been decided --

$$\psi_n(t, r) = \sum_p^P a_n^p(t) \eta_n^p(\bar{r}) \quad (3.2.3)$$

and

$$\psi_n^\dagger(r) = \sum_p^P a_n^{p\dagger} \eta_n^p(\bar{r}) \quad (3.2.4)$$

-- the form of the basis functions must be determined. A major requirement for these functions is that they vanish at

the edge of the reactor (ignoring extrapolation distances). In a one dimensional (axial) problem, using the cylindrical coordinates chosen in section 2.1,

$$\eta_n^p(0) = 0 \quad (3.2.5)$$

and

$$\eta_n^p(L) = 0 \quad (3.2.6)$$

are the restrictions when the origin is at the bottom of the reactor and L is the height of the reactor. In all three dimensions the restrictions become

$$\eta_n^p(r, \zeta, 0) = 0 \quad , \quad (3.2.7)$$

$$\eta_n^p(r, \zeta, L) = 0 \quad , \quad (3.2.8)$$

and

$$\eta_n^p(R, \zeta, z) = 0 \quad . \quad (3.2.9)$$

The inclusion of the azimuthal direction, ζ , imposes the additional restriction that the function be periodic in that dimension. Mathematically expressed,

$$\eta_n^p(r, \zeta, z) = \eta_n^p(r, 2\pi i + \zeta, z) \quad (3.2.10)$$

for any nonzero integer i.

With only these restrictions (zero flux at the boundary, specification of geometry, and the number of dimensions

required), any number of simple functions could be used. However, the boundaries between regions of the reactor must be considered. The fact that the fluxes and currents must be continuous throughout a reactor requires that

$$\phi_n(h^-) = \phi_n(h^+) \quad (3.2.11)$$

and

$$-D_n(h^-) \nabla \phi_n(h^-) = -D_n(h^+) \nabla \phi_n(h^+) \quad (3.2.12)$$

where h^- and h^+ indicate the diffusion coefficients and fluxes are evaluated at the boundary $r=h$ for adjacent regions. Using the expansions, Eqs. 3.2.11 and 3.2.12 can be expressed as

$$\sum_p^P a_n^p(t) \eta_n^p(h^-) = \sum_p^P a_n^p(t) \eta_n^p(h^+) \quad (3.2.13)$$

and

$$\begin{aligned} -D_n(h^-) \sum_p^P a_n^p(t) \nabla \eta_n^p(h^-) \\ = -D_n(h^+) \sum_p^P a_n^p(t) \nabla \eta_n^p(h^+) \end{aligned} \quad (3.2.14)$$

respectively. The simplest way to satisfy these conditions is to require the basis functions to be continuous across an interface, i.e.

$$\eta_n^p(h^-) = \eta_n^p(h^+) \quad (3.2.15)$$

and their corresponding currents,

$$-D_n(h^-) \nabla \eta_n^p(h^-) = -D_n(h^+) \nabla \eta_n^p(h^+) \quad (3.2.16)$$

be equal.

The isotopic concentrations will not be continuous in a heterogeneous reactor -- where there is no fuel, no fission products will be produced. For simplicity, however, the fission product expansions are assumed to be the same form as the flux expansions. The cases with large homogeneous regions considered with this model makes this assumption valid. These constraints also applied to the adjoint system and so the same expansions are used when solving the adjoint nonlinear system of equations.

The computer program discussed in Chapter Four and the numerical results given in Chapter Five will be one-dimensional calculations. Use of one dimension results in a computer code with region requirements small enough to be solved on the computer system available. Of the three possible dimensions, axial, radial, and azimuthal, the axial dimension is of greatest concern. Because of the partial length rods and the the axial temperature variations, axial oscillations are easy to initiate and maintain in a reactor. The symmetry of the core reduces the azimuthal oscillatory problem and the radial flattening of the flux reduces the oscillatory problem in the radial direction.

All of the constraints on η_n^p increase the difficulties of expressing the basis functions. There are, however, an infinite number of forms that can be chosen, for example, in one dimension,

$$\eta_n^p(z) = \text{Sin}(b_n^p z) + c_n^p \text{Cos}(b_n^p z) \quad (3.2.17)$$

and

$$\eta_n^p(z) = c_n^p + b_n^p \left(\frac{z}{L}\right) - \left(\frac{z}{L}\right)^{p+1} \quad (3.2.18)$$

are valid with the proper choice of c_n^p and b_n^p which are region dependent. The ease of determining these b's and c's will vary greatly between the forms. It will be shown that the polynomial representation, which will be used in the one-dimensional problem, will result in a simpler set of equations to solve over the Fourier series.

Both forms for η_n^p (Eqs. 3.2.17 and 3.2.18) will result in a set of simultaneous equations due to the boundary conditions (Eqs. 3.2.15 and 3.2.16). The sine and cosine basis functions will result in the equations being transcendental of the form

$$\begin{aligned} \text{Sin}(b_n^p h^-) + c_n^p \text{Cos}(b_n^p h^-) \\ = \text{Sin}(b_n^p h^+) + c_n^p \text{Cos}(b_n^p h^+) \end{aligned} \quad (3.2.19)$$

and

$$\begin{aligned} -D_n(h^-) \nabla [\text{Sin}(b_n^p h^-) + c_n^p \text{Cos}(b_n^p h^-)] \\ = -D_n(h^+) \nabla [\text{Sin}(b_n^p h^+) + c_n^p \text{Cos}(b_n^p h^+)]. \end{aligned} \quad (3.2.20)$$

Solving these equations for the b's and c's can be very complex and time consuming. The polynomial basis functions result in equations of the form

$$\begin{aligned} c_n^p + b_n^p \left(\frac{h^-}{L} \right) - \left(\frac{h^-}{L} \right)^{p+1} \\ = c_n^p + b_n^p \left(\frac{h^+}{L} \right) - \left(\frac{h^+}{L} \right)^{p+1} \end{aligned} \quad (3.2.21)$$

and

$$\begin{aligned} -D_n(h^-) \nabla \left[c_n^p + b_n^p \left(\frac{h^-}{L} \right) - \left(\frac{h^-}{L} \right)^{p+1} \right] \\ = -D_n(h^+) \nabla \left[c_n^p + b_n^p \left(\frac{h^+}{L} \right) - \left(\frac{h^+}{L} \right)^{p+1} \right]. \end{aligned} \quad (3.2.22)$$

These can be written as a simple set of linear equations for which the solution can easily be found for the b's and c's. It is a variation on this polynomial basis function that will be used for the one-dimensional numerical solutions presented in chapter five and the appropriate system of equations needed to solve for the b's and c's is given in appendix B.

3.3 The Time Derivative

The nonlinear Eqs. 3.1.3 and 3.1.4 expressed in section 3.5 requires the evaluation of the time derivative da/dt . A finite differencing technique is used for the time domain instead of the Galerkin technique. The Galerkin method would require a large number of profiles in the time domain for accurate results and this would yeild a large system of simultaneous equations to be solved for. The finite differencing technique results in a much smaller system which must be solved many times; once for each time-step. Because of the computer core storage constraints, the large system is unacceptable and the finite differencing method is used.

The simplest finite approximation is Euler's formula which states

$$\frac{d a(t)}{d t} = \frac{a(t) - a(t - \Delta t)}{\Delta t} \quad , \quad (3.3.1)$$

where Δt is a finite time increment. This results in a set of time dependent approximations as shown in Fig. 3.3.1. The obvious problem with this scheme is that, at the beginning of the time step, the derivative is actually known and Euler's approximation violates this information.

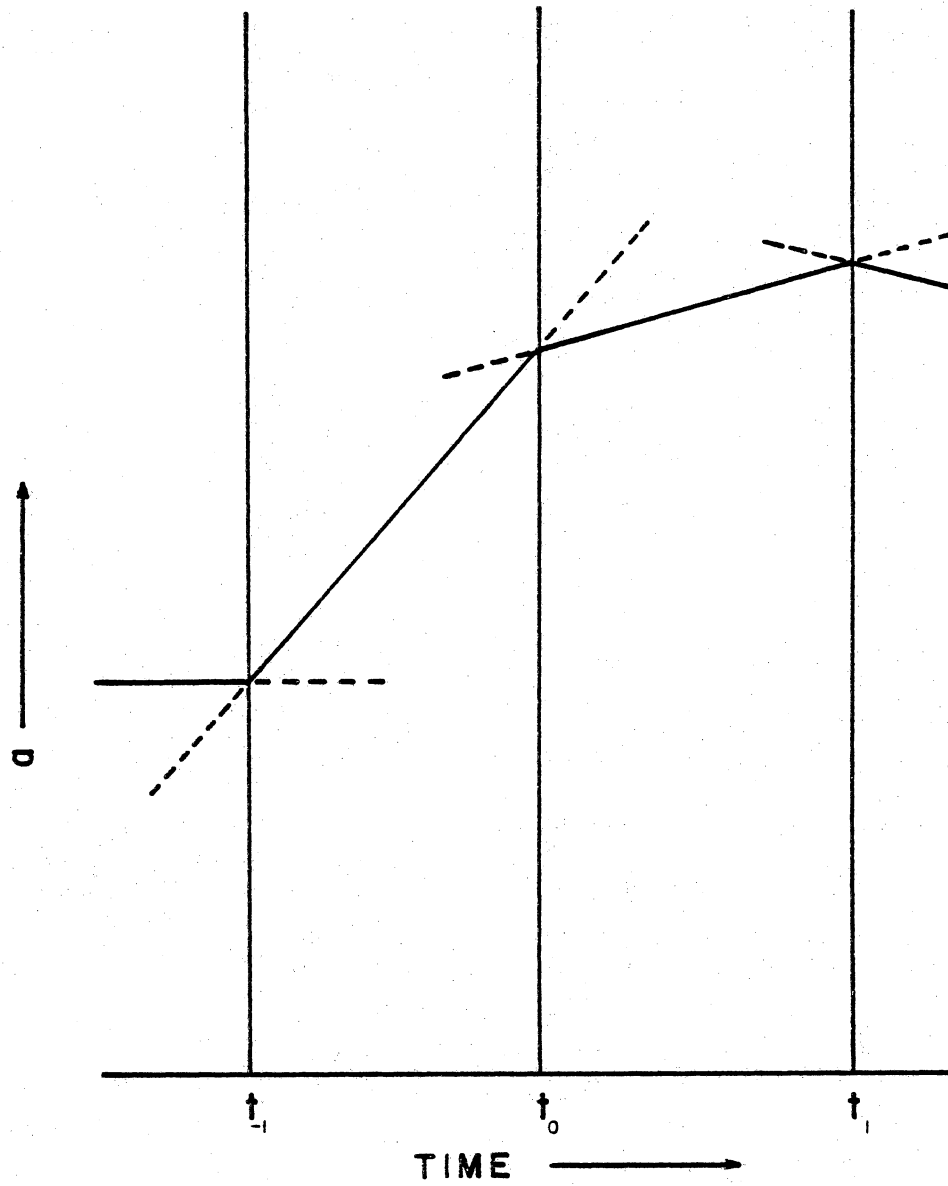


FIGURE 3.3.1 Euler's Approximation to the Time Derivative

To use this information, a second-order polynomial fit can be used. This polynomial,

$$a(t) = a_2 t^2 + a_1 t + a_0 \quad , \quad (3.3.2)$$

has three unknown coefficients and therefore, three equations must be used to evaluate them. These equations consist of the function values at each endpoint of the step and the derivative at the beginning of the time step (see Fig. 3.3.2). In matrix form, these three equations can be written as

$$\begin{bmatrix} 2t_0 & 1 & 0 \\ t_0^2 & t_0 & 1 \\ t_1^2 & t_1 & 1 \end{bmatrix} \begin{bmatrix} a_2 \\ a_1 \\ a_0 \end{bmatrix} = \begin{bmatrix} \frac{da}{dt}|_{t_0} \\ a(t_0) \\ a(t_1) \end{bmatrix} \quad . \quad (3.3.3)$$

The derivative at the end of the timestep is

$$\frac{da}{dt} = 2 \left(\frac{a(t_0) - a(t_0 + \Delta t)}{\Delta t} \right) - \frac{da}{dt}|_{t_0} \quad , \quad (3.3.4)$$

where the coefficients are found by solving the matrix Eq. 3.3.3 and substituting Δt for $t_1 - t_0$. This approximation is the one used when it is necessary to evaluate any of the time derivatives.

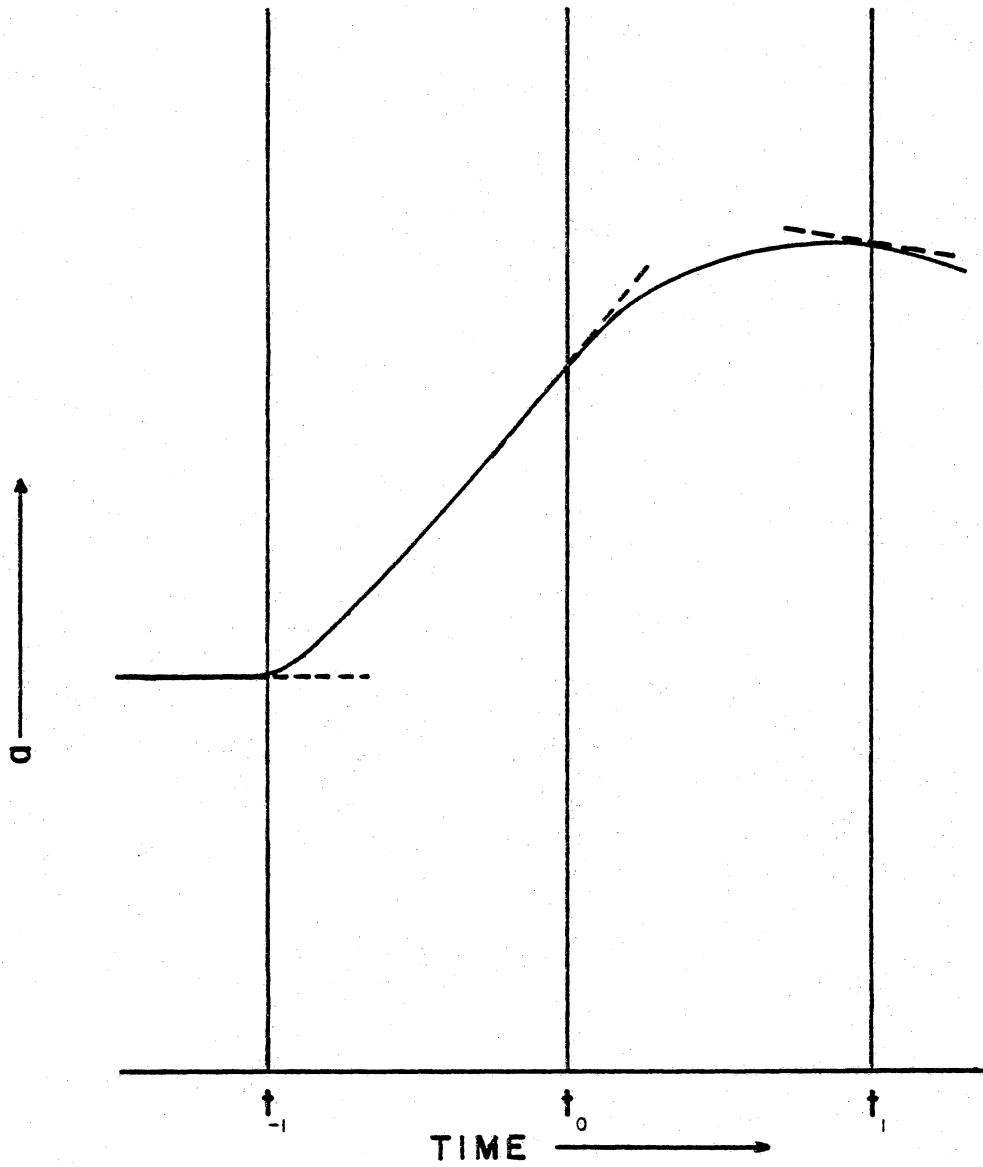


FIGURE 3.3.2 The Second Order Approximation to the Time Derivative

3.4 Power and Adjoint Constraints

The nonlinear systems of equations incompletely describe the reactor system without the power constraint which will allow a unique flux level to the nonlinear equations to be obtained. A nuclear reactor can have an infinite number of flux levels, each of which will have a unique power level associated with it. This is, of course, assuming that parameters, such as cross sections, remain constant (as we assume here) over all power levels. If this is not the case, temperature and power dependent parameters and their associated equations would have to be added to the system of state equations.

The thermal power of a reactor is related to the flux by the fission reaction rate. Assuming the same average thermal power generation in all groups for the fission process, the total power output can be expressed as

$$P_{th} = G_c \int \sum_g^G \Sigma_g^f \phi_g d\bar{r} \quad (3.4.1)$$

or,

$$0 = \frac{P_{th}}{G_c} - \sum_g^G \int \Sigma_g^f \phi_g d\bar{r} \quad (3.4.2)$$

This equation permits the flux, iodine, and xenon levels to be uniquely determined for the system.

The adjoint system still needs to be constrained. This is done by requiring the same number of "adjoint" neutrons as actual neutrons in the reactor core. Mathematically this is expressed as

$$0 = \sum_g \int \phi_g^\dagger d\bar{r} - \sum_g \int \phi_g d\bar{r} \quad (3.4.3)$$

This will require that the equilibrium direct system be solved before the adjoint system.

3.5 The Nonlinear Equations

Expanding and inserting the series profiles into Eq. 3.1.3 results in the direct nonlinear equations

$$\begin{aligned}
 0 &= \int e_s \eta_s^i d\bar{r} \\
 &= \sum_t^N \sum_r^R (s_{ts} - \frac{p_{ts}}{k_{ts}}) \sum_o^P a_t^o \int_r \eta_t^o \eta_s^i d\bar{r} \\
 &+ \left[\sum_o^P a_s^o \left(- \sum_r^R D_s \int_r \eta_s^i (\nabla \eta_s^o) d\bar{r} \right. \right. \\
 &\quad + \sum_r^R \alpha_s \Sigma_s^a \phi_s \int_r \eta_s^o \eta_s^i d\bar{r} \\
 &\quad \left. \left. + \sum_e^E \sigma_s^e \sum_h^P a_{G+e}^h \sum_r^R \int_r \eta_s^o \eta_{G+e}^h \eta_s^i d\bar{r} \right) ; \quad s \leq G \right. \\
 &+ \left[\sum_o^P \left(- \frac{d a_s^o}{d t} \sum_r^R \int_r \eta_s^o \eta_s^i d\bar{r} \right. \right. \\
 &\quad \left. \left. - a_s^o \sum_u^G \sigma_u^{s-G} \sum_h^P a_u^h \sum_r^R \int_r \eta_s^o \eta_u^h \eta_s^i d\bar{r} \right) ; \quad s > G \right. \\
 &\hspace{15em} (3.5.1)
 \end{aligned}$$

where

$$s = 1, 2, 3, \dots, G \quad (3.5.2)$$

and

$$i = 1, 2, 3, \dots, P \quad (3.5.3)$$

The power constraint for the direct nonlinear system of

equations is

$$0 = \frac{P_{rh}}{G_c} - \sum_g^G \sum_r^R \sum_g^G \sum_p^P a_g^p \int_r \eta_g^p d\bar{r} \quad (3.5.4)$$

The adjoint nonlinear equations (3.1.4) become

$$\begin{aligned} 0 &= \int e_s^t \eta_s^i d\bar{r} \\ &= \sum_t^N \sum_r^R (s_{st} - \frac{p_{st}}{k_{st}}) \sum_o^P a_o^t \int \eta_o^t \eta_s^i d\bar{r} \\ &\quad \left[\sum_o^P a_o^t \left(- \sum_r^R D_s \int_r \eta_s^i (\nabla \eta_s^o) d\bar{r} \right. \right. \\ &\quad \left. \left. + \sum_r^R a_s^a \Sigma_s^a \bar{\phi}_s^t \int_r \eta_s^o \eta_s^i d\bar{r} \right. \right. \\ &\quad \left. \left. + \sum_e^E \sigma_s^e \sum_h^P a_{G+e}^t \sum_r^R \int_r \eta_s^o \eta_{G+e}^h \eta_s^i d\bar{r} \right) ; \quad s \leq G \right. \\ &\quad \left. - \left[\sum_o^P a_o^t \sum_u^G \sigma_u^{s-G} \sum_h^P a_u^t \sum_r^R \int_r \eta_s^o \eta_u^h \eta_s^i d\bar{r} ; \quad s > G \right. \right. \end{aligned} \quad (3.5.5)$$

and their constraint is

$$\begin{aligned} 0 &= \sum_k^G \sum_o^P a_k^o \sum_r^R \int_r \eta_k^o d\bar{r} \\ &\quad - \sum_k^G \sum_o^P a_k^o \sum_r^R \int_r \eta_k^o d\bar{r} \end{aligned} \quad (3.5.6)$$

These equations are used in the numerical computer model described in the following chapter.

Chapter IV

Computational Methods - the XORA Program

4.1 XORA

The solutions for the direct and adjoint systems of nonlinear equations, with constraints, are calculated by the computer code XORA (Xenon Oscillations - a Residual Approach). This code is written in the FORTRAN IV (H-Extended) language and runs on the IBM computers located at VPI & SU. A one-dimensional model is used in XORA in order to reduce computing time and region requirements. The program is capable of solving multigroup (or single group) problems. The time-dependent problem may be solved using the nonlinear model developed in the previous chapters or with a linearized version discussed in section 4.3.

The overall logic flow in XORA can be broken down into five major sections as shown in Fig. 4.1.1. Detailed logic flow diagrams of the sections are given in Appendix C. A partial listing of the computer program is given as Appendix E. For brevity, common computational routines, such as Gaussian elimination, are not included.

The first logic section, INPUT, reads in from a data set (or interactive terminal) which describes the problem to be

solved. This input includes such parameters as the number of regions, groups, and profiles along with the nuclear properties of the core. A sample input is given in Appendix D.

The INITIALIZATION logic section is called next. This section changes the input to the form required by the program. It also causes parameters used for the profiles and integrations to be calculated and stored for future use. The final purpose of this section is to give initial values to variables such as the effective multiplication factor and the time.

The next logic section actually has the direct nonlinear system of equations solved. This section is called DIRECT. Because the dominant eigenvalue is required, the Wielandt method [40] is employed. This scheme requires the solution of the nonlinear equations for each iteration on the eigenvalue. Two methods are provided in XORA. The first method is a standard Newton-Raphson technique [45] and is normally called by the program. If convergence seems to be failing, another method, called the Kane-Yakolev method, is incorporated. Theoretically, this method, described in section 4.2, will result in a solution to the system of equations regardless of the initial guess at the solution.

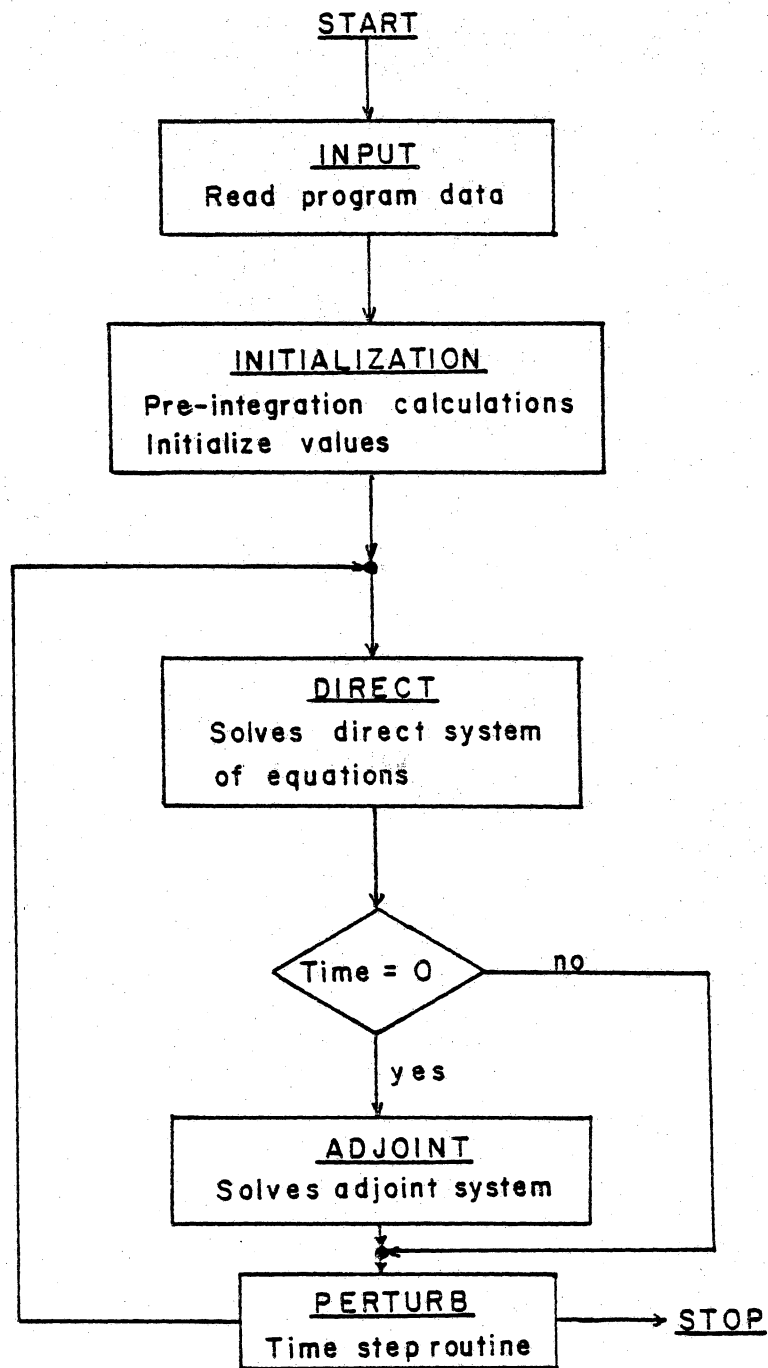


FIGURE 4.1.1 Major Logic Sections in XORA

The major drawback of the Kane-Yakolev method is that it can require large numbers of calculations to be able to get a valid solution, thus making the Newton-Raphson method a more desirable routine to use when possible.

The adjoint system of nonlinear equations is evaluated by the logic section ADJOINT. This section is called only once, at equilibrium, and uses information from the solution of the equilibrium direct system. The method of solution is identical to that used in the DIRECT logic section described in the preceding paragraph.

The last major logic section, PERTURB, has the function of controlling the time dependency of the program. Its functions include testing to see if the end time of the simulation has been reached and, if not, causing another time-step to be taken. Any variations in reactor parameters is also controlled by PERTURB. When the end time of the simulation is detected, this section causes the program to halt execution.

Throughout all of these logic sections appropriate output is generated. This output includes a listing of the input information and any error messages deemed necessary along with the actual calculational output. The actual output corresponding to the sample input of Appendix D is given as Appendix F.

4.2 Kane-Yakolev Method for Simultaneous Equations

The Kane-Yakolev method for solving simultaneous linear, nonlinear, algebraic, or transcendental equations is a noniterative approach. The method involves formation of a differential system of equations from the original set of equations. An integration routine, like the Runge-Kutta method used in XORA, is then employed to solve the system from the initial point to the endpoint that are determined by the formation of the differential equations. The result of the integration is the solution to the original system.

Development of the Kane-Yakolev method begins with the original system of equations

$$\begin{aligned}
 f_1(x_1, x_2, \dots, x_N) &= 0 \\
 f_2(x_1, x_2, \dots, x_N) &= 0 \\
 \vdots & \\
 \vdots & \\
 \vdots & \\
 f_N(x_1, x_2, \dots, x_N) &= 0
 \end{aligned}
 \tag{4.2.1}$$

which can be expressed in compact form as

$$\underline{f}(\underline{x}) = \underline{0}
 \tag{4.2.2}$$

Using a guess for the solution, \underline{x}^0 , it is possible to express the system of equations as

$$\underline{f}(\underline{y}) = \underline{f}(\underline{x}^0) (1 - \tau)
 \tag{4.2.3}$$

Differentiating 4.2.3 with respect to τ results in

$$\frac{d \underline{f}}{d \underline{y}} \frac{d \underline{y}}{d \tau} = - \underline{f}(\underline{x}^0) \quad (4.2.4)$$

or

$$\frac{d \underline{y}}{d \tau} = - \left[\frac{d \underline{f}}{d \underline{y}} \right]^{-1} \underline{f}(\underline{x}^0) \quad (4.2.5)$$

Next, the differential Eqs. 4.2.5 must be solved. The initial condition is

$$\underline{y} = \underline{x}^0 \quad (4.2.6)$$

which comes from Eq. 4.2.3 when $\tau = 0$. Using this initial condition, Eq. 4.2.5 is integrated. At $\tau = 1$, Eq. 4.2.3 becomes

$$\underline{f}(\underline{y}) = \underline{f}(\underline{x}^0) (1 - 1) = 0 \quad (4.2.7)$$

so the endpoint of the integration will occur when $\tau = 1$ and the resulting \underline{y} is the required solution vector.

4.3 Alterations of the Nonlinear Xenon Model to a Linear Model

The nonlinearities of the xenon-induced flux oscillation problem are contained in the fission product absorption terms of the form

$$\sigma_g^e N^e \phi_g \quad (4.3.1)$$

which are located in the [N] matrix of equation 2.2.3 ([R] contains [N]). To obtain a linear expression for equation 4.3.1, variations in both the flux and isotopic concentration are taken about their equilibrium points, resulting in

$$\phi_g = \phi_{g_0} + \delta \phi_g \quad , \quad (4.3.2)$$

where the subscript 0 indicates the equilibrium conditions,

$$N^e = N_0^e + \delta N^e \quad , \quad (4.3.3)$$

and

$$\sigma_g^e N^e \phi_g = \sigma_g^e (N_0^e + \delta N^e) (\phi_{g_0} + \delta \phi_g) \quad . \quad (4.3.4)$$

Rewriting 4.3.4, the equation becomes

$$\sigma_g^e N^e \phi_g = \sigma_g^e (N_0^e \phi_{g_0} + \delta N^e \phi_{g_0} + N_0^e \delta \phi_g + \delta N^e \delta \phi_g) \quad . \quad (4.3.5)$$

To linearize, the second order variation term is assumed negligible giving

$$\sigma_g^e N^e \phi_g = \sigma_g^e (N_0^e \phi_{g_0} + \delta N^e \phi_{g_0} + N_0^e \delta \phi_g) \quad . \quad (4.3.6)$$

Now that there is a linear expression (equation 4.3.6) for the nonlinear terms, the original, time dependent state equations 2.2.3 can be written as

$$\begin{aligned} & ([D] + [S] + [a]) (\underline{\Phi} + \delta \underline{\Phi}) + [N] \underline{\Phi} \\ & + [N] \delta \underline{\Phi} + [\delta N] \underline{\Phi} = \frac{[P]}{k} (\underline{\Phi} + \delta \underline{\Phi}) \quad . \quad (4.3.7) \end{aligned}$$

Subtracting the equilibrium system from equation 4.3.7 results in

$$([D] + [S] + [\alpha] + [N])\delta\Phi + [\delta N]\Phi = \frac{[P]}{k}\delta\Phi \quad (4.3.8)$$

where the eigenvalue is assumed to be constant and equal to the equilibrium value.

Solution of the linear system requires that the equilibrium nonlinear solution be known along with the solution at the end of at least the first perturbation. If it were attempted to use the linear system from before the first perturbation, the new state variables ($\delta\Phi_0$) would be initially zero and this trivial solution would result for all time. It is this linear system that is used for comparative purposes in Chapter Five.

Chapter V

Numerical Results

5.1 The Cases and the Input Cross Sections

Solutions of the xenon-induced flux oscillation model are computed by the computer program XORA. The specific problems considered are chosen to show the effects of the nonlinearities of the model when compared to the linear model. Considerations are also given to the effects of varying the number of energy groups and profile expansions. The cases used are listed in table 5.1.1. The identification used for the cases are derived by the following scheme. The first character is an L for a linear model or an N for a nonlinear one. The next number, followed by a G, is the number of energy groups. The number preceeding the R is the number of spatial regions, and the last number, which preceeds the P, is the number of profiles. The final character indicates which set of input cross sections is being used.

A consistent set of input cross sections are required for valid comparisons between these cases. These cross sections are for a unit cell of a Babcock & Wilcox reactor with a burnup of approximately 16000 MWD/MTU. Table 5.1.2 gives

the reactor parameters used. The cross sections are obtained from the computer code VIM[50]. VIM is a Monte Carlo program, developed at Argonne National Laboratory, used to calculate the collision history of neutrons in a reactor. The particular calculations used are for an infinite lattice of heterogeneous (fuel pellet, clad, and moderator regions) fuel cells with no axial leakage. The fine energy group structure is composed of 54 half lethargy width groups starting with a maximum energy of 10MeV. A 55th group is included which has 10^{-5} eV, the minimum energy allowed in VIM, as its lower energy bound. The results of the calculations are homogenized and then collapsed into a variety of few-group energy structures for use as input into XORA.

The results from VIM did not specifically include scattering between groups or the diffusion coefficients. The diffusion coefficients are approximated by

$$D_g = \frac{1}{3(\Sigma^t - \bar{\mu} \Sigma_{H_2O}^s)} \quad , \quad (5.1.1)$$

since $\bar{\mu} \Sigma_{H_2O}^s$ is the only significant contribution to the scattering. It is assumed that scattering occurs only between adjacent groups and no upscattering is present, even in the thermal groups. Then, the three group downscattering

Table 5.1.1 The XORA Cases

<u>Case ID</u>	Nonlinear or <u>Linear</u>	<u>#Groups</u>	<u>#Regions</u>	<u>#Profiles</u>	<u>Data set</u>
N1G2R2PA	Non	1	2	2	A
N1G2R3PA	Non	1	2	3	A
N1G2R4PA	Non	1	2	4	A
N3G2R3PB	Non	3	2	3	B
N3G2R2PC	Non	3	2	2	C
N3G2R3PC	Non	3	2	3	C
N3G2R6PC	Non	3	2	6	C
N3G2R3PD	Non	3	2	3	D
L1G2R3PA	Lin	1	2	3	A
L3G2R3PC	Lin	3	2	3	C

Table 5.1.2 Babcock & Wilcox PWR Reactor Parameters

Overall Core

Thermal Power Level	2568 MW
Height	366 cm
Equivalent Diameter	327 cm

Equivalent Fuel Cell

(15 x 15 Rectangular Fuel Assemblies)

Pellet Outside Diameter	0.9398 cm
Cladding Outside Diameter	1.0922 cm
Cell Pitch	1.4427 cm

Homogeneous Cell Composition

• Densities are in atoms /cm-barn

Element	Density	Element	Density
H (H ₂ O)	$2.6070 \cdot 10^{-2}$	U ²³⁵	$1.1218 \cdot 10^{-4}$
B ¹⁰	$3.9970 \cdot 10^{-6}$	U ²³⁶	$1.8554 \cdot 10^{-5}$
B ¹¹	$1.7728 \cdot 10^{-5}$	U ²³⁸	$6.9456 \cdot 10^{-3}$
O ¹⁶	$2.7278 \cdot 10^{-2}$	Pu ²³⁹	$3.1572 \cdot 10^{-5}$
Xe ¹³⁵	$2.8101 \cdot 10^{-9}$	Pu ²⁴⁰	$6.2656 \cdot 10^{-6}$
Sm ¹⁴⁹	$6.4490 \cdot 10^{-8}$	Pu ²⁴¹	$5.0759 \cdot 10^{-6}$
Zirc2	$4.4253 \cdot 10^{-3}$	Pu ²⁴²	$8.4520 \cdot 10^{-7}$

equations, based on neutron balance, are

$$\Sigma_{1 \rightarrow 2}^s = \frac{\chi_1 \left[\begin{array}{c} \text{production} \\ \text{rate} \end{array} \right] - \left[\begin{array}{c} \text{absorption} \\ \text{rate} \end{array} \right]}{\phi_1} \quad (5.1.2)$$

and

$$\Sigma_{2 \rightarrow 3}^s = \frac{\chi_2 \left[\begin{array}{c} \text{production} \\ \text{rate} \end{array} \right] - \left[\begin{array}{c} \text{absorption} \\ \text{rate} \end{array} \right] + \Sigma_{1 \rightarrow 2}^s \phi_1}{\phi_2} \quad (5.1.3)$$

In order to check the validity of these assumptions, the absorption cross section for the lowest energy group is calculated using the neutron balance equation and the results of Eqs. 5.1.2 and 5.1.3, i.e.,

$$\Sigma_3^a = \frac{\chi_3 \left[\begin{array}{c} \text{production} \\ \text{rate} \end{array} \right] + \Sigma_{2 \rightarrow 3}^s \phi_2}{\phi_3} \quad (5.1.4)$$

This cross section is then compared to that obtained by VIM. The results in all cases indicate that no appreciable upscattering occurs with the presence of xenon in the reactor. These results along with the group cross sections used are given in tables 5.1.3 thru 5.1.6.

5.2 Direct Solution - the Equilibrium Problem

The first step in the xenon induced flux oscillation problem is to obtain the equilibrium direct solution. A

Table 5.1.3 One-Group Parameters - Case A

Lower Energy Bound	$1.000 \cdot 10^{-5}$
Chi	1.000
Nu	2.622
Fission Cross Section	0.008716
Absorption Cross Section (without Xe)	0.02219
Diffusion Coefficient	0.3900
Microscopic Xenon Cross Section	$1.224 \cdot 10^6$
Fission Yield of Iodine	6.1
Fission Yield of Xenon	0.3

- All energies are in eV.
- All cross sections are macroscopic (cm^{-1}) unless noted otherwise.
- All microscopic cross sections are in barns.
- All diffusion coefficients are in cm.
- All fission yields are in per cent.

Table 5.1.4 Three-Group Parameters - Case B

	Energy Group		
	<u>1</u>	<u>2</u>	<u>3</u>
Lower Energy Bound	1.855	0.0206	$1.000 \cdot 10^{-5}$
Chi	1.000	0.000	0.000
Nu	2.673	2.622	2.556
Fission Cross Section	0.002003	0.04291	0.02153
Absorption Cross Section (without Xe)	0.009216	0.08565	0.1183
Downscattering Cross Section Group i into i+1	0.01675	0.01658	---
Diffusion Coefficient	1.0880	0.6900	0.4500
Microscopic Xenon Cross Section	---	$1.224 \cdot 10^6$	$2.611 \cdot 10^6$
Fission Yield of Iodine	6.1	6.1	6.1
Fission Yield of Xenon	0.3	0.3	0.3

- All energies are in eV.
- All cross sections are macroscopic (cm^{-1}) unless noted otherwise.
- All microscopic cross sections are in barns.
- All diffusion coefficients are in cm.
- All fission yields are in per cent.

Table 5.1.5 Three-Group Parameters - Case C

	Energy Group		
	<u>1</u>	<u>2</u>	<u>3</u>
Lower Energy Bound	1.855	0.0924	$1.000 \cdot 10^{-5}$
Chi	1.000	0.000	0.000
Nu	2.673	2.683	2.565
Fission Cross Section	0.002003	0.03202	0.06947
Absorption Cross Section (without Xe)	0.009216	0.06939	0.1281
Downscattering Cross Section Group i into i+1	0.01675	0.1019	---
Diffusion Coefficient	1.0880	0.6692	0.4327
Microscopic Xenon Cross Section	---	$4.431 \cdot 10^6$	$2.483 \cdot 10^6$
Fission Yield of Iodine	6.1	6.1	6.1
Fission Yield of Xenon	0.3	0.3	0.3

- All energies are in eV.
- All cross sections are macroscopic (cm^{-1}) unless noted otherwise.
- All microscopic cross sections are in barns.
- All diffusion coefficients are in cm.
- All fission yields are in per cent.

Table 5.1.6 Three-Group Parameters - Case D

	Energy Group		
	<u>1</u>	<u>2</u>	<u>3</u>
Lower Energy Bound	1.855	0.2511	$1.000 \cdot 10^{-5}$
Chi	1.000	0.000	0.000
Nu	2.673	2.714	2.590
Fission Cross Section	0.002003	0.02356	0.06098
Absorption Cross Section (without Xe)	0.009216	0.05944	0.1131
Downscattering Cross Section Group i into i+1	0.01675	0.02267	---
Diffusion Coefficient	1.0880	0.7312	0.4772
Microscopic Xenon Cross Section	---	$2.253 \cdot 10^6$	$2.000 \cdot 10^6$
Fission Yield of Iodine	6.1	6.1	6.1
Fission Yield of Xenon	0.3	0.3	0.3

- All energies are in eV.
- All cross sections are macroscopic (cm^{-1}) unless noted otherwise.
- All microscopic cross sections are in barns.
- All diffusion coefficients are in cm.
- All fission yields are in per cent.

determination of the validity of the results is of prime importance. This is determined by a direct comparison to the VIM results. In all cases, comparable results are obtained including the flux ratios and k effective. The differences, as seen in Tables 5.2.1 through 5.2.4 are attributable to the fact that, in VIM, the xenon concentration is inputted at a constant concentration across the fuel pellet. The XORA program, however, calculates a spatial distribution for the xenon concentration. This spatial distribution of xenon is more realistic than the constant distribution making the XORA model better than VIM for xenon.

The use of a multi-energy group structure causes a small alteration in the results due to a better treatment of the xenon cross section. The absorption rate due to xenon differs in the XORA results from the VIM results because of a change in the neutron energy spectrum due to the different amount of xenon in the XORA calculation compared to the VIM input. The multi-energy group treatment allows for a change in the effective flux weighting of the xenon cross section which is substantial because of the high neutron dependency of the xenon cross section (as shown in Fig. 1.1.3). The different multigroup structures used in cases N3G2R3PB,

Table 5.2.1 One-Group Equilibrium Results for Data Set A

	<u>VIM</u>	<u>N1G2R2PA</u>	<u>N1G2R3PA</u>	<u>N1G2R4PA</u>
Effective Multiplication	1.0302	1.0316	1.0317	1.0317
Total Rate of Production ⁽¹⁾	1.0311	1.0362	1.0356	1.0356
Total Rate of Absorption ⁽¹⁾	1.0009	1.0000	1.0000	1.0000
Xenon Absorption Rate ⁽¹⁾	0.0244	0.0186	0.0192	0.0192
Flux Level (cm ⁻² -sec ⁻¹) ⁽¹⁾	45.106	45.327	45.307	45.307
Leakage Rate ⁽¹⁾	--	0.0046	0.0038	0.0038
Iodine Concentration ⁽²⁾	--	5.8335	5.8335	5.8335
Xenon Concentration ⁽²⁾	2.8105	1.7795	1.9615	1.9615

-
1. Normalized to total absorption rate
 2. Concentrations are in 10¹⁵ atoms per cm³

Table 5.2.2 Equilibrium Results for Data Set B

	<u>VIM</u>	<u>N3G2R3PB</u>
Effective Multiplication	1.0302	1.0315
Group One Flux ($\text{cm}^{-2}\text{-sec}^{-1}$) ⁽¹⁾	38.541	38.531
Group Two Flux ($\text{cm}^{-2}\text{-sec}^{-1}$) ⁽¹⁾	6.1104	6.1466
Group Three Flux ($\text{cm}^{-2}\text{-sec}^{-1}$) ⁽¹⁾	0.4550	0.4609
Flux Level ($\text{cm}^{-2}\text{-sec}^{-1}$) ⁽¹⁾	45.106	45.138
Total Rate of Production ⁽¹⁾	1.0311	1.0359
Total Rate of Absorption ⁽¹⁾	1.0009	1.0000
Xenon Absorption Rate ⁽¹⁾	0.0244	0.0192
Leakage Rate ⁽¹⁾	--	0.0043
Iodine Concentration ⁽²⁾	--	5.8335
Xenon Concentration ⁽²⁾	2.8105	1.9620

-
1. Normalized to total absorption rate
 2. Concentrations are in 10^{15} atoms per cm^3

Table 5.2.3 Equilibrium Results for Data Set C

	<u>VIM</u>	<u>N3G2R2PC</u>	<u>N3G2R3PC</u>	<u>N3G2R6PC</u>
Effective Multiplication	1.0302	1.0324	1.0326	1.0326
Group One Flux ($\text{cm}^{-2}\text{-sec}^{-1}$) ⁽¹⁾	38.541	38.572	38.527	38.525
Group Two Flux ($\text{cm}^{-2}\text{-sec}^{-1}$) ⁽¹⁾	3.742	3.748	3.745	3.744
Group Three Flux ($\text{cm}^{-2}\text{-sec}^{-1}$) ⁽¹⁾	2.824	2.856	2.856	2.856
Flux Level ($\text{cm}^{-2}\text{-sec}^{-1}$) ⁽¹⁾	45.106	45.176	45.128	45.126
Total Rate of Production ⁽¹⁾	1.0311	1.0374	1.0370	1.0369
Total Rate of Absorption ⁽¹⁾	1.0009	1.0000	1.0000	1.0000
Xenon Absorption Rate ⁽¹⁾	0.0244	0.0187	0.0192	0.0193
Leakage Rate ⁽¹⁾	--	0.0050	0.0044	0.0042
Iodine Concentration ⁽²⁾	--	5.8330	5.8335	5.8335
Xenon Concentration ⁽²⁾	2.8105	1.7750	1.9585	1.9970

-
1. Normalized to total absorption rate
 2. Concentrations are in 10^{15} atoms per cm^3

Table 5.2.4 Equilibrium Results for Data Set D

	<u>VIM</u>	<u>N3G2R3PD</u>
Effective Multiplication	1.0302	1.0330
Group One Flux ($\text{cm}^{-2}\text{-sec}^{-1}$) ⁽¹⁾	38.541	38.527
Group Two Flux ($\text{cm}^{-2}\text{-sec}^{-1}$) ⁽¹⁾	2.256	2.255
Group Three Flux ($\text{cm}^{-2}\text{-sec}^{-1}$) ⁽¹⁾	4.310	4.349
Flux Level ($\text{cm}^{-2}\text{-sec}^{-1}$) ⁽¹⁾	45.106	45.131
Total Rate of Production ⁽¹⁾	1.0311	1.0372
Total Rate of Absorption ⁽¹⁾	1.0009	1.0000
Xenon Absorption Rate ⁽¹⁾	0.0244	0.0192
Leakage Rate ⁽¹⁾	--	0.0042
Iodine Concentration ⁽²⁾	--	5.8330
Xenon Concentration ⁽²⁾	2.8105	1.9595

-
1. Normalized to total absorption rate
 2. Concentrations are in 10^{15} atoms per cm^3

N3G2R3PC, and N3G2R3PD indicate that, when the neutron energy spectrum can change from the initially assumed profile used for calculating the group constants, careful consideration must be given to the thermal group structure. As is shown below in the transient section, the effect due to the energy structure is substantial. This structure includes the number of thermal groups as well as the energy widths of these groups.

Another fact surfaced during the calculations of the group transfer cross sections. Typically, upscattering of neutrons between the thermal groups occurs. The presence of xenon, with its high thermal cross section, causes the absorption rate to overshadow the upscattering rate. Combined with the fact that upscattering is negligible in the higher energy regions, the xenon absorption effectively eliminates the upscattering terms from the model. If the model is expanded to include nonfuel regions, such as the reflectors, the lack of xenon in these regions will result in the upscattering terms becoming important in the thermal groups.

The other major result from the equilibrium cases deals with the profile expansions. The one-group model has results for two, three, and four profile expansions for each

flux group and isotopic concentration. The results, at equilibrium, for these cases were quite close for the three and four profile cases. The two profile case, however, had an 11 per cent decrease in the amount of xenon present. This difference is due to the constraints being imposed on the system. First, the correct averages are being sought for each region. Secondly, the number of neutrons leaking from the reactor is required. Since the number of neutrons leaking from the system is being dictated by the profiles chosen, the two profile case will be unable to vary the leakage and still maintain the regional averages. The three and four profile cases can alter the ratios of the profiles, thus altering the leakage, while still maintaining the proper regional averages. This indicates that the minimum number of profiles that should be used is, for one dimension, one higher than the number of regions chosen. Also, for equilibrium calculations, increasing the number of profiles beyond this minimum will result in an increase in computing time with little increase in the accuracy of the results. The three energy group cases gave the same type of results.

The proper choice of the number of profiles is important in the XORA model. Combining this choice with an

appropriate energy structure will result in accurate solutions to the equilibrium system of equations.

5.3 Adjoint Solution - the Equilibrium Problem

The adjoint system can be considered the backwards problem. Here, the "adjoint neutrons" are produced at thermal energies and upscatter to higher energies. Also there is no adjoint xenon or iodine being produced. This is the result of treating the entire system as a single set of equations rather than trying to determine separate adjoint equations for the isotopic concentrations. When the complete adjoint system is expanded, the equations

$$-\lambda^2 N^2 - N^2 \sum_g^G \sigma_g^2 \phi_g = 0 \quad (5.3.1)$$

and

$$-\lambda^1 N^1 - N^1 \sum_g^G \sigma_g^1 \phi_g + \lambda^2 N^2 = 0 \quad (5.3.2)$$

are found. The only valid solution to the first is $N^2=0$ (xenon) since all of the terms are positive. With N^2 being zero, the second equation requires that N^1 (iodine) be zero also. Thus the adjoint system reduces to the adjoint of the diffusion system of equations without the individual isotopic absorptions.

The results for the adjoint system are given in Tables 5.3.1 through 5.3.3. The same features as found in the direct system are seen in the adjoint problem. The one exception is that, without adjoint xenon, downscattering (the adjoint of upscattering) becomes important. However, if upscattering is neglected in the direct system, the downscattering of adjoint neutrons must also be neglected to keep the two systems consistent.

5.4 Direct Solution - the Transient Problem

Xenon-induced flux oscillations occur when the equilibrium state of the reactor is perturbed. The cause of the perturbation can be any change in the reactor that forces the spatial distribution of the xenon concentration or flux to alter. Such a change may result from the insertion of a control rod into one region of the reactor with a decrease in boron poisoning throughout the reactor in order to remain critical. This is simulated by altering the macroscopic cross sections in the XORA program. The transient cases considered are with this form of perturbation. In particular, a 0.25 per cent increase in the absorption cross sections of region one and a corresponding 0.25 per cent decrease in region two is

Table 5.3.1 One-Group Adjoint Results for Data Set A

	<u>N1G2R2PA</u>	<u>N1G2R3PA</u>	<u>N1G2R4PA</u>
Effective Multiplication	1.0524	1.0525	1.0525
Total Rate of Production ⁽¹⁾	1.0558	1.0558	1.0558
Total Rate of Absorption ⁽¹⁾	1.0000	1.0000	1.0000
Flux Level (cm ⁻² -sec ⁻¹) ⁽¹⁾	46.193	46.193	46.193
Leakage Rate ⁽¹⁾	0.0034	0.0033	0.0033

1. Normalized to total absorption rate

Table 5.3.2 Adjoint Results for Data Set C

	<u>N3G2R2PC</u>	<u>N3G2R3PC</u>	<u>N3G2R6PC</u>
Effective Multiplication	1.0598	1.0599	1.0599
Group One Flux ($\text{cm}^{-2}\text{-sec}^{-1}$) ⁽¹⁾	3.784	3.784	3.7831
Group Two Flux ($\text{cm}^{-2}\text{-sec}^{-1}$) ⁽¹⁾	4.744	4.744	4.744
Group Three Flux ($\text{cm}^{-2}\text{-sec}^{-1}$) ⁽¹⁾	4.936	4.966	4.963
Flux Level ($\text{cm}^{-2}\text{-sec}^{-1}$) ⁽¹⁾	13.492	13.493	13.491
Total Rate of Production ⁽¹⁾	1.3127	1.3125	1.3124
Total Rate of Absorption ⁽¹⁾	1.0000	1.0000	1.0000
Leakage Rate ⁽¹⁾	0.2529	0.2526	0.2525

1. Normalized to total absorption rate

Table 5.3.3 Adjoint Results for Data Sets B and D

	<u>N3G2R3PB</u>	<u>N3G2R3PD</u>
Effective Multiplication	1.0579	1.0606
Group One Flux ($\text{cm}^{-2}\text{-sec}^{-1}$) ⁽¹⁾	2.487	4.300
Group Two Flux ($\text{cm}^{-2}\text{-sec}^{-1}$) ⁽¹⁾	3.117	5.392
Group Three Flux ($\text{cm}^{-2}\text{-sec}^{-1}$) ⁽¹⁾	3.299	5.662
Flux Level ($\text{cm}^{-2}\text{-sec}^{-1}$) ⁽¹⁾	8.904	15.354
Total Rate of Production ⁽¹⁾	1.3600	1.2619
Total Rate of Absorption ⁽¹⁾	1.0000	1.0000
Leakage Rate ⁽¹⁾	0.3019	0.2013

 1. Normalized to total absorption rate

imposed for 2.0 hours and then removed. Results from all cases are normalized by dividing the regional averages by the total core averages. In particular the total flux averages of each region and the isotopic concentrations of each region are considered, i.e.,

$$\frac{\phi_1^T}{\phi^T}, \quad \frac{I_1^T}{I^T}, \quad \frac{Xe_1^T}{Xe^T}, \quad \frac{\phi_1^T}{\phi^T}, \quad \frac{I_1^T}{I^T}, \quad \text{and} \quad \frac{Xe_1^T}{Xe^T} \quad (5.4.1)$$

are used.

Using this form of normalization, the total flux oscillations for the one- (N1G2R3PA) and three- (N3G2R3PC) energy group cases are compared. As seen in figure 5.4.1, a substantial difference in both amplitude and phase of the oscillations occurs. As is mentioned in section 5.2, this is attributable to the treatment of the xenon cross section. In the three group case, the total effective xenon cross section is the flux-weighted average of the three groups. This averaged cross section changes with the flux oscillations and is better than the constant cross section that is assumed with only one energy group.

The structure of the multiple energy groups is also important. Figure 5.4.2 shows the flux oscillations for the three different energy structures used in cases N3G2R3PB, N3G2R3PC, and N3G2R3PD. The peak amplitude of the

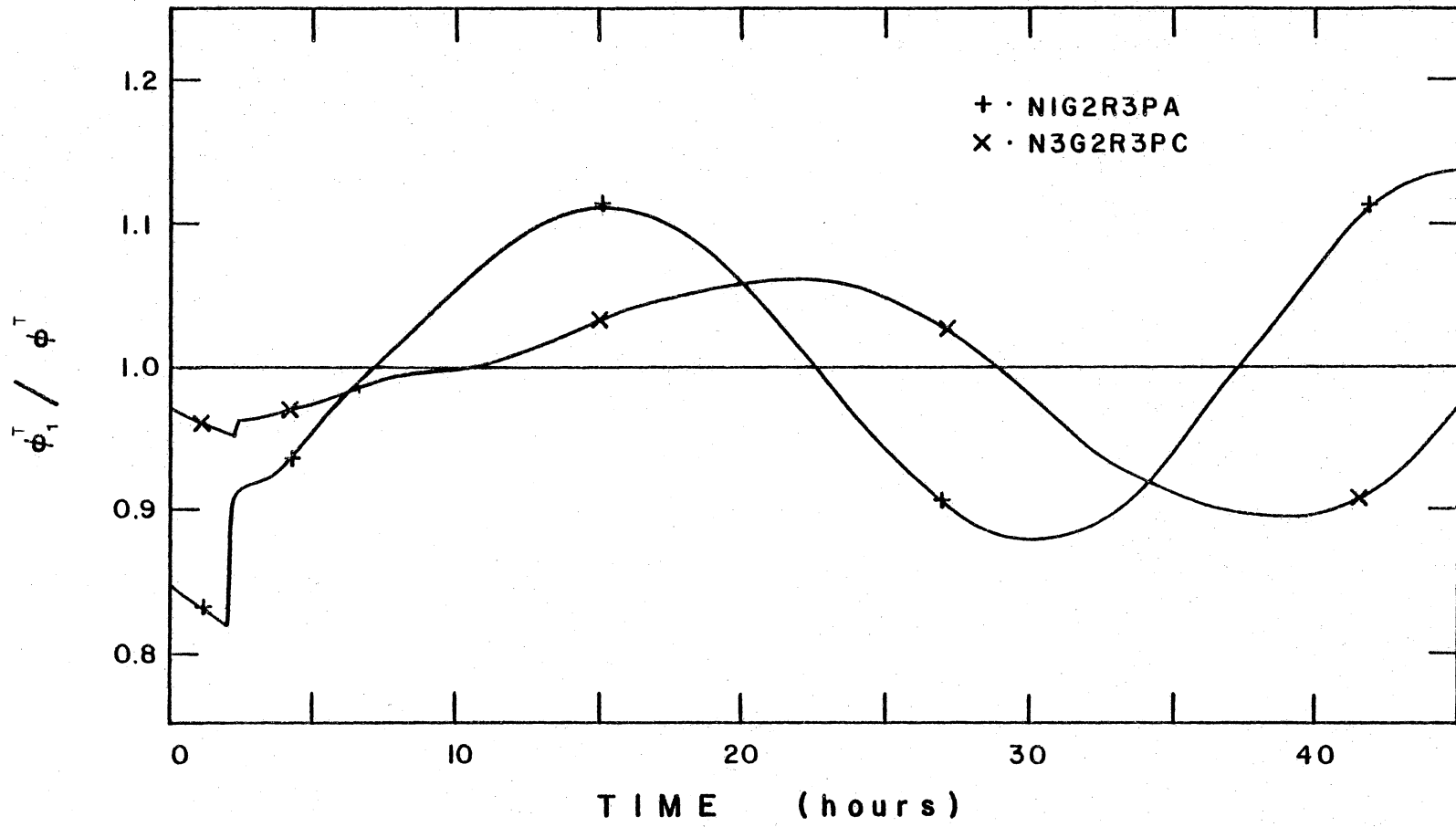


FIGURE 5.4.1 Comparison of Three- and One-Energy-Group Model Flux Oscillations

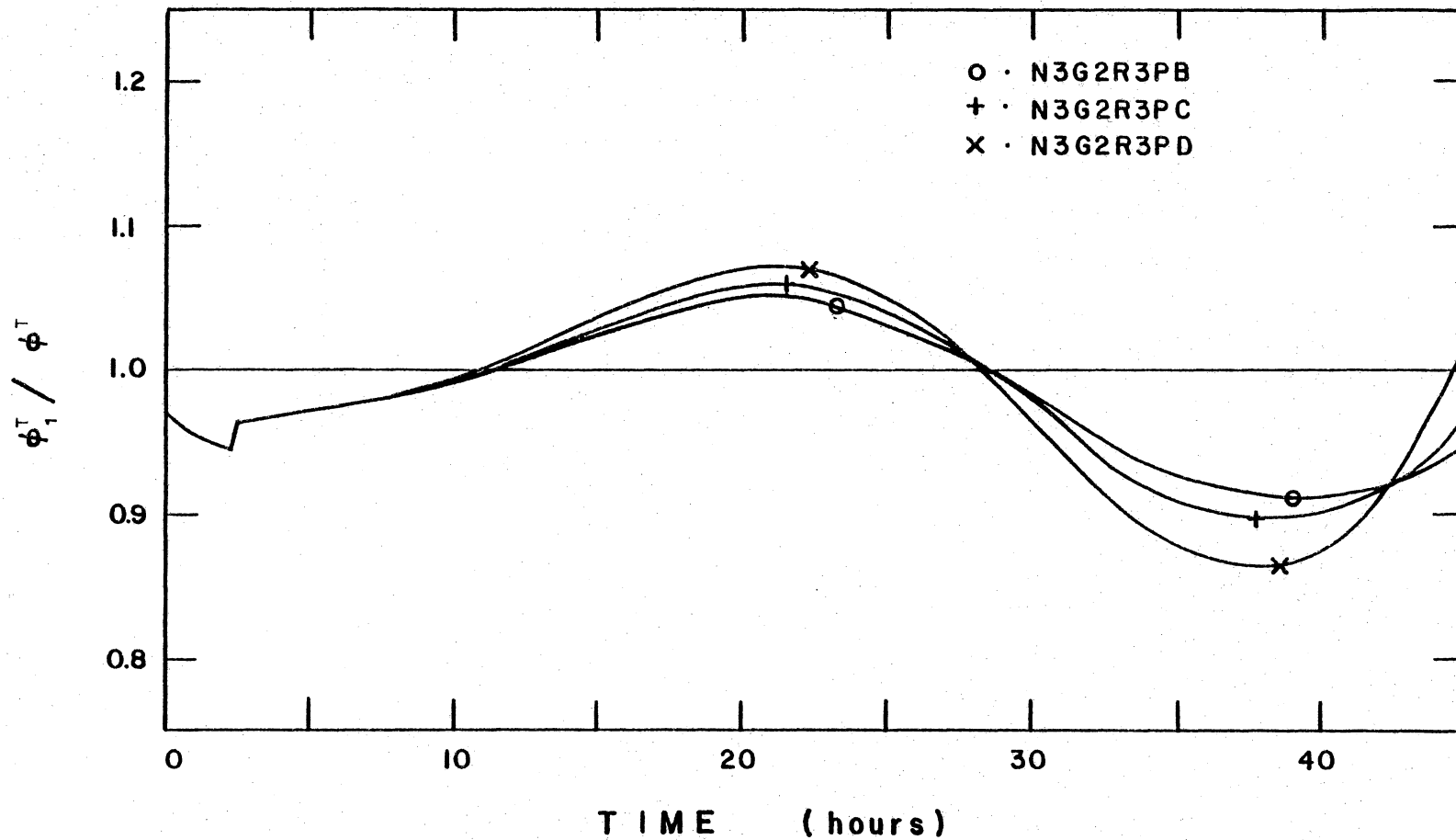


FIGURE 5.4.2 Comparison of Flux Oscillations due to Alternative Three-Energy-Group Structures

oscillations was found to increase as the energy boundary between the two thermal groups was raised. The differences in the flux weighting of the xenon causes the differences in the amplitudes predicted by the three models.

The amplitude of the oscillation is also affected by the number of profiles used to model the flux. In the one group case, the difference between the use of two and three profiles (N1G2R2PA and N1G2R3PA) was 16 per cent whereas the difference between the three and four profile cases (N1G2R3PA and N1G2R4PA) was only 4 per cent. As explained in the equilibrium cases, the large difference between using two and three profiles is the number of constraints on the system.

An increase in the number of profiles will result in a more accurate solution (theoretically exact with an infinite number of profiles) at the expense of computational time. The increase in computational time is quite dramatic. For the three-group cases (N3G2R2PC, N3G2R3PC, and N3G2R6PC) Table 5.4.1 lists the number of time steps performed and the amount of computer time required. Table 5.4.1 also shows the estimated time required to complete 80 hours of reactor simulation time. As seen, the six-profile case takes about six times as long to execute than the three-profile case.

Table 5.4.1 Computational Times for Selected XORA Cases

<u>Case</u>	<u>Simulated Time (hour)</u>	<u>Actual Run Time (s)</u>	<u>Estimated Run Time for 80 hrs (s)</u>
N1G2R2PA	24	120	380
N1G2R3PA	50	333	525
N1G2R4PA	22	360	1250
N3G2R2PC	100	506	410
N3G2R3PC	81	660	655
N3G2R6PC	15	900	4650

Usually, the increase in accuracy is outweighed by the increased cost of the calculations.

The limit cycle is obtained for the N3G2R3PC case. Figure 5.4.3 shows the flux oscillations along with the xenon and iodine isotopic concentration oscillations for region one of the reactor. In Chapter One, it is stated that the xenon would be approximately 180° out of phase with the flux and iodine. This is true if only one perturbation was caused in the reactor. The perturbation used in all of the cases is actually two changes in the absorption cross sections, the second change being the return to the initial values. This second perturbation causes a shift in the phase of the oscillations between the flux, iodine, and xenon as seen in Fig. 5.4.3. This shift depends on both the length of the perturbation and the rate that iodine decays into xenon. It is the combination of the perturbation and iodine decay rate that makes optimal control of xenon oscillations difficult.

5.5 The Linear Model Results

The linear model is developed at the end of Chapter Four and implemented by the XORA model. Results from the linear model are given in Figs. 5.5.1 and 5.5.2. In both the one-

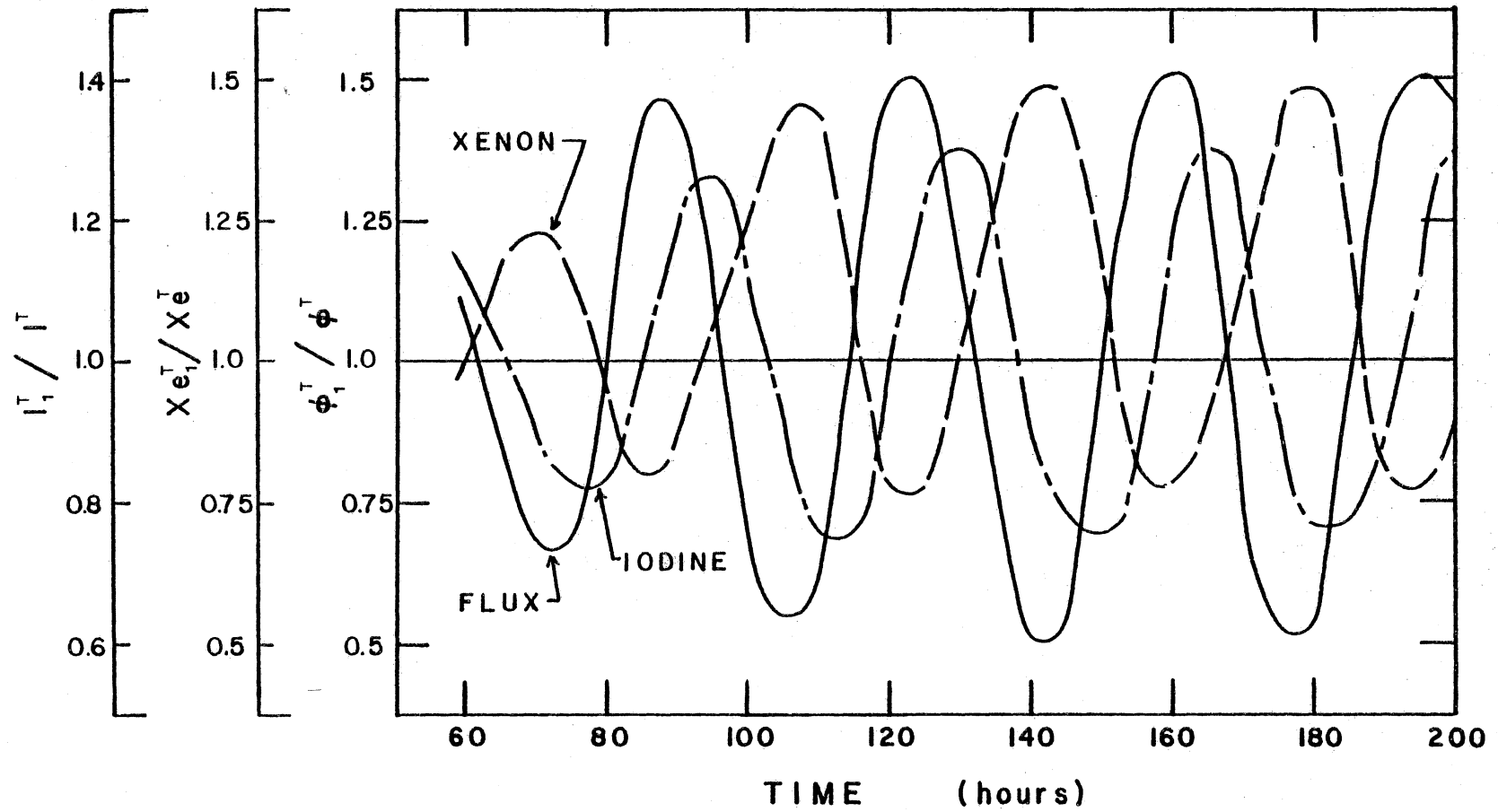


FIGURE 5.4.3 Model Response Exhibiting Limit Cycle

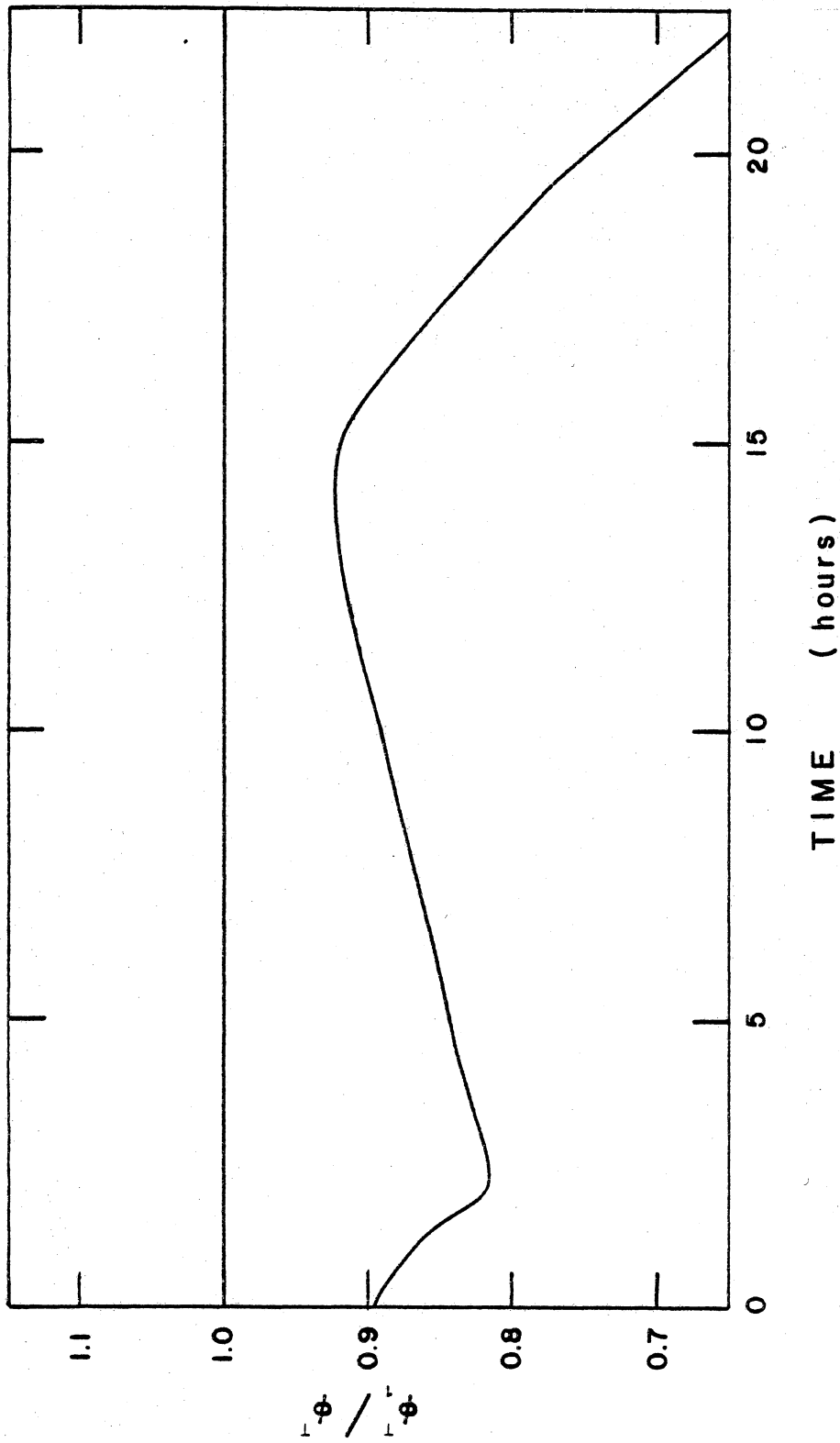


FIGURE 5.5.1 One-Group Linear Model Flux Response

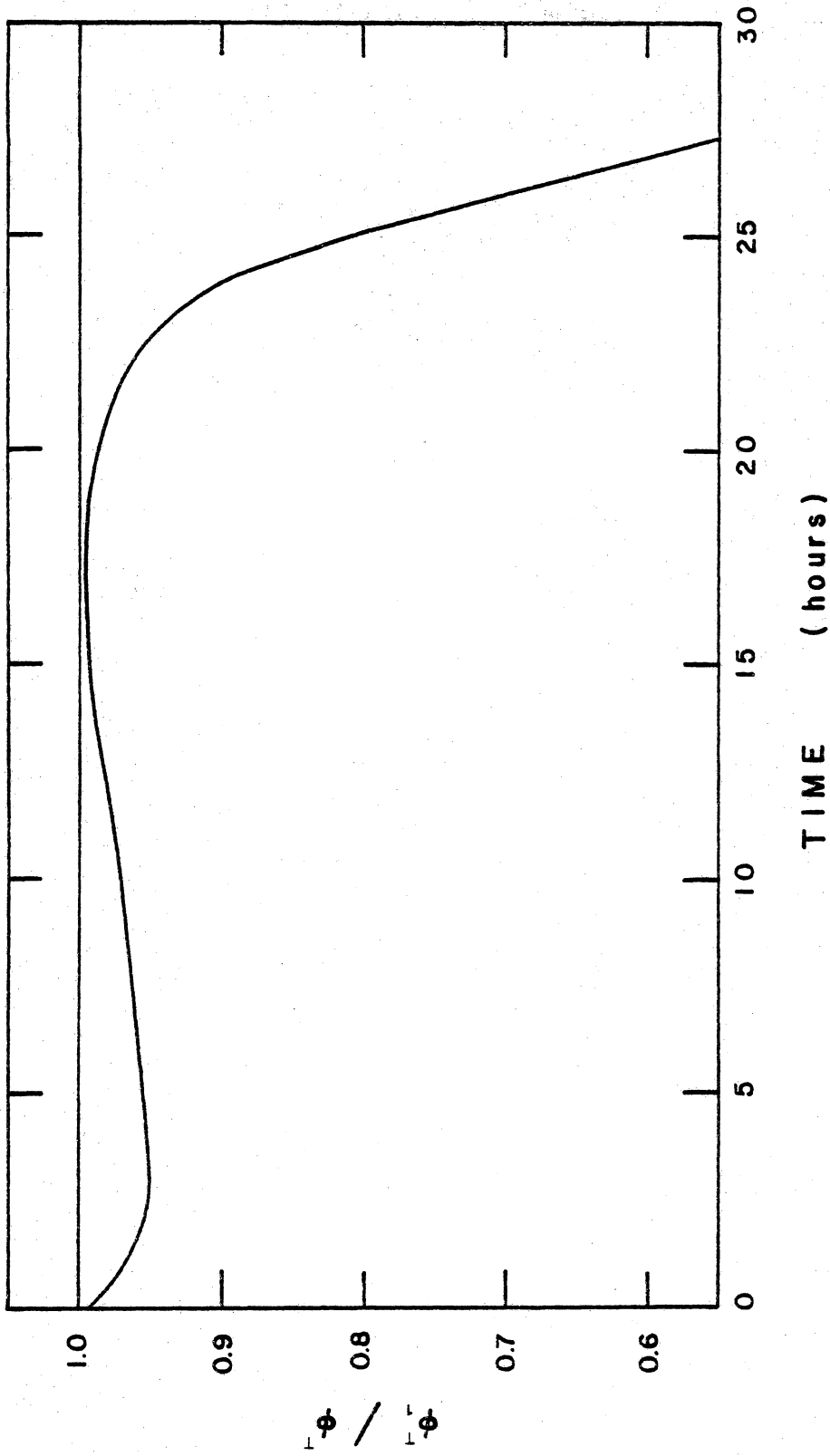


FIGURE 5.5.2 Three-Group Linear Model Flux Response

energy group and three-energy group models the flux levels begin reducing quite quickly and soon no power is being produced in the reactor. The oscillation of xenon causes the total absorption cross section in the reactor to vary dramatically for the input parameters of the system. When the power in a region of the reactor begins to decrease, the amount of xenon increases. This increase, without the nonlinear effects, quickly reduces the power level. Since the effects of the reduction of iodine due to the decreased power lags by some hours, the increased xenon absorption is able to reduce the power to zero before its production rate, from iodine, decreases. Thus, for the given input, the nonlinear effects becomes large and the linear model quickly becomes invalid.

Illustration of a difference in periods between the linear and nonlinear model is shown in Fig. 5.5.3. A different set of input data given in Table 5.5.1, was used along with a low flux level. The resulting periods of oscillations exhibit the divergent behavior indicated in Fig. 1.3.1. Fortunately, in a real reactor, operating limits, such as the axial offset, are strict enough that the reactor will automatically shutdown before the xenon oscillations have a chance to grow to the magnitudes shown in Fig. 5.5.3.

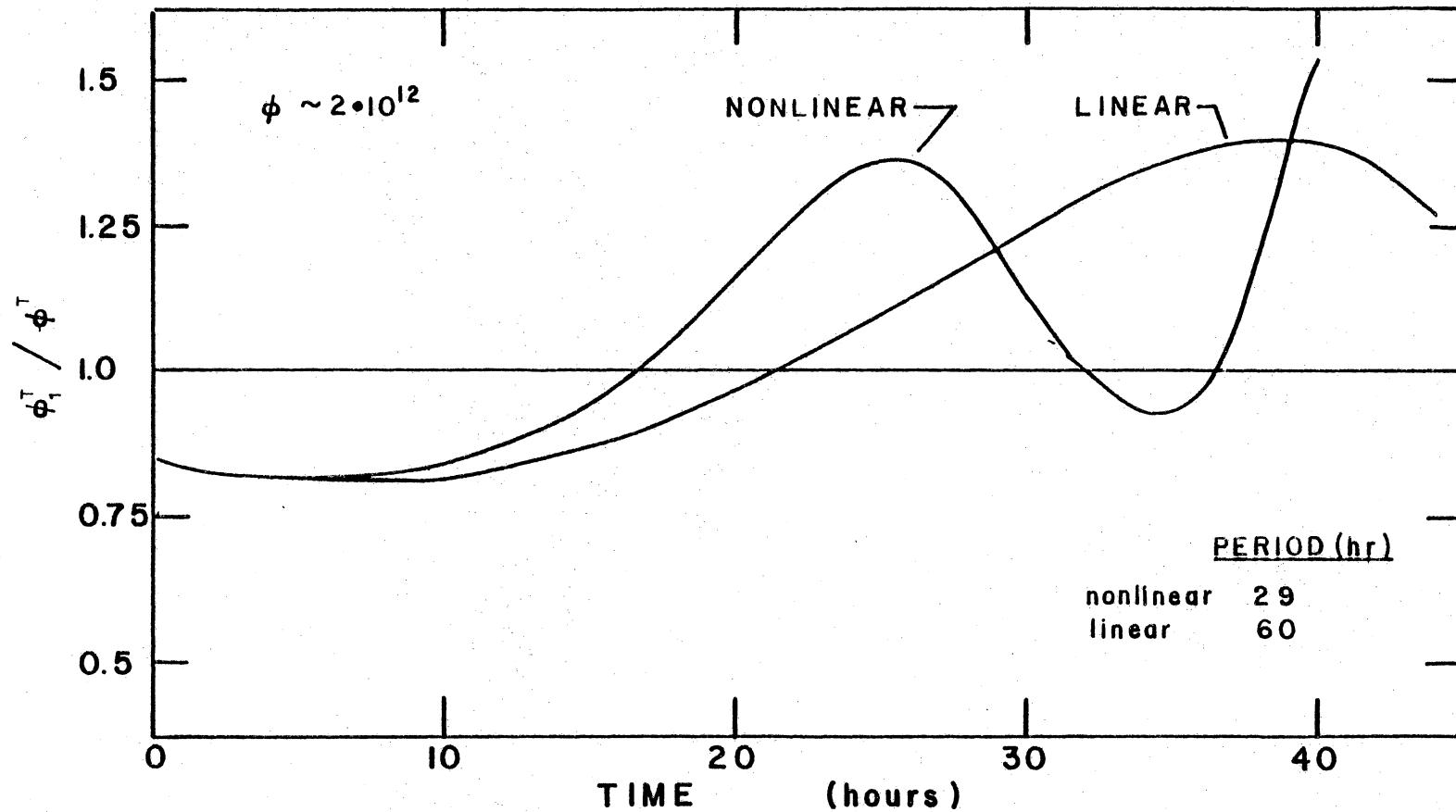


FIGURE 5.5.3 Low Flux Level, Linear & Nonlinear Models
Showing Period Difference

Table 5.5.3 Parameters for Low Flux Level Case

Lower Energy Bound	$1.000 \cdot 10^{-5}$
Chi	1.000
Nu	2.438
Fission Cross Section	0.6400
Absorption Cross Section (without Xe)	1.530
Diffusion Coefficient	0.3950
Microscopic Xenon Cross Section	$2.720 \cdot 10^6$
Fission Yield of Iodine	6.1
Fission Yield of Xenon	0.3

- All energies are in eV.
- All cross sections are macroscopic (cm^{-1}) unless noted otherwise.
- All microscopic cross sections are in barns.
- All diffusion coefficients are in cm.
- All fission yields are in per cent.

Chapter VI

Conclusions - Recommendations

6.1 Overview of Results

The specific cases considered in Chapter Five explored the effects of alternative energy-group structures and changes in the number of profiles used, along with the nonlinearities of the system. The one and three energy group models give substantial differences in results for the 0.25 per cent perturbation in the absorption cross sections. As the size of the perturbation is increased, the results differ even more, with the multigroup model being more accurate.

The effect of the number of profiles is pronounced. If too few profiles are chosen, the system is unable to adequately balance the regional averages along with the leakage of neutrons from the reactor. The minimum number of profiles needed is one higher than the number of regions being considered in the one-dimensional model. The use of additional profiles causes a small increase in the accuracy of the results at the expense of a dramatic increase in computational time.

The effects of the nonlinearities are pronounced for the cases chosen. In the linear evaluations, the flux levels in the reactor begins first to follow the nonlinear results but after a few hours the fluxes start to reduce to zero. The results of the nonlinear model, however, do not go to zero but started to oscillate, going to a limit cycle as shown in Fig. 5.4.3.

From these results it is seen that a multigroup treatment of xenon oscillations is required for accurate results. Also the appropriate number of profiles should be chosen to balance the accuracy requirements against the amount of computational time required.

The use of a linear model will result in invalid results for low flux levels and for inputs that have a large change in flux and xenon concentrations. Even with these restrictions, a simple one-group, linear model is dequate for practical reactor control. Long before any of the differences between the nonlinear and linear models become important, the reactor will have exceeded other operating limits and be shut down. Since the one-group model overpredicts the xenon effect, a margin of safety is inherently included in the calculations. It is only when considering the xenon oscillations problem form the more

theoretical viewpoint than pure reactor control, that the multigroup, nonlinear model is required.

6.2 Associated Problems

The nonlinear property associated with the xenon induced flux oscillation problem is also found in the fuel depletion problem. The major difference in the depletion problem is that the fuel isotopes, rather than the fission products, are changing with time. This results in the addition of a nonlinear fissioning rate. Also, the initial isotopic rates of change are not zero and a different set of initial conditions must be supplied. Such a set would be a "best fit" in the Galerkin sense to the initial spatial fuel concentrations. One final point of consideration is that the time span of the fuel depletion problem is on the order of months rather than hours so short term effects, like temperature feedback, are neglected.

Another area of use for the Galerkin method is in reactor kinetics. Instead of considering isotopic concentrations, delayed neutron concentrations, which form a linear system, are studied. Galerkin's method is valid for linear as well as nonlinear systems of equations. A major problem in reactor kinetics is the rate at which the transients occur.

Typically, times of 10^{-5} seconds are of concern for durations of at least a few seconds, requiring solution of a large number of finite time steps. By expanding Galerkin's method of weighted residuals to include time as part of the inner product, it should be possible to speed solution of the system over that of the conventional finite differencing in both time and space.

6.3 Recommendations

The use of Galerkin's method of weighted residuals makes it possible to solve many of the nonlinear problems associated with nuclear reactor systems. In particular, the xenon-induced flux oscillation problem has been modeled in three dimensions and solved, numerically, in one dimension. The success of the results indicates further research is necessary. Among the areas of interest are three-dimensional effects, sensitivity analysis, and a refinement in the use of different profiles in the various regions of the reactor. By allowing different profiles in the various regions, nonfissioning regions, such as reflectors, can be considered in the model.

This additional work on xenon induced flux oscillations can lead to a better understanding of the problem. This can

result in better prediction methods for controlling nuclear reactors during xenon transients. Better computer models can also be created to study the effects on the reactor with respect to xenon transients during emergency situations leading to a better evaluation of their safety.

References

1. Shotkin, Louis M., "Centers and Limit Cycles in Reactor Kinetics." Neutron Dynamics and Control, CONF-650413, 1966, pp 88-109.
2. Chernick, J., Lellouche, G., and Wollman, W., "The Effect of Temperature on Xenon Instability." Nuclear Science and Engineering: 10, 1961, pp 120-131.
3. Shotkin, Louis M., "Reactor Stability Against Xenon Oscillations." Reactor Kinetics and Control, March 25-27, 1963, University of Arizona
4. Karppinen, J., Versluis, R., and Blonsnes, B., "Core Control Optimization for Scheduled Load Changes in Large Pressurized Water Reactors." Nuclear Science and Engineering: 71, 1979, pp 1-17.
5. Kern, R. C., Coppersmith, W. C., and Rosztoczy, Z. R., "A Three-Dimensional Method for Design Studies of Xenon-Induced Spatial Power Oscillations." Nuclear Applications and Technology, Vol 9, July 1970, pp 70-82.
6. Congdon, M. E., "Space-Dependent Noise with Xenon Feedback." Transactions of the American Nuclear Society.
7. Kaplan, S., and Yasinsky, J., "Natural Modes of the Xenon Problem with Flow Feedback - An Example." Nuclear Science and Engineering: 25, 1966, pp 430-438.
8. Rydin, R. A., "A Critical Evaluation of the Mu-Mode and Lamda-Mode Methods of Evaluating Reactor Stability with Respect to Xenon-Induced Spatial Power Oscillations: Design Implications for the High Temperature Reactor." Derichte der Kernforschungsanlage Julich, Nr. 1272, Feburary 1976, pp 75-88.
9. El-Bassioni, A. A., Impink, A. J., and Poncelet, C. G., "Load Follow Studies of a Power Reactor Subject to Spatial Xenon Oscillations." Proceedings of the Conference on Computational Methods in Nuclear Engineering, Charleston, South Carolina: CONF-750413, April 15-17, 1975, Vol I, pp 67-85.

10. Summary of Report by T. Y. Tsai; File no. Lr:72:2974-01:01
11. Josephson, J., and Geets, J., "A Comparison with Experiment of Xenon Oscillation Stability Calculations Using a Two-Point Kinetics Model." Transactions of the American Nuclear Society, 23, 1976, pp 594-596.
12. Rydin, R. A., "A Lambda-Mode Evaluation of Time Step Corrections in Xenon Oscillation Simulation." Atomkernenergie (ATKE) Bd. 28, 1976, Lfg. 2.
13. Kern, Coppersmith, and Rosztoczy, "Three-Dimensional Method for Design Studies of Xenon-Induced Spatial Oscillations." Transactions of the American Nuclear Society.
14. Lellouche, Gerald S., "Space Dependent Xenon Oscillations." Nuclear Science and Engineering: 12, 1962, pp 482-489.
15. Randall, D., and St. John, D., "Xenon Spatial Oscillations." Nucleonics, 16, no. 3, 1958, pp 82.
16. Tiihonen, Olli, "XISPO - A One Dimensional Computer Code for PWR Xenon Transients." Technical Research Centre of Finland; VTT-YDI-133; UDK 621.0399.56:681.3.06.
17. Asaki, Yoshiro, and Akcasu, A. Ziya, "An Investigation of Nonlinear Xenon Oscillation by Method of Averaging." Journal of Nuclear Energy, Vol 27, pp 839-855.
18. Jorge, H. M., Long, R. L., and Purohit, S. N., "Axial Power Shaping in Large Pressurized Water Reactors." Second Power Plant Dynamics, Control and Testing Symposium, Knoxville, Tennessee: September 3-5, 1975.
19. Chernick, J., "The Dynamics of a Xenon Controlled Reactor." Nuclear Science and Engineering: 8, 1960, pp 233-243.
20. Canosa, J., and Brooks, H., "Xenon-Induced Oscillations." Nuclear Science and Engineering: 26, 1966, pp 237-253.

21. Graves, W. E., "Experience with Xenon Oscillations." Nuclear Applications and Technology: Vol 9, November 1970, pp 651-661.
22. "XISPO - A One Dimensional Computer Code for PWR Xenon Transients." Technical Research Centre of Finland; June 1974.
23. Akhtar, P., and Trojan, O. A., "Xenon-Induced Power Oscillations in CANDU." Transactions of the American Nuclear Society: 23, 1976, pp 596.
24. Omega, R. J., and Kisner, R. A., "Parameter Identification for Spatial Xenon Transient Analysis and Control." Annals of Nuclear Energy: Vol 6, 1979, pp 369-374.
25. Omega, R. J., and Kisner, R. A., "An Axial Xenon Oscillation Model." Annals of Nuclear Energy: Vol 5, 1978, pp 13-19.
26. Kisner, R., A Two-Point Variational Model for the Reactor Core Subject to Xenon-Induced Flux Oscillations. Blacksburg, VA: Master Thesis, Virginia Polytechnic Institute and State University, 1976.
27. Mastroianni Jr., V., Parameter Optimization fo the Nonlinear and Linear Xenon Oscillation Models. Blacksburg, VA: Master Thesis, Virginia Polytechnic Institute and State University, 1979.
28. Personal Correspondence with Dr. R. J. Omega, Professor of Mechanical Engineering, Virginia Polytechnic Institute and State University, Blacksburg, VA.
29. Omega, Ronald J., An Introduction to Fission Reactor Theory. Blacksburg, VA: University Publications, 1975.
30. Goldberg, Mughabghab, Magurno, and May, Neutron Cross Sections. Brookhaven National Laboratory, BNL 325 (Physics - TID-4500), 1966
31. Chart of the Nuclides; General Electric Company, 1977.
32. Hetrick, D., Dynamics of Nuclear Reactors. Chicago: University of Chicago Press, 1971.

33. Reactor Theory and Power Reactors. Trieste: International Center for Theoretical Physics, IAEA-SMR-44, 1980.
34. Strieder, W., and Aris, R., Variational Methods Applied to Problems of Diffusion and Reaction. New York: Springer-Verlag, 1970.
35. Lewins, Jeffery, Importance, The Adjoint Function. Oxford: Pergamon Press Ltd., 1965.
36. Becker, Martin, The Principles and Applications of Variational Methods. Cambridge, Massachusetts: MIT Press, Research Monograph No. 27, 1964.
37. Stacey, Jr., Weston M., "Variational Methods in Nuclear Reactor Physics." Nuclear Science and Technology, vol 10, 1974.
38. Schechter, R. S., The Variational Method in Engineering. New York: McGraw-Hill Book Company, Chemical Engineering Series, 1967.
39. Ketter, R. L., and Prawel, Jr., S. P., Modern Methods of Engineering Computation. New York: McGraw-Hill Book Company, 1969.
40. Nakamura, Shoichiro, Computational Methods in Engineering and Science (with Applications to Fluid Dynamics and Nuclear Systems). New York: John Wiley and Sons, Inc., 1977, pp 207-237
41. Stacey, Jr., Weston M., Variational Methods in Nuclear Reactor Physics. New York: Academic Press, Nuclear Science and Technology Series, 1974
42. Adams, C. H. "Current Trends in Methods for Neutron Diffusion Calculations." Nuclear Science and Engineering: 64, 1977, pp 552-562
43. Ober, T. G., Stork, J. C., Rickard, I. C., and Gasper, J. K., "Theory, Capabilities and use of the Three-Dimensional Reactor Operation and Control Simulator (ROCS)." Nuclear Science and Engineering: 64, 1977, pp 605-623.

44. Nelson, Paul, and Meyer, Harold, "Convergence Results and Asymptotic Error Estimates for Galerkin-Type Spectral Synthesis." Nuclear Science and Engineering: 64, 1977, pp 638-643.
45. Rydin, Roger A., Nuclear Reactor Theory and Design. Blacksburg, VA: University Publications, 1977.
46. Lamarsh, John R., Introduction to Nuclear Reactor Theory. Reading, Massachusetts: Addison-Wesley Publishing Company, Inc., 1972.
47. Ash, Milton, Nuclear Reactor Kinetics. New York: McGraw-Hill Inc., 1979.
48. Meghreblian, R., and Holmes, D., Reactor Analysis. New York: McGraw-Hill Inc., 1960.
49. Henry, Allan, Nuclear-Reactor Analysis. Cambridge, Massachusetts: The MIT Press, 1975.
50. Duderstadt, J., and Hamilton, L., Nuclear Reactor Analysis. New York: John Wiley & Sons, Inc., 1976.
51. Raymond, William J., Pressurized Water Reactor Startup Testing. Blacksburg, VA: Master Thesis, Virginia Polytechnic Institute and State University, 1975.
52. Pressurized Water Reactor Technology (volume 1). Lynchburg, VA: Babcock & Wilcox (TRG-72-77), 1972.
53. Glasstone, S., and Sesonske, A., Nuclear Reactor Engineering. New York: Van Nostrand Reinhold Company, 1967.
54. Bell, G., and Glasstone, S., Nuclear Reactor Theory. New York: Van Nostrand Reinhold Company, 1970.
55. Stacey, Jr., W., Space-Time Nuclear Reactor Kinetics. New York: Academic Press, 1969.
56. Conte, S., and de Boor, C., Elementary Numerical Analysis. New York: McGraw-Hill Inc., 1965.

Appendix A

Quantities Requiring the Adjoint Flux

A.1 Perturbation Theory and Reactor Kinetics

A major use of the adjoint flux is in perturbation theory and reactor kinetics. Perturbation theory deals with the effects induced by a local change in the material properties of the reactor system. Examples of how such changes can be induced are by control rod movement and addition of a soluble poison to the coolant system. Often perturbation theory is applied to the reactor kinetics equations. Reactor kinetics consider the effects of the delayed neutrons by the inclusion of the time-dependent precursor balance equations.

The spatial flux shape changes are negligible during a transient when the reactor is sufficiently small so that it is well-coupled. Then, the reactor can be treated as a point having certain weighted average properties. The point reactor kinetics equations can be written as

$$\frac{dn}{dt} = \frac{\rho - \beta}{\Lambda} n + \sum_i \lambda_i c_i + q \quad (\text{A.1.1})$$

1. Based entirely on Nuclear Reactor Theory and Design by Roger Ryden[48]

and

$$\frac{dc_i}{dt} = \frac{\beta_{in}}{\Lambda} - \lambda_i c_i \quad ; i = 1, 2, \dots, 6 \quad . \quad (\text{A.1.2})$$

where

$$\underline{\Phi} = [\phi_1 \quad \phi_2 \quad \dots \quad \phi_G] \quad , \quad (\text{A.1.3})$$

$$\underline{F} = [\nu_1 \Sigma_1^f \quad \nu_2 \Sigma_2^f \quad \dots \quad \nu_G \Sigma_G^f] \quad , \quad (\text{A.1.4})$$

$$\underline{\chi}_p = [\chi_{p_1} \quad \chi_{p_2} \quad \dots \quad \chi_{p_G}] \quad , \quad (\text{A.1.5})$$

$$\underline{\chi}_i = [\chi_{i_1} \quad \chi_{i_2} \quad \dots \quad \chi_{i_G}] \quad , \quad (\text{A.1.6})$$

$$[\text{T}] = \text{dia} [1/\nu_1 \quad 1/\nu_2 \quad \dots \quad 1/\nu_G] \quad , \quad (\text{A.1.7})$$

and

$$[\text{L}] = [\text{R}] - [\text{N}] \quad . \quad (\text{A.1.8})$$

The matrices $[\text{P}]$, $[\text{R}]$, and $[\text{N}]$ are as defined in Chapter Two. The actual quantities used in Eqs. A.1.1 and A.1.2 are given in the the next section.

A.2 Adjoint Weighted Point Kinetics Quantities

Equations A.1.1 and A.1.2 are obtained by making the following definitions.

1. Effective Neutron Density. The neutrons in a reactor have different importance depending on their location. Weighting them to get the same importance that they have in the actual situation results in the effective neutron density and is given by

$$n(t) = \langle \Phi_0^\dagger, [T] \Phi \rangle = \left[\begin{array}{l} \text{weighted neutron} \\ \text{population in} \\ \text{the core} \end{array} \right] \quad (\text{A.2.1})$$

2. Effective Precursor Concentration. Like the neutrons, the importance of the delayed neutron precursors depends on their locations. Weighting them to get the same importance that they have in the actual reactor results in the effective precursor concentration and is given by

$$c_i(t) = \langle \Phi_0^\dagger, \chi c_i \rangle \quad (\text{A.2.2})$$

3. Effective Source. A source, Q , in a reactor has its effectiveness altered by its spatial distribution. To obtain the effective source for the situation, the actual

source is weighted resulting in

$$q = \langle \underline{\Phi}_0^\dagger, \underline{Q} \rangle \quad (A.2.3)$$

4. Lifetime. The lifetime is the weighted integral time that the average neutron lives before being captured or being leaked from the core. In words, it is

$$[\text{Lifetime}] = \frac{\text{Mean free path for loss}}{\text{Average velocity of neutron}}$$

The perturbation theory equivalent is to adjoint weight the $1/v$ factors in the numerators and the $[L]$ in the denominator to obtain

$$l = \frac{\langle \underline{\Phi}_0^\dagger, [T] \underline{\Phi}_0 \rangle}{\langle \underline{\Phi}_0^\dagger, [L] \underline{\Phi}_0 \rangle} \quad (A.2.4)$$

5. Generation Time. The generation time is the weighted integral time until a neutron is produced. In words, it is

$$[\text{Generation time}] = \frac{\text{Mean free path for production}}{\text{Average velocity of neutron}}$$

The perturbation theory equivalent is

$$\Lambda = \frac{\langle \underline{\Phi}_0^\dagger, [T] \underline{\Phi}_0 \rangle}{\langle \underline{\Phi}_0^\dagger, [P] \underline{\Phi}_0 \rangle} \quad (A.2.5)$$

6. Effective Delayed Neutron Fraction. Delayed neutrons are born as a physical fraction of the total neutron production, but are more important than fission neutrons because they are born at a lower energy. Weighting them to get the same importance that they have in the actual situation, the resulting equation, in words is

$$\bar{\beta}_i = \beta_i \frac{[\text{Weighted production rate of group } i \text{ delayed neutrons}]}{\text{Total weighted production rate}}$$

The perturbation theory equivalent is

$$\bar{\beta}_i = \beta_i \frac{\langle \Phi_0^\dagger, \chi_i \underline{F} \Phi_0 \rangle}{\langle \Phi_0^\dagger, \chi_p \underline{F} \Phi_0 \rangle} \quad (\text{A.2.6})$$

7. Reactivity. The reactivity is the change in the effective multiplication factor for a change in the production and loss terms of an amount [P] and [L]. The reactivity, in words, is

$$\text{Reactivity} = \frac{\left[\begin{array}{c} \text{Weighted total} \\ \text{production} \\ \text{rate change} \end{array} \right] \left[\begin{array}{c} \text{Weighted total} \\ \text{loss rate} \\ \text{change} \end{array} \right]}{\text{Weighted total production rate}}$$

The perturbation theory equivalent is

$$\rho = \frac{\langle \Phi_0^\dagger, (\delta[P]/k_0 - \delta[L]) \Phi_0 \rangle}{\langle \Phi_0^\dagger, [P]/k_0 \Phi_0 \rangle} \quad (\text{A.2.7})$$

The use of the adjoint flux as the weighting factor in perturbation theory assigns the correct importance to the various quantities.

Appendix B

Basis Function Expansions

B.1 The Linear System of Equations

Using the polynomial form of the basis functions --

$$\eta_n^p(z) = c_n^p(z) + b_n^p(z) (z/L) - (z/L)^{p+1} \quad (\text{B.1.1})$$

-- it is possible to form a linear system of equations in order to find the coefficients b_n^p and c_n^p . Applying the interface conditions to each profile,

$$0 = c_n^p(h_i^-) - c_n^p(h_i^+) + (b_n^p(h_i^-) - b_n^p(h_i^+)) (h_i/L) \quad (\text{B.1.2})$$

and

$$\begin{aligned} 0 = & D_n(h_i^-) c_n^p(h_i^-) - D_n(h_i^+) c_n^p(h_i^+) \\ & + (D_n(h_i^-) b_n^p(h_i^-) - D_n(h_i^+) b_n^p(h_i^+)) (h_i/L) \\ & - (D_n(h_i^-) - D_n(h_i^+)) (h_i/L)^{p+1} \end{aligned} \quad (\text{B.1.3})$$

The additional constraint imposed by the boundary conditions are written as

$$0 = c(0) \quad (\text{B.1.4})$$

and

$$0 = c_n^p(L) + b_n^p(L) - 1 \quad (\text{B.1.5})$$

Rewriting these equations in matrix form,

$$[M] \underline{X} = \underline{R} \quad (B.1.6)$$

where the group and profile are implied and where

$$[M] = \begin{bmatrix} 1 & 0 & 0 & 0 & \dots & 0 & 0 \\ 1 & (h_1/L) & -1 & -(h_1/L) & \dots & 0 & 0 \\ 1 & D(h_1^-) & 0 & D(h_1^+) & \dots & 0 & 0 \\ \cdot & \cdot & \cdot & \cdot & & \cdot & \cdot \\ \cdot & \cdot & \cdot & \cdot & & \cdot & \cdot \\ \cdot & \cdot & \cdot & \cdot & & \cdot & \cdot \\ 0 & 0 & 0 & 0 & \dots & 0 & D(L^-) \\ 0 & 0 & 0 & 0 & \dots & 1 & 1 \end{bmatrix} \quad (B.1.7)$$

$$\underline{X} = [\begin{matrix} b(h_1^-) & c(h_1^-) & b(h_2^-) & c(h_2^-) \\ & & \dots & b(L^-) & c(L^-) \end{matrix}]^T \quad (B.1.8)$$

$$\underline{R} = [\begin{matrix} 0 & 0 & s(1) & 0 & s(2) \\ & & \dots & 0 & s(R) & 1 \end{matrix}]^T \quad (B.1.9)$$

and

$$s(n) = (p+2) (D(h_n^-) - D(h_n^+)) (h/L)^{p+1} \quad (B.1.10)$$

Gaussian elimination can be performed on Eq. B.1.6 to obtain the required b's and c's for each profile. Thus, for a problem with G energy groups, E isotopes (N=2 for the

xenon problem), and P profiles for each group or isotopes, $(G+E) * P$ sets of simultaneous linear equations must be solved for the complete set of b 's and c 's.

Appendix C

Logic Flow Charts for XORA

C.1 Logic Flow Charts

This appendix contains the logic flow charts for the XORA program. Figure C.1.1 shows the logic flow for the INPUT section. Figure C.1.2 shows the logic flow for the INITIALIZATION section. Figures C.1.3 and C.1.4 shows the logic flow for the DIRECT and ADJOINT sections respectively. Finally, figure C.1.5 is the logic flow for the PERTURB logic section.

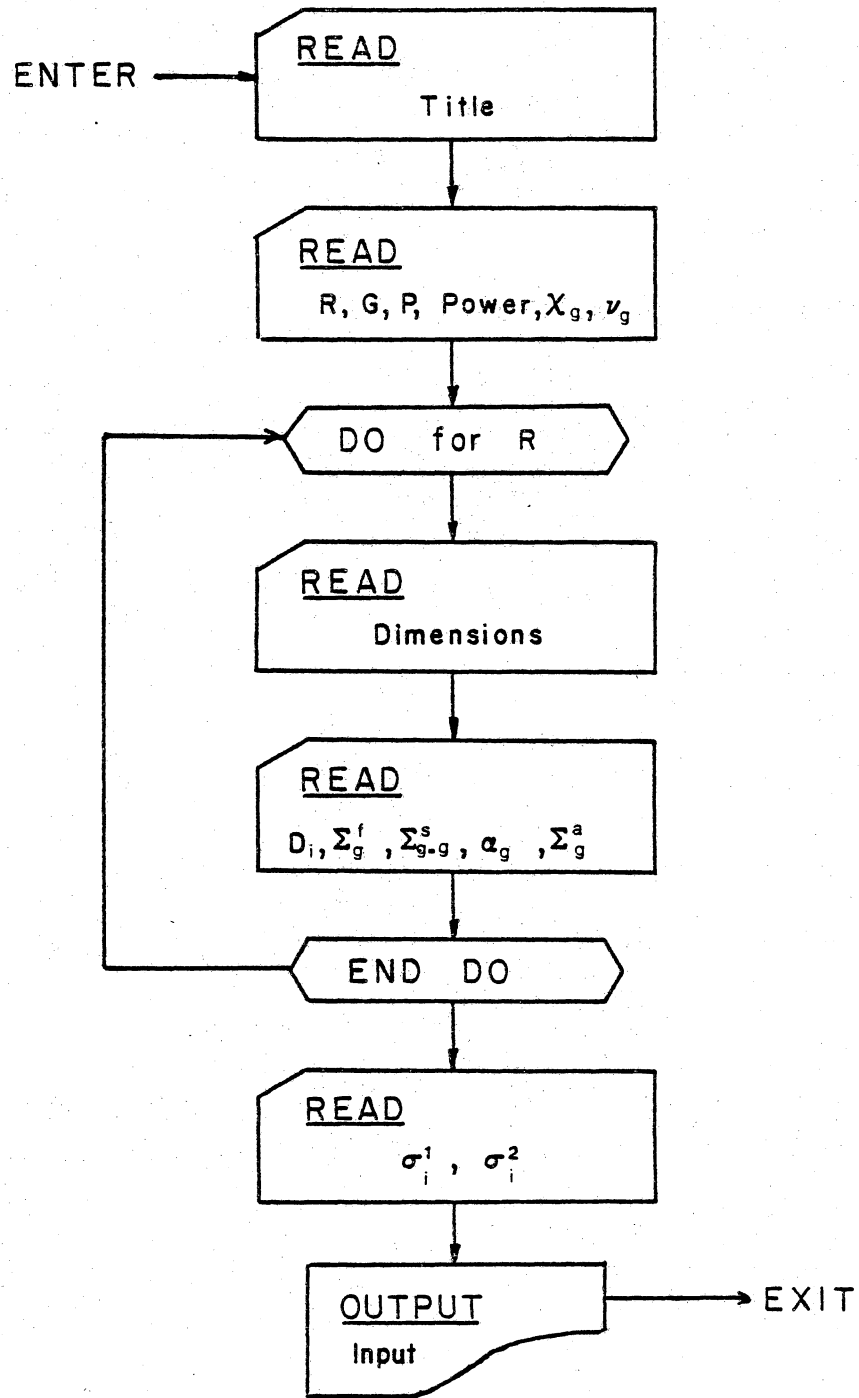


FIGURE C.I.I INPUT Logic Flow Section

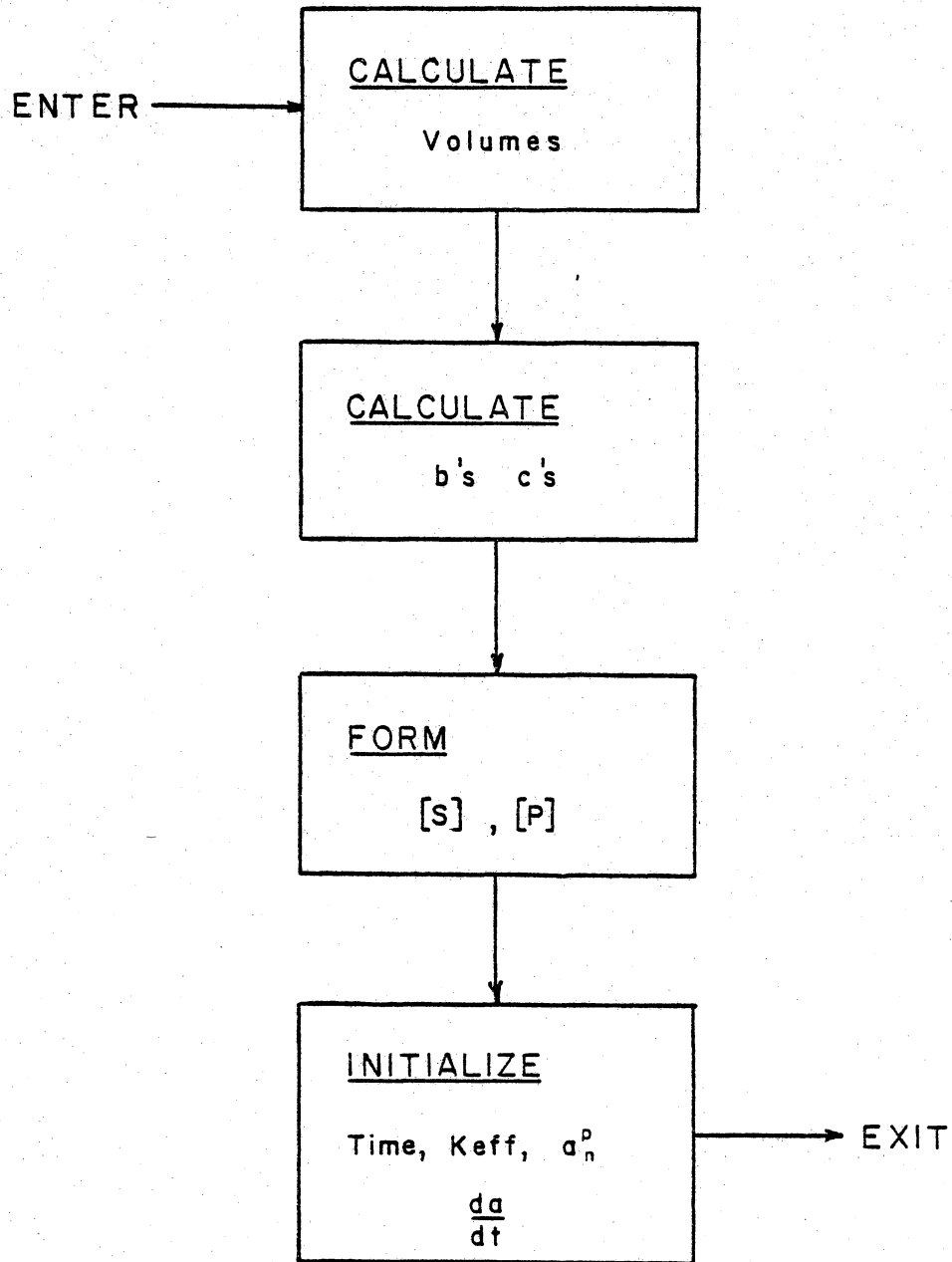


FIGURE C.1.2 INITIALIZATION Logic Flow Section

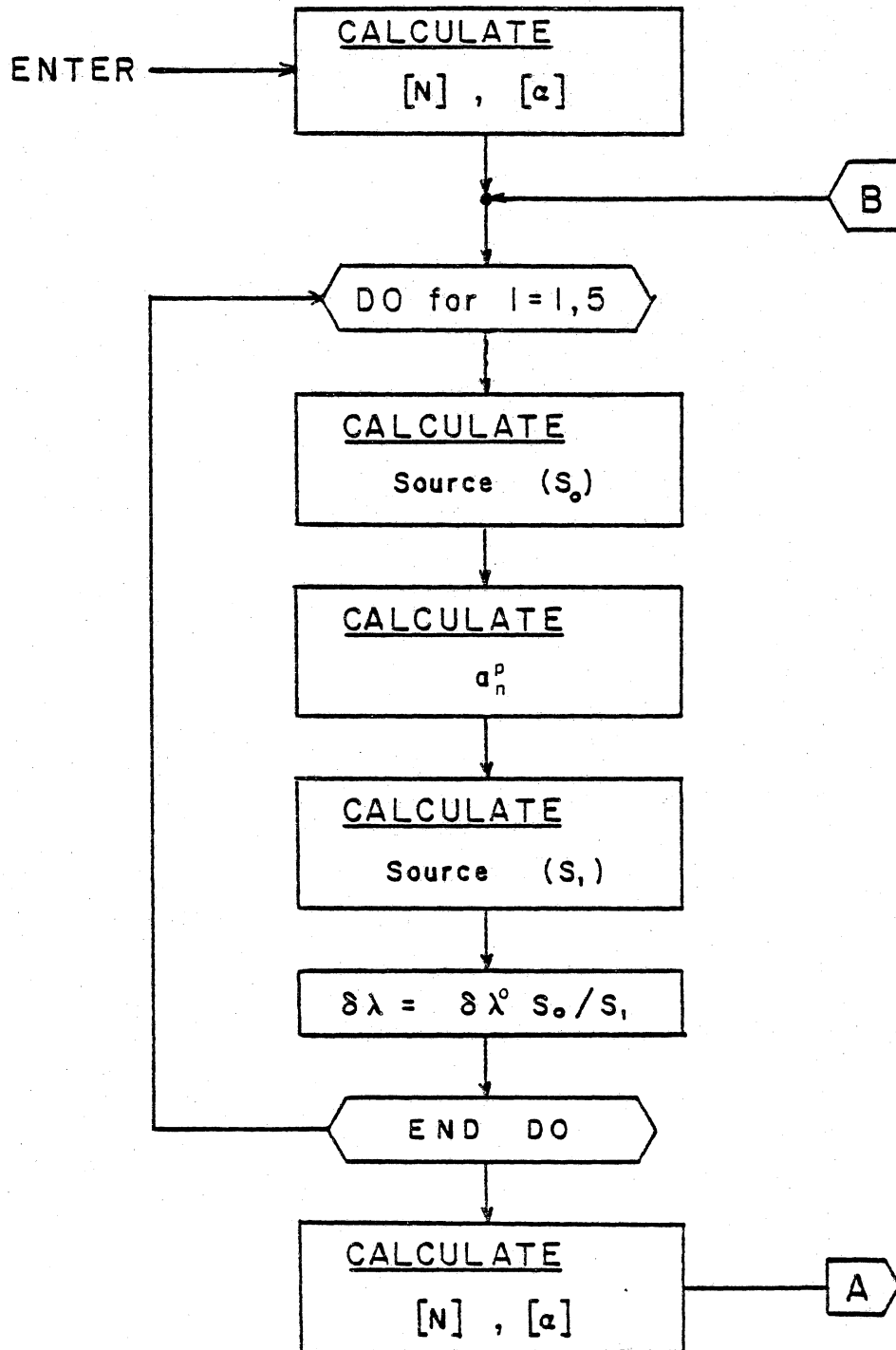


FIGURE C.1.3 DIRECT Logic Flow Section

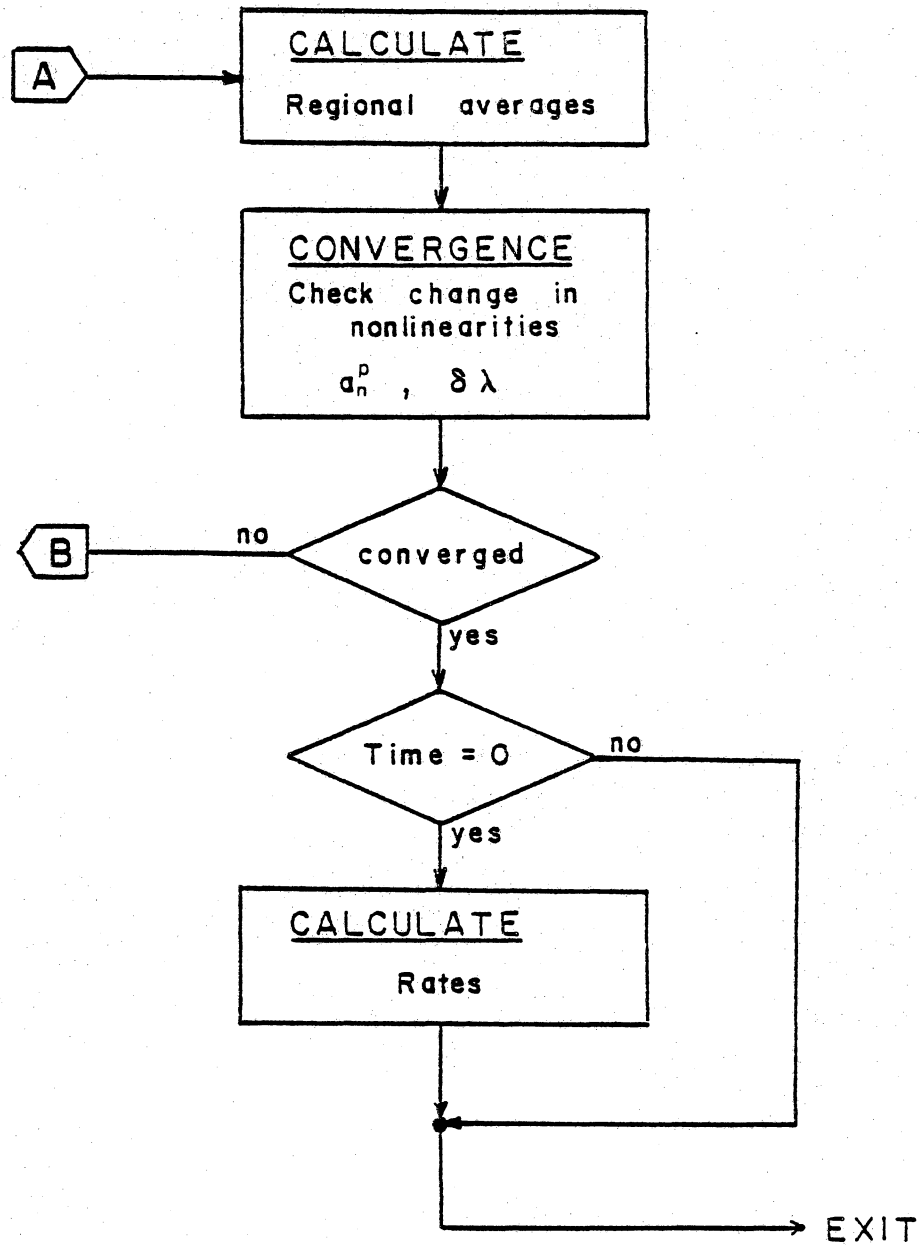


FIGURE C.1.3 DIRECT Logic Flow Section
(con't)

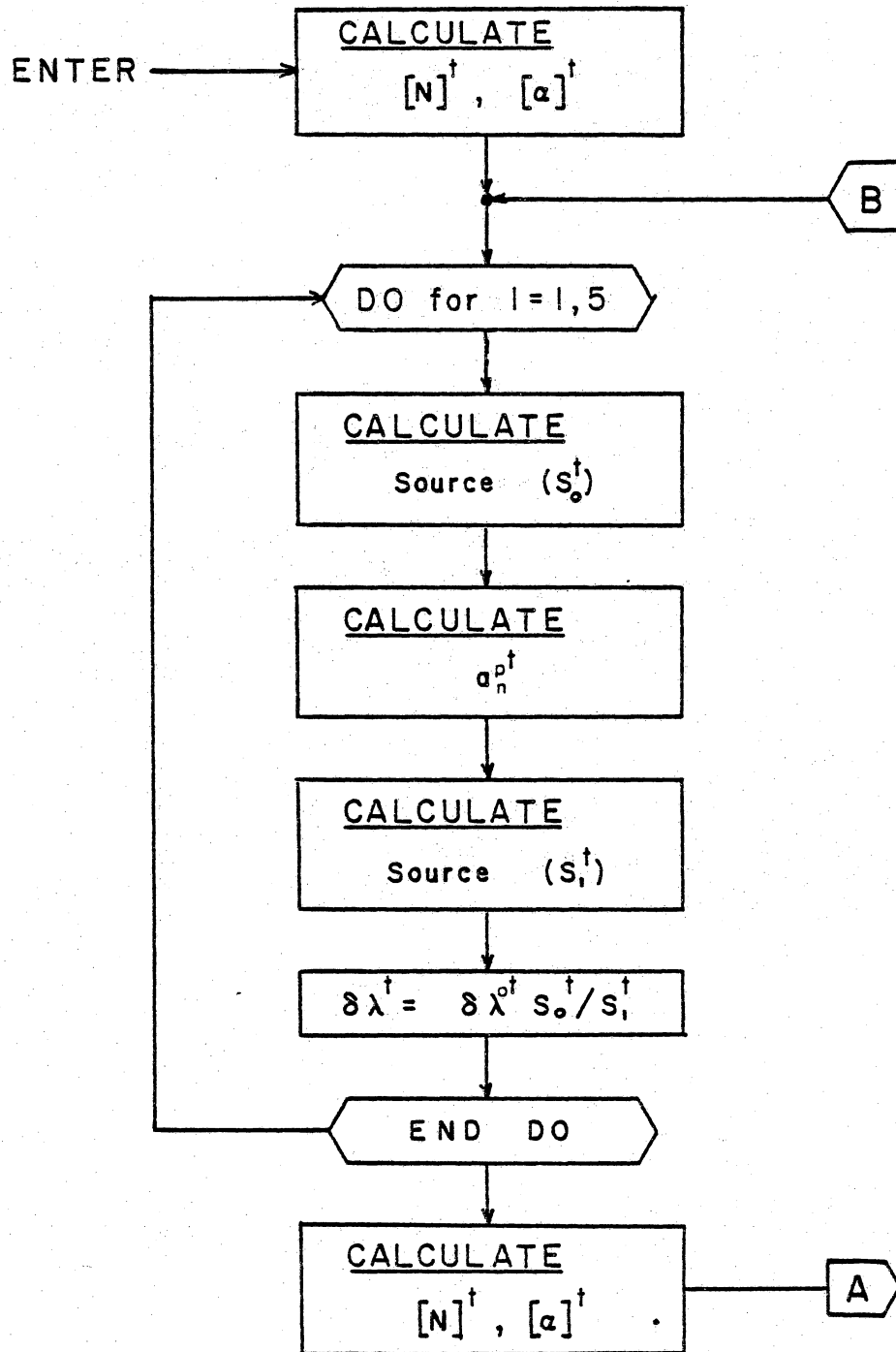


FIGURE C.1.4 ADJOINT Logic Flow Section

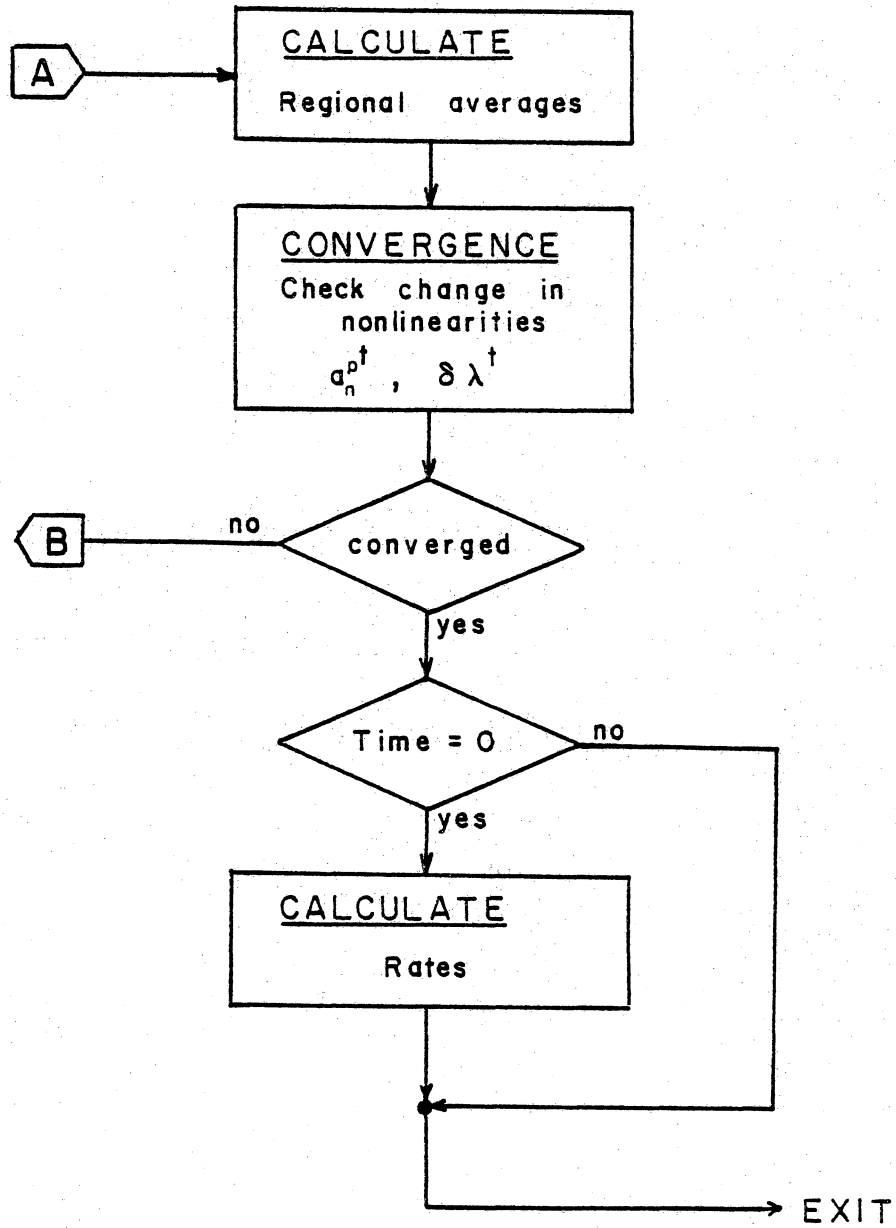


FIGURE C.1.4 ADJOINT Logic Flow Section
(con't)

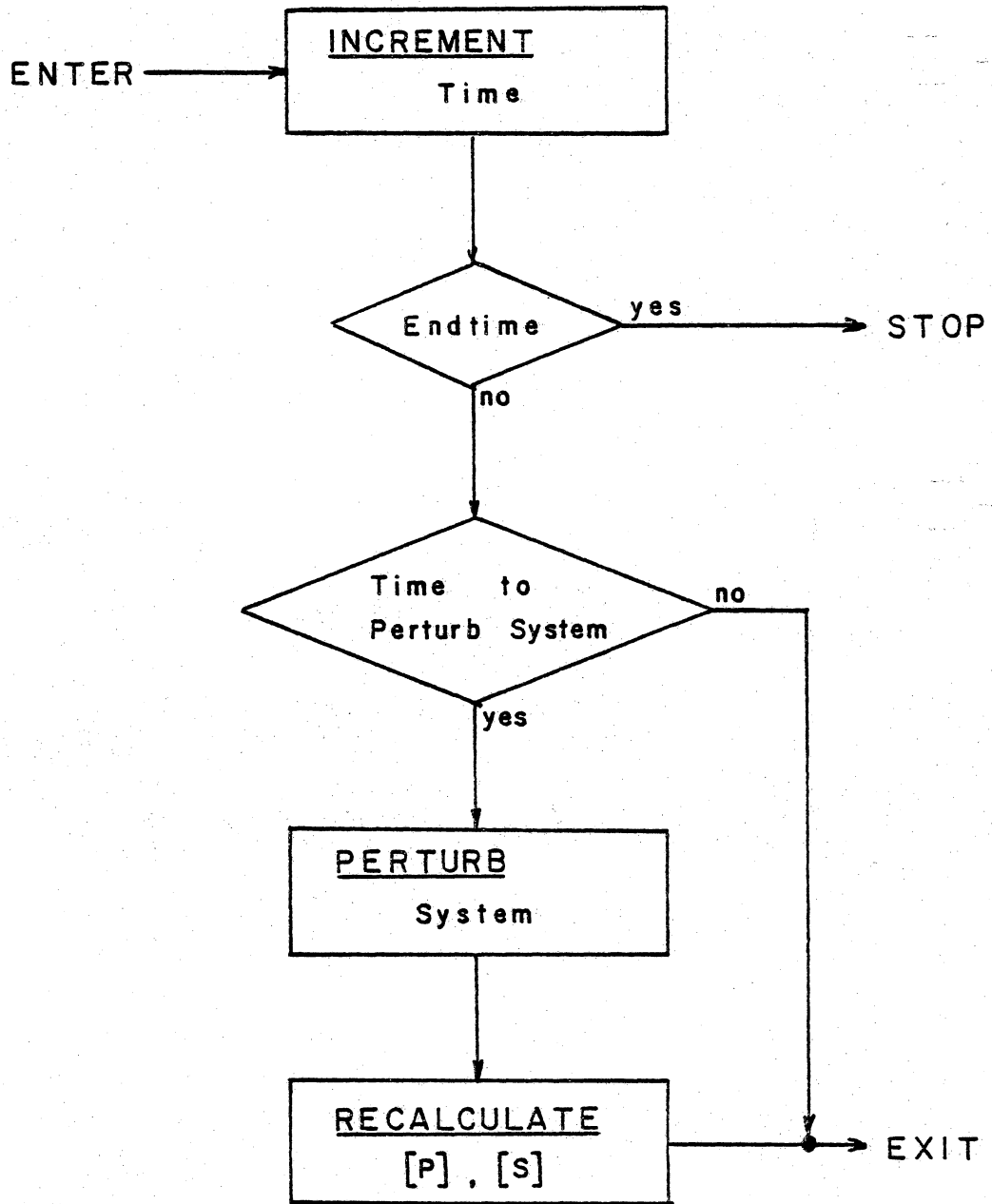


FIGURE C.1.5 PERTURB Logic Section

Appendix D

Sample Input to XORA

D.1 Three-Group Sample Input for Case N3G2R3PC

The input data set for N3G2R3PC is given below. All lines preceded with an "*" are editorial comment cards and should NOT be included in the input deck.

* front page title cards are first, with a ,END ending them.

N3G2R3PC - NONLINEAR, 3 GROUP, 2 REGION, 3 PROFILE
DATASET C

* 0 = not terminal input, 0 = nonlinear

0 0

* 2 region, 3 group

2 3

* 1 radial, 3 axial, 1 azimuthal profiles

* (only the axial is present in the 1-D model)

1 3 1

* power level, then chi for each group

2568.0

1.0 0.0 0.0

* nu for each group

2.67264 2.68253 2.56496

* region 1 input. First dimensions, radial, axial, azimuthal

0.0 163.5 0.0 183.0 0.0 360.0

* by groups, first Diffusion coefficient, sigma-fission,

* sigma absorption, temperature coefficient of reactivity

1.087601 .6692375 .4327365

9.2156562E-3 6.93907E-2 .1280889

2.0027E-3 3.2022E-2 6.9467E-2

0.0 0.0 0.0

* this is the scattering matrix. The last two rows

* contain gammas and decay constants

0.0 0.0 0.0 0.0 0.0

1.675306E-2 0.0 0.0 0.0 0.0

0.0 .10191339 0.0 0.0 0.0

0.061 0.061 0.061 -2.87E-5 0.0

0.003 0.003 0.003 2.87E-5 -2.09E-5

* region 2 input, like region 1

0.0 163.5 183.0 366.0 0.0 360.0

1.087601 .6692375 .4327365

9.2156562E-3 6.93907E-2 .1280889

2.0027E-3 3.2022E-2 6.9467E-2

0.0 0.0 0.0

0.0 0.0 0.0 0.0 0.0

1.675306E-2 0.0 0.0 0.0 0.0

0.0 .10191339 0.0 0.0 0.0

0.061 0.061 0.061 -2.87E-5 0.0

0.003 0.003 0.003 2.87E-5 -2.09E-5

* for each isotope, the group cross sections

0.0 0.0 0.0

0.0 4.4309E-19 2.4826E-18

Appendix E
Partial XORA Listing

E.1 Source Code for XORA

This appendix contains a partial listing of the XORA code. Utility routines, such as Gaussian elimination and Newton-Raphson iteration, have been excluded for brevity.

SUBROUTINE XORA

XORA - CONTROLING PROGRAM

MAIN

THIS IS THE DRIVER PROGRAM FOR THE XORA CODE
THIS PROGRAM DICTATES THE CALLING OF THE MAJOR
SECTIONS AND HELPS SET UP SOME SPECIAL PARAMETERS
LIKE THE MAXIMUM SIZES ALLOWS FOR NUMBER OF
REGIONS, GROUPS, ETC.

IMPLICIT INTEGER (I,N,\$), REAL(A-H,J-M,O-Z)

COMMON /ANS / COEFF(7,20),KEFF
COMMON /CONSAT/ NPOWK
COMMON /WHICH / DIRNUT, NADJ
COMMON /ANP2 / NREG, NGRP, NELE, NPRO, NEQU, NTOT
COMMON /TCTIM / TTIME, DELTI
COMMON /AIOT / NR, NW1, NW2, NW3
COMMON /EMSGC / NWE, IER
COMMON /WRKIN / WORK2(5000)
COMMON /ALINSR/ NLINER
COMMON /PERTS / IPERT

CALL ERRSET(207,256,-1,1)
CALL XVAL
CALL OUTS

NR = 1
NPOWK = 0
NW2 = 2
NWE = 3
NW3 = 4
NW1 = 3

CALL TOP

KEFF = 2.0

REGIONS
\$MAX1 = 10
GROUPS
\$MAX2 = 5

```
C      ELEMENTS
C      $MAX3 = 2
C      NUMBER EQUATIONS
C      $MAX4 = 7
C      NUMBER PROFILES TOTAL
C      $MAX5 = 20
C      NUMBER COEFFS. TOTAL
C      $MAX6 = $MAX4 * $MAX5
C
C      CALL THE INPUTING ROUTINE TO GET THE MAJOR DATA
C
C      CALL SINP
C
C      IPERT = 0
C      IKEPTS = NLINER
C      NLINER = 0
C
C      NOW, FORM SIGOUT AND CNSFIS WHICH CONTAINS THE
C      MAJOR LINEAR FACTORS
C
C      CALL SMAT
C
C      LETS OUTPUT THE INPUT INFORMATION SO THAT WE
C      KNOW WHAT THE DARN RUN IS ALL ABOUT.
C
C      CALL OUT1
C
C      IT IS NOW NECESSARY TO SPLIT SOME WORK SPACE UP SO
C      THAT WE CAN PREFORM PRELIMINARY INTEGRAL WORK IN .....
C
C      NR22 = NREG * 2
C      NNN = NR22 * NR22 + 1
C      N4 = NNN + NR22
C
C      ..... AINTGL
C
C      A = AINTGL(NR22,WORK2(1),WORK2(NNN),WORK2(N4))
C
C      NOW LETS JUST OUTPUT THE REGIONAL VOLUMES CAUSES
C      THEY HAVE BEEN CALCULATED AND IT MIGHT BE OF USE
C      TO WHOM, I DON'T KNOW.
C
C      CALL OUT3(1)
C
C      NOW WE MUST BEGIN THE MAJOR WORK OF CALLING THE DIRECT
C      SYSTEM (AND EQUILIBRIUM ADJOINT SYSTEM) ALONG WITH THE
C      PERTURBATION ROUTINE IN ORDER TO GET ANY SORT OF
C      USEFUL (DEBATABLE) INFORMATION OUT.
```

```

C
C FIRST, SET THE TIME TO ZERO SO THAT WE KNOW THE
C EQUILIBRIUM CONDITIONS MUST FIRST BE CALCULATED.
C
  TTIME = 0.0
  DELTI = 0.0
  IKEEP = 0
C
C BEGINNING OF THE LOOP.....
C
100 CONTINUE
  IF ( IPERT .EQ. 1 ) NLINER = IKEEP
  IF ( IKEEP .NE. 0 ) GOTO 210
  IF ( NLINER .NE. 1 ) GOTO 210
  IF ( TTIME .LT. 1.E-20 ) GOTO 210
  IKEEP = IKEEP + 1
  NPOWK = 1
  A = STOLIN(5)
210 CONTINUE
C
C FIRST WE CALCULATE THE DIRECT SYSTEM.
C
  NADJ = 0
  CALL DIRREC($MAX1,$MAX2,$MAX3,$MAX4,$MAX5,$MAX6)
C
C IF THIS IS AT TIME ZERO, STOR THE EQUILIBRIUM
C COEFFICIENTS
C
  IF ( TTIME .LE. 1.E-20) A1 = STOLIN(1)
C
C IER WILL NOW BE ZERO ONLY IF THE DIRECT SYTEM
C CONVERGED. IF IT DIDN'T LETS GET OUT OF THE BLASTED
C PROGRAM
C
  IF ( IER .NE. 0 ) GOTO 999
C
C IF TTIME IS LESS THAN 1.E-18 (I.E. ZERO), CALCULATE
C THE ADJOINT SYSTEM.
C
  IF ( TTIME .GT. 1.E-20 ) GOTO 1300
C
  WRITE(6,3364)
3364 FORMAT(//' DIRECT SYSTEM COEFFICIENTS'//)
  DO 3365 IG = 1,NEQU
  WRITE(6,*) (COEFF(IG,IP),IP=1,NPRO)
3365 CONTINUE
C
  NADJ = 1

```

```
      CALL DIRREC($MAX1,$MAX2,$MAX3,$MAX4,$MAX5,$MAX6)
C
      WRITE(6,11732)
11732  FORMAT(///' ADJOINT SYTEM COEFFICEINTS'///)
      DO 11733 IG = 1, NEQU
      WRITE(6,*) (COEFF(IG,IP),IP=1,NPRO)
11733  CONTINUE
C
C      GET DIRECT SYSTEM BACK
C
      A1 = STOLIN(3)
1300  CONTINUE
C
C      NOW LETS PERTURB THE SYSTEM BY CALLIN THE
C      USER SUPPLIED ROUTINE PERT.
C
      CALL PERT(IK)
C
C      THE ARGUMENT OF PERT SHOULD BE SET TO 1 TO CONTINUE
C      THE CALCULATIONS OR 2 TO END THEM
C
      GOTO (100,110), IK
110  CONTINUE
C
C-----
C-----
999  CONTINUE
      CALL TOP
      RETURN
      END
```

FUNCTION AINTGL(NREG2, JACK, RES, IWK)

 THIS FUNCTION COMPUTES THE "V" AND "W" CONSTANTS
 FOR THE 1-D POLYNOMIAL EXPANSIONS

ENTRY POINTS ALSO INCLUDED ARE:

SIINT	-	SINGLE INTEGRAL
DOINT	-	DOUBLE INTEGRAL
TRINT	-	TRIPLE INTEGRAL
DEINT	-	DELSQUARE INTEGRAL

NREG2 = 2 *NREG
 JACK IS A WORK ARRAY OF 2 X NREG2
 RES IS A WORK ARRAY OF NREG2
 IWK IS A WORK ARRAY OF NREG2

 IMPLICIT REAL(A-H, J-M, O-Z), INTEGER(I, N, \$)

DATA CONST /1.0/
 COMMON /POLY\$ / THEVS(10,7,20), THEWS(10,7,20),
 & THEBS(10,140)
 COMMON /MVAL / MAXRAD, MAXAXI, MAXAZM
 COMMON /ANP2 / NREG, NGRP, NELE, NPRO, NEQU, NTOT
 COMMON /ANP3 / SIGABS(10,5), ALPHA(10,5),
 & DIFFUS(10,5), SIGELE(2,5),
 & ANU(5), CHI(5), SIGSCT(10,7,7)
 COMMON /BOUD / RIN(10), ROUT(10), AXTP(10),
 & AXBT(10), AZSD(10), AZED(10), VOL(10)
 COMMON /PRFS / NRAD, NAXI, NAZM
 COMMON /EMSGC / NWE, IER

DIMENSION JACK(NREG2, NREG2), RES(NREG2), IWK(NREG2)

CONST = 3.14159 * ROUT(1)**2
 CALCULATE VOLUMES

MAXRAD = 0.0
 MAXAXI = 0.0
 MAXAZM = 0.0
 VOLUME = 0.0

DO 500 IR = 1, NREG
 IF (MAXRAD .LT. ROUT(IR)) MAXRAD = ROUT(IR)

```

IF ( MAXAXI .LT. AXTP(IR) ) MAXAXI = AXTP(IR)
IF ( MAXAZM .LT. AZED(IR) ) MAXAZM = AZED(IR)

```

C

```

VOL(IR) = ( ROUT(IR) ** 2 - RIN(IR) ** 2 )
& * (AXTP(IR)-AXBTP(IR) ) * (AZED(IR)-AZSD(IR) )/360.
& * 3.14159

```

500

```

VOLUME = VOLUME + VOL(IR)
CONTINUE

```

C

```

DO 40 IG = 1, NGRP
DO 30 IP = 1, NPRO

```

C

```

DO 6 I1 = 1, NREG2
DO 5 I2 = 1, NREG2
JACK(I1,I2) = 0.0

```

5

```

CONTINUE

```

6

```

RES(I1) = 0.0

```

C

```

CONTINUE

```

```

JACK(1,1) = 1.0
RES(1) = 0.0
IREG = NREG - 1

```

C

```

DO 10 IR1 = 1, IREG
ILOC1 = IR1 * 2
ILOC2 = ILOC1 + 1
ILOC3 = ILOC1 - 1
ILOC4 = ILOC3 + 1
ILOC5 = ILOC4 + 1
ILOC6 = ILOC5 + 1
IR2 = IR1 + 1

```

C

```

A1 = MAXAXI
TE1 = AXTP(IR1) / A1

```

C

```

RES(ILOC1) = 0.0
JACK(ILOC1,ILOC3) = 1.0
JACK(ILOC1,ILOC4) = TE1
JACK(ILOC1,ILOC5) = -1.0
JACK(ILOC1,ILOC6) = -TE1

```

C

```

TE2 = (IP+2) * ( TE1**(IP+1) )
RES(ILOC2) = TE2 * (DIFFUS(IR1,IG)
& -DIFFUS(IR2,IG) )
JACK(ILOC2,ILOC3) = 0.0
JACK(ILOC2,ILOC4) = DIFFUS(IR1,IG)
JACK(ILOC2,ILOC5) = 0.0
JACK(ILOC2,ILOC6) = -DIFFUS(IR2,IG)

```



```

C
10 CONTINUE
C
  ILOC2 = NREG2 - 1
  RES(NREG2) = +1.0
  JACK(NREG2, ILOC2) = 1.0
  JACK(NREG2, NREG2) = 1.0
C
  CALL GAUSS(JACK, RES, NREG2, IWK)
C
  DO 20 IR = 1, NREG
  IK = IR * 2
  IJ = IK - 1
  THEWS(IR, IG, IP) = RES(IJ)
  THEVS(IR, IG, IP) = RES(IK)
20 CONTINUE
30 CONTINUE
40 CONTINUE
C
C THE ISOTOPIC GROUPS
C
C
  N1 = NGRP + 1
  DO 50 IR = 1, NREG
  DO 60 IG = N1, NEQU
  DO 70 IP = 1, NPRO
  THEVS(IR, IG, IP) = +1.0
  THEWS(IR, IG, IP) = 0.0
70 CONTINUE
60 CONTINUE
50 CONTINUE
  AINTGL = 0.0
C
C THE B S
C
  I1 = 3*NPRO + 5
  DO 90 IR = 1, NREG
  T = AXP(IR)
  B=AXB(IR)
  THEBS(IR, 1) = T - B
  T1 = T / MAXAXI
  B1 = B / MAXAXI
  DO 80 I = 2, I1
  T2 = T * ( T1 ** (I-1) )
  B2 = B * ( B1 ** (I-1) )
  THEBS(IR, I) = (T2 - B2) / I
80 CONTINUE
90 CONTINUE

```

GOTO 999

C
C
C

ENTRY SIINT (IR, IG, IN)

C
C
C
C
C

THIS FUNCTION COMPUTES THE INTEGRAL OF A SINGLE
PROFILE EXPANSION.

B1 = THEBS(IR, 1)
B2 = THEBS(IR, 2)
B3 = THEBS(IR, (IN+2))

C

AINTGL = THEWS(IR,IG,IN) * B1
& + THEVS(IR,IG,IN) * B2
& - B3
AINTGL = CONST * AINTGL
GOTO 999

C
C
C

ENTRY DOINT(IR,IG,IN,IK,II)

C
C
C
C
C
C

THIS FUNCTION COMPUTES THE INTEGRAL OF TWO PROFILE
EXPANSIONS MULTIPLIED TOGETHER BEFORE INTEGRATION

WN = THEWS(IR,IG,IN)
WI = THEWS(IR,IK,II)
VN = THEVS(IR,IG,IN)
VI = THEVS(IR,IK,II)

C

B1 = THEBS(IR,1)
B2 = THEBS(IR, 2)
B3 = THEBS(IR, 3)
B4 = THEBS(IR, (II+2))
B5 = THEBS(IR, (IN+2))
B6 = THEBS(IR, (II+3))
B7 = THEBS(IR, (IN+3))
B8 = THEBS(IR, (II+IN+3))

C

AINTGL = WN * WI * B1
& + (WN * VI + VN * WI) * B2
& + (VN * VI) * B3
& - WN * B4 - WI * B5

```
& - VN * B6 - VI * B7
& + B8
```

C

```
AINTGL = AINTGL * CONST
GOTO 999
```

C

C

C

```
ENTRY TRINT (IR, IG, IN, IK, II, IP, IH)
```

C

C

C

C

C

C

```
THIS FUNCTION COMPUTES THE INTEGRAL OF THREE PROFILE
EXPANSIONS MULTIPLIED TOGETHER BEFORE INTEGRATION
```

```
VI = THEVS (IR, IK, II)
VH = THEVS(IR, IP, IH)
VN = THEVS(IR, IG, IN)
WN = THEWS(IR, IG, IN)
WI = THEWS(IR, IK, II)
WH = THEWS(IR, IP, IH)
```

C

```
B1 = THEBS(IR, 1 )
B2 = THEBS(IR, 2 )
B3 = THEBS(IR, 3 )
B4 = THEBS( IR, 4 )
B5 = THEBS(IR, (II+2) )
B6 = THEBS(IR, (IN+2) )
B7 = THEBS(IR, (IH+2) )
B8 = THEBS(IR, (II+2) )
B9 = THEBS(IR, (IN+2) )
B10 = THEBS(IR, (IH+2) )
```

C

```
B11 = THEBS(IR, (II+4) )
B12 = THEBS(IR, (IN+4) )
B13 = THEBS(IR, (IH+4) )
B14 = THEBS(IR, (IN+II+3) )
B15 = THEBS(IR, (II+IH+3) )
B16 = THEBS(IR, (IN+IH+3) )
```

C

```
B17 = THEBS(IR, (IN+II+4) )
B18 = THEBS(IR, (II+IH+4) )
B19 = THEBS(IR, (IN+IH+4) )
B20 = THEBS(IR, (IN+II+IH+4) )
```

C

```
AINTGL = WP * WN * WI * B1
& + (WP*WN*VI + WP*VN*WI + VH*WN*WI) * B2
& + (WP*VN*VI + VH*WN*VI + VH*VN*WI) * B3
```

```

& + VH*VN*VI * B4
& - WH*WN * B5      - WH*WI * B6      - WN*WI * B7
& -(WH*VN + VH*WN) * B8 -(WH*VI+VH*WI) * B9
& - (WN*VI + VN*WI) * B10

```

C

```

AINTGL = AINTGL
& -VH*VN * B11 - VH*VI * B12 - VN*VI * B13
& + WH * B14 + WN * B15 + WI * B16
& + VH * B17 + VN * B18 + VI * B19 - B20

```

C

```

AINTGL = CONST * AINTGL
GOTO 999

```

C

C

C

```

ENTRY DEINT(IR, IK, II, IG, IN)

```

C

C

C

C

C

C

C

C

C

C

C

C

C

C

```

A1 = (IN) * (IN+1) / (MAXAXI * MAXAXI)

```

```

AINTGL = THEBS(IR, (II+IN+1) )
& - THEVS(IR, IK, II) * THEBS(IR, (IN+1) )
& - THEWS(IR, IK, II) * THEBS(IR, (IN) )
AINTGL = CONST * AINTGL * A1
GOTO 999

```

C

C

C

999

```

CONTINUE
RETURN
END

```

SUBROUTINE DIRREC(\$MAX1,\$MAX2,\$MAX3,\$MAX4,\$MAX5,\$MAX6)

C
C
C
C
C
C
C
C
C
C
C

DIRREC CONTROLS THE OUTER (WIELANDT) ITERATIONS FOR
DETERMINING THE SOLUTION OF THE DIRECT OR ADJOINT
SYSTEMS.

IMPLICIT REAL(A-H,J-M,O-Z),INTEGER(I,N,\$)

C

```

COMMON /ANS      / COEFF(7,20),KEFF
COMMON /PERTS    / IPERT
COMMON /ST1      / EQUIL(7,20), KEQUI, LAMEQU
COMMON /ALINSR   / NLINER
COMMON /DER      / DCOEFO(2,20),COEFOD(7,20),DCOEF(2,20)
COMMON /AIOT     / NR, NW1, NW2, NW3
COMMON /EMSGC    / NWE, IER
COMMON /ANP2     / NREG, NGRP, NELE, NPRO, NEQU, NTOT
COMMON /ANP1     / POWER, SIGFIS(10,5)
COMMON /ANP3     / SIGABS(10,5), ALPHA(10,5),
&                DIFFUS(10,5), SIGELE(2,5),
&                ANU(5), CHI(5), SIGSCT(10,7,7)
COMMON /MATR     / SIGOUT(10,7,7), CNSFIS(10,7,7)
COMMON /BOUD     / RIN(10), ROUT(10), AXTP(10),
&                AXBT(10), AZSD(10), AZED(10), VOL(10)
COMMON /TCTIM    / TTIME, DELTI
COMMON /A$VE     / AVETOT(7), AVERA(10,7), TOTNUT, VOLUME,
&                EQUTOT(7), EQAVE(10,7)
COMMON /POW1     / MULT, PMULT
COMMON /IWKL     / ITY1
COMMON /EST      / DLAM
COMMON /GONLY    / DLIN(7,20,7,20), LINS(7,20,7,20),
&                ANON(7,20,20)
COMMON /WHICH    / DIRNUT, NADJ
COMMON /$GAUSS$  / DIAG, LAST
COMMON /$NEW1$   / ANORM, AFIST
COMMON /ST2      / KEST
COMMON /WRKIN    / WK(4720), X(140), XOLD(140)
COMMON /CONSAT   / NPOWK

```

C

```

DATA          IFIRST/O/
EXTERNAL      KY1,KYFUN,KYDER

```

C
C
C
C

```

DETERMINE NUMBER OF EQUATIONS IN EIGEN PROBLEM
AND THE NUMBER REMAINING FOR THE ISOTOPES

```

```

INUM = NGRP
IF ( NLINER .EQ. 1 ) INUM= NEQU
NEIGEN = INUM * NPRO
WRITE(6,*) NEIGEN, INUM
NONEIG = NPRO * NEQU - NEIGEN
C
C   IF THIS IS THE FIRST TIME, LETS TAKE A FEW
C   GUESSES
C
C   IF ( IFIRST .NE. 0 ) GOTO 30
C
ANONN = 0.0
LAMDA = 1.0/KEFF
KEST = KEFF
A1 = GDNLIN(0)
DLAM = .001
C
DO 10 IG = 1, NEQU
DO 20 IP = 1, NPRO
DO 17 IH = 1, NPRO
ANON(IG,IP,IH) = 0.0
17  CONTINUE
COEFF(IG,IP) = +1.E00
IF ( IG .GT. NGRP ) COEFF(IG,IP) = 50.
20  CONTINUE
10  CONTINUE
C
DO 27 IE = 1, NELE
DO 28 IP = 1, NPRO
DCOEFO(IE,IP) = 0.0
28  CONTINUE
27  CONTINUE
C
A = POW(0)
CALL AVE1(COEFF,7,20)
C
IFIRST = IFIRST + 1
GOTO 32
C
C   THIS ISN'T THE FIRST TIME, SO USE INFORMATION
C   FROM THE PREVIOUS TIME.
C
30  CONTINUE
C
DLAM = 1.0/KEFF - 1.0/KEST
LAMDA = 1.0/KEST
KEFF = KEST
C

```

```

A1 = SOURC(1,NGRP)
A = POW(0)
A3 = GDNLIN(0)
ANONN = AONL(0)
32 CONTINUE
C
C
C NOW THE LOOP FOR THE SYSTEM OF EQUATIONS TO BE SOLVED
C
ICNT = 0
IST = 1
IFLAG1 = 0
IFLAG2 = 0
NTOT1 = NTOT - 1
IMAIN = 0
NITER = 50
IINNER = 0
GOTO 100
C
C NOW, FIRST WE WILL ASSUME THAT THE NONLINEARITIES,
C ALONG WITH TEMPERATURE FEEDBACK, IS KNOWN.
C THATS WHY WE SKIP TO 100
C
188 CONTINUE
C
C NONLINEARITY UPDATING
C
IMAIN = IMAIN + 1
A3 = AONL(0)
IF ( ANONN .NE. 0. )
& AN = ABS (( A3 - ANONN )/ANONN)
IF ( ANONN .EQ. 0. ) AN = ABS(A3)
ANONN = A3
IF ( NLINER.EQ.0 .AND. AN.LT.1.E-4) GOTO 5000
IF(NLINER.EQ.1 .AND. DXMAX.LE.1.E-4) GOTO 5000
IF (IMAIN .GT. NITER ) GOTO 8011
IINNER = 0
C
C NOW WE PREFORM THE WIELANDT METHOD OF SOLVING FOR THE
C FLUXES AND ISOTOPIC CONCENTRATIONS, ASSUMING THAT THE
C NONLINEARITIES ARE KNOWN AND CORRECT. WE SHALL GO
C BACK AND UPDATE THE NONLINEARITES AT A LATER STEP
C (SEE 188 ABOVE)
C
100 IER = 0
IINNER = IINNER + 1
C
C IF WE HAVE DONE A FEW WIELANDT ITERATIONS, GO

```

```
C      BACK AND UPDATE NONLINEARITIES
C
C      IF ( IINNER .GT. 9 ) GOTO 188
C
C      GET THE INITIAL SOURCE BEFORE UPDATING FLUXES
C
C      A1 = SOURC (1,NGRP)
C      A = POW(0)
C      CALL AVE1(COEFF,7,20)
C
C      NOW, INDICATE THAT THIS IS A FLUX ITERATION
C      AND COPY THE FLUX COEFFICIENTS INTO THE
C      SOLUTION VECTOR FOR THE NEWTON METHOD.
C
C      ITY1 = 0
C      ASSIGN 50 TO IBACK1
C      GOTO 7100
C
C      50 CONTINUE
C
C      1717 CONTINUE
C
C      ICNT = ICNT + 1
C      39822 CONTINUE
C
C      IF WE HAVE DONE TOO MANY, ASSUME WE CAN'T GET THE
C      PROBLEM SO GET OUT OF IT.
C
C      IF ( ICNT .GT. 300 ) GOTO 8011
C
C      SOLVE FOR THE FLUXES.
C
C      CALL NEWTON(KY1,+5,NEIGEN, 15,X,WK(IST),0.00)
C
C      13433 FORMAT(//)
C      IF ( IER .EQ. -113) IER = 0
C      IF ( IER .NE. 0 ) IFLAG1 = IFLAG1 + 1
C      IF ( IER .EQ. 0 ) IFLAG1 = 0
C      IER = 0
C      IF ( IFLAG1 .EQ. 10)
C      & CALL KANE(KYFUN,KYDER,X,NTOT1,WK(IST),0.25)
C      IER = 0
C
C      7223 CONTINUE
C
C      PUT THE SOLUTION VECTOR BACK INTO THE FLUX COEFFICIENT
C
C      ASSIGN 400 TO IBACK2
```



```

GOTO 7200
400 CONTINUE
DXMAX2 = DXMAX
C
C GET NEW SOURCE TO CALCULATE THE CHANGE IN THE
C DELTA EIGENVALUE.
C
A2 = SOURC(2,NGRP)
KHOLD = 0.0
IF ( NLINER .EQ. 1 ) GOTO 12344
C
C UPDATE DLAM IF THIS IS NOT A CONSTANT KEFF MODEL
C I.E. NOT LINEAR AND KCONST EQ 0
C
RES = A1 / A2
KHOLD = DLAM
DLAM = DLAM * RES
DELT = ABS(DLAM - KHOLD)
C
K2 = 1.0/ (LAMDA + DLAM)
KHOLD = ABS(DLAM - KHOLD)
C
12344 CONTINUE
C
C UPDATE SOURCE, WITH NORMALIZATION AND POWER
C BEFORE GOING TO THE ISOTOPIC EQUATIONS
C
A1 = SOURC (1,NGRP)
A = POW(0)
CALL AVE1(COEFF,7,20)
C
IF(NLINER .EQ. 1 ) GOTO 34234
C UPDATE THE IODINE AND XENON
C
C TELL THAT IT'S ISOTOPES, AND COPY ISOTOPE
C COEFFICIENTS INTO SOLUTION VECTOR FOR NEWTON
C
ITY1 = 1
ASSIGN 47 TO IBACK1
GOTO 7100
C
47 CONTINUE
C
C SOLVE FOR THE ISOTOPES
C
CALL NEWTON(KY1,-5,NONEIG, 15,X,WK(IST),0.00)
C
IF ( IER .EQ. -113) IER = 0

```

```

      IF ( IER .NE. 0 ) IFLAG2 = IFLAG2 + 1
      IF ( IER .EQ. 0 ) IFLAG2 = 0
      IER = 0
      IF ( IFLAG2 .EQ. 10)
& CALL KANE(KYFUN,KYDER,X,NTOT1,WK(IST),0.25)
      IER = 0
C
C   UNSCRAMBLE THE SOLUTION VECTOR BACK INTO THE
C   ISOTOPE'S COEFFICIENTS
C
      ASSIGN 478 TO IBACK2
      GOTO 7200
478  CONTINUE
      IF ( DXMAX2 .GT. DXMAX) DXMAX = DXMAX2
34234 IF(NLINER.EQ.1 ) DXMAX = DXMAX2
C
C   CHECK FOR CONVERGENCE ON KEFF
C   AND COEFFICIENTS
C
      IF ( KHOLD .GT. 1.E-7) GOTO 100
      IF ( DXMAX .GT. 1.E-6 ) GOTO 100
C
C   GO BACK AND UPADTE NONLINEARITIES.
C
      GOTO 188
C
C   WHEN WE HAVE CONVERGED, COME HERE AND CONTINUE
C
5000 CONTINUE
C
      GOTO 8873
C
C   IN CASE OF ERRORS .....
C
8011 CONTINUE
      IER = 400
      WRITE(NWE,8012)
8012 FORMAT(/' DIRECT(F): ',
& 'NO CONVERGENCE ON DIRECT SYSTEM')
      GOTO 8873
C
8873 CONTINUE
      A3 = POW(0)
C
C   COPY NEW INTO OLD
C   ONLY IF NOT ADJOINT
C
      IF ( NADJ .EQ. 1 ) GOTO 883

```

```

C
  IF ( TTIME .LE. 1.E-20) GOTO 8867
  DO 886 IE = 1, NELE
  IG = NGRP + IE
  DO 887 IP = 1, NPRO

C
C  WE WANT TO SAVE THE ACTUAL FLUX LEVEL, NOT THE
C  CHANGE IN FLUX LEVEL IN COEFOD.  ALSO THE DERIVATIVE
C

  A1 = COEFF(IG,IP) * MULT
  B1 = COEFOD(IG,IP)
  IF ( NLINER .EQ. 1 ) B1 = B1 -EQUIL(IG,IP)
  C1 = DCOEFO(IE,IP)
  DCOEFO(IE,IP) = DERTIM(DELTI,A1,B1,C1)
887  CONTINUE
886  CONTINUE
8867 CONTINUE

C
C  WRITE(6,13481)
C13481 FORMAT(/)
C  WRITE(6,*) TTIME
C  WRITE(6,*) COEFF
C  WRITE(6,*) DCOEFO
C

  DO 888 IG = 1, NEQU
  DO 889 IP = 1, NPRO
  COEFOD(IG,IP) = COEFF(IG,IP) * MULT
  IF ( NLINER .EQ. 1 ) COEFOD(IG,IP) = COEFOD(IG,IP)
&                                     + EQUIL(IG,IP)
889  CONTINUE
888  CONTINUE

C
883  CONTINUE

C
C  NOW LETS OUTPUT SOME STUFF SO IT WON'T HAVE BEEN
C  A TOTAL WASTE OF CALCULATIONS
C

  TAIME = TTIME / 3600.
  IF ( NADJ.EQ.1) WRITE(NW1,7444)
7444  FORMAT('1',,10X,'ADJOINT SYSTEM'//)
  KEFF = 1.0/ ( LAMDA + DLAM)
  WRITE(NW1,3343) TAIME, KEFF
3343  FORMAT(//,10X,'TIME: ',F8.4,' HOURS',/
& /, 10X,'KEFF: ',F9.7,/)
  CALL AVE1(COEFF,7,20)
  CALL OUT3(2)

C
  IF ( TTIME .GT. 1.E-20 ) GOTO 999

```

```

      IF ( NADJ .EQ. 0 ) DIRNUT = TOTNUT
C
      N2 = NREG * NGRP + 1
      N3 = N2 + NREG * NGRP
      N4 = N3 + NREG * NGRP
      N5 = N4 + NREG * NGRP * NELE
      N7 = (NREG + NELE )
C
      CALL RATES ($MAX1,$MAX2,$MAX3,$MAX4,$MAX5,$MAX6,
& COEFF, SIGABS, SIGFIS,ALPHA,SIGELE,DIFFUS,VOL,
& WK(1), WK(N2), WK(N3), WK(N4), WK(N5), NREG, NGRP,
& NELE, NEQU, NPRO, N7, MULT, AVETOT)
      IER = 0
      IF(NADJ .EQ.1 ) WRITE(NW1,7445)
7445  FORMAT('1',/,10X,'DIRECT TIME DEPENDENT SYSTEM'/)
C
      GOTO 999
C-----
C
7100  CONTINUE
      IF ( ITY1 .EQ. 0 ) IS = 1
      IF ( ITY1 .EQ. 0 ) IE = INUM
      IF ( ITY1 .EQ. 1 ) IS = INUM + 1
      IF ( ITY1 .EQ. 1 ) IE = NEQU
      IO = 0
      DO 7101 IG = IS, IE
      DO 7102 IP = 1, NPRO
      IO = IO + 1
      X(IO) = COEFF(IG,IP)
      XOLD(IO) = X(IO)
7102  CONTINUE
7101  CONTINUE
      GOTO IBACK1, (47, 50 )
C-----
C
7200  CONTINUE
      IF ( ITY1 .EQ. 0 ) IS = 1
      IF ( ITY1 .EQ. 0 ) IE = INUM
      IF ( ITY1 .EQ. 1 ) IS = INUM + 1
      IF ( ITY1 .EQ. 1 ) IE = NEQU
      DXMAX = 0.0
      IO = 0
      DO 7201 IG = IS, IE
      DO 7202 IP = 1, NPRO
      IO = IO + 1
      COEFF(IG,IP) = X(IO)
      DX = X(IO) - XOLD(IO)

```

```
IF ( X(IO) .NE. 0.0 ) DX = ABS(DX/X(IO))
IF ( X(IO) .EQ. 0.0 ) DX = ABS(DX)
IF (DX .GT. DXMAX ) DXMAX = DX
7202 CONTINUE
7201 CONTINUE
GOTO IBACK2, ( 400, 478 )
C
C-----
999 CONTINUE
RETURN
END
```

FUNCTION GDNL (IJ, II)

 GDNL FORMS THE GALERKINS NONLINEAR ALGEBRAIC EQUATIONS

THIS ENTIRE ROUTINE CONTAINS ALL OF THE EQUATIONS FOR
 THE DERIVATIVES, POWER CONSTRAINTS, ETC. PLUS A FEW
 UTILITY PROGRAMS.

THEY ALL REQUIRE THE SAME INFORMATION FROM COMMON
 AND OFTEN INVOLVES THE USE OF THE SAME CODE SECTIONS.

IMPLICIT REAL (A-H,J-M,O-Z), INTEGER (I,N,\$)

COMMON /ANS / COEFF(7,20),KEFF
 COMMON /CONSAT/ NPOWK
 COMMON /ALINSR/ NLINER
 COMMON /EMSGC / NWE, IER
 COMMON /ANP1 / POWER, SIGFIS(10,5)
 COMMON /ANP2 / NREG, NGRP, NELE, NPRO, NEQU, NTOT
 COMMON /ANP3 / SIGABS(10,5), ALPHA(10,5),
 & DIFFUS(10,5), SIGELE(2,5),
 & ANU(5), CHI(5), SIGSCT(10,7,7)
 COMMON /MATR / SIGOUT(10,7,7), CNSFIS(10,7,7)
 COMMON /TCTIM / TTIME, DELTI
 COMMON /POW1 / MULT, PMULT
 COMMON /BOUD / RIN(10), ROUT(10), AXTP(10),
 & AXBT(10), AZSD(10), AZED(10), VOL(10)
 COMMON /A\$VE / AVETOT(7), AVERA(10,7), TOTNUT, VOLUME,
 & EQUTOT(7), EQAVE(10,7)
 COMMON /DER / DCOEFO(2,20), COEFOD(7,20), DCOEF(2,20)
 COMMON /EST / DLAM
 COMMON /GDONLY/ DLIN(7,20,7,20), LINS(7,20,7,20),
 & ANON(7,20,20)
 COMMON /WHICH / DIRNUT, NADJ
 COMMON /SORE / SOUR(7,20)
 COMMON /AIOT / NR, NW1, NW2, NW3
 COMMON /ST1 / EQUIL(7,20), KEQUI, LAMEQU

DATA IFLAG1 / 0 /

IENT = 0

FORM THE LINEAR SECTION
 WITHOUT DIFFUSION OR TIME DERIVATIVES.

```

SUM = 0.
DO 10 IK = 1, NEQU
DO 30 IP = 1, NPRO
SUM = SUM + COEFF(IK,IP) * LINS(IJ,II,IK,IP)
30 CONTINUE
10 CONTINUE
C
DO 32 IP = 1, NPRO
SUM = SUM + COEFF(IJ,IP) * ANON(IJ,II,IP)
32 CONTINUE
C
IF ( IJ .GT. NGRP ) GOTO 12434
C
SUM = SUM - SOUR(IJ,II)
12434 CONTINUE
C
DIFFUSION IF IJ <= NGRP
C
IF ( IJ .GT. NGRP ) GOTO 80
C
DO 50 IR = 1, NREG
SUM2 = 0.
DO 60 IP = 1, NPRO
SUM2 = SUM2 + COEFF(IJ,IP) * DEINT(IR,IJ,II,IJ,IP)
60 CONTINUE
SUM = SUM + DIFFUS(IR,IJ) * SUM2
50 CONTINUE
C
GOTO 129
C
80 CONTINUE
IF ( NADJ .EQ. 1 ) GOTO 129
IE = IJ - NGRP
C
C TIME DERIVATIVE
C
IF ( DELTI .LE. 1.E-50) GOTO 129
DO 121 IP = 1, NPRO
SUM1 = 0.0
DO 122 IR = 1, NREG
SUM1 = SUM1 + DOINT(IR,IJ,IP,IJ,II)
122 CONTINUE
C
C NOTE THAT IF WE WITHDRAW THE EQUIL AMOUNT FROM THE
C COEFOD, WE GET SAME RESULT
C
AA2 = COEFF(IJ,IP)
BB2 = COEFOD(IJ,IP)

```

```

      IF ( NLINER .EQ. 1 ) BB2 = BB2 - EQUIL(IJ,IP)
      SUM = SUM - SUM1 *
& (( AA2 * MULT - BB2 )
& * 2.0 / DELTI - DCOEFO(IE,IP) ) / MULT
121  CONTINUE
129  CONTINUE
      SUM5 = 0.0
C
C   LINERAIZED  IJ, II
C
      IF ( TTIME .LT. 1.E-20 ) GOTO 560
      IF ( NLINER.EQ. 0 ) GOTO 560
      IF ( IJ .GT. NGRP) GOTO 540
C
      DO 521 IE = 1, NELE
      A = SIGELE(IE,IJ)
      IF ( A .LT. 1.E-50) GOTO 521
      IEG = IE + NGRP
      SUM2 = 0.0
      DO 522 IM = 1, NPRO
      DO 523 IL = 1, NPRO
      SUM1 = 0.0
      DO 524 IR = 1, NREG
      SUM1 = SUM1 + TRINT(IR,IEG,IL,IJ,IM,IJ,II)
524  CONTINUE
      SUM2 = SUM2 + SUM1 *
& (EQUIL(IEG,IL) * COEFF(IJ,IM)
& + EQUIL(IJ,IM) * COEFF(IEG,IL) )
523  CONTINUE
522  CONTINUE
      SUM5 = SUM5 + SUM2 * A
521  CONTINUE
      GOTO 560
C
540  CONTINUE
      IE = IJ - NGRP
      DO 541 IG = 1, NGRP
      A = SIGELE(IE,IG)
      IF ( A.LT.1.E-50) GOTO 541
      SUM2 = 0.0
      DO 542 IM = 1, NPRO
      DO 543 IL = 1, NPRO
      SUM1 = 0.0
      DO 544 IR = 1, NREG
      SUM1 = SUM1 + TRINT(IR,IG,IL,IJ,IM,IJ,II)
544  CONTINUE
      SUM2 = SUM2 + SUM1 *
& ( EQUIL(IJ,IM) * COEFF(IG,IL)

```



```

&      + EQUIL(IG,IL) * COEFF(IJ,IM) )
543  CONTINUE
542  CONTINUE
      SUM5 = SUM5 - SUM2 * A
541  CONTINUE
      GOTO 560
C
560  CONTINUE
      SUM = SUM + SUM5 * MULT
C
      GDNL = SUM
      GOTO 999
C
C-----
C
C      ENTRY AONL(IDUM)
C-----
C
      GDNL = 0.0
      DO 7777 IJ = 1, NEQU
C      IF ( TTIME .LE. 1.E-20) ATOT = AVETOT(IJ)
C      IF ( TTIME .GT. 1.E-20) ATOT = EQUTOT(IJ)
      ATOT = AVETOT(IJ)
      DO 7776 II = 1, NPRO
      DO 7774 IP = 1, NPRO
      ANON(IJ,II,IP) = 0.0
      SUM = 0.0
C
C      ALPHA TERMS IF IJ <= NGRP
C
      IF ( IJ .GT. NGRP ) GOTO 170
C
      DO 130 IR = 1, NREG
      SUM = DOINT(IR,IJ,IP,IJ,II) * ATOT * ALPHA(IR,IJ) *
& SIGABS(IR,IJ) + SUM
130  CONTINUE
C
170  CONTINUE
C
      NOW FOR THE NON-LINEAR ABSORPTIONS
C      FIRST, IF IJ <= NGRP
C
      IF ( ( TTIME .GT. 1.E-20) .AND. (NLINER .EQ. 1) )
&      GOTO 7676
C
      SUM14 = 0.0
      SUM15 = 0.0

```

```

IF ( IJ .GT. NGRP ) GOTO 240
C
SUM1 = 0.
DO 190 IE = 1, NELE
SUM2 = 0.
IGE = NGRP + IE
A1 = SIGELE(IE,IJ)
IF ( A1 .LE. 1.E-50) GOTO 190
DO 200 IH = 1, NPRO
SUM3 = 0.
DO 210 IR = 1, NREG
SUM3 = SUM3 + TRINT(IR, IJ, IP, IJ, II, IGE, IH)
210 CONTINUE
SUM2 = SUM2 + SUM3 * COEFF(IGE, IH)
200 CONTINUE
SUM1 = SUM1 + SUM2 * A1
190 CONTINUE
SUM14 = SUM14 + SUM1 * MULT
C
GOTO 300
240 CONTINUE
C
C NOW IF IJ > NGRP
C
IJG = IJ - NGRP
SUM1 = 0.
DO 260 IG = 1, NGRP
A1 = SIGELE(IJG, IG)
IF ( A1 .LE. 1.E-50) GOTO 260
SUM2 = 0.
DO 270 IH = 1, NPRO
SUM3 = 0.
DO 2880 IR = 1, NREG
SUM3 = SUM3 + TRINT(IR, IJ, IP, IG, IH, IJ, II)
2880 CONTINUE
SUM2 = SUM2 + SUM3 * COEFF(IG, IH)
270 CONTINUE
C
SUM1 = SUM1 + SUM2 * A1
260 CONTINUE
SUM15 = SUM15 - SUM1 * MULT
C
300 CONTINUE
SUM = SUM + SUM14 + SUM15
7676 GDNL = GDNL + SUM
ANON(IJ, II, IP) = SUM
7774 CONTINUE
7776 CONTINUE

```

7777 CONTINUE
GOTO 999

C

C-----

C

ENTRY DGDNL (IJ,II,IG,IP)

C

C-----

C

C

C

THE LINEAR TERMS

DSF = DLIN(IJ,II,IG,IP)

IF (IJ .EQ. IG) DSF = DSF + ANON(IJ,II,IP)

290

CONTINUE

C

C

C

LINEARIZED, IJ,II, IG,IP

IF (NLINER .EQ. 0) GOTO 7999

IF (TTIME .LT. 1.E-20) GOTO 7999

C

LINERIZED

C

SUM5 = 0.0

IF (IJ .GT. NGRP) GOTO 750

IF (IG .GT. NGRP) GOTO 720

C

IF (IG.NE.IJ) GOTO 799

DO 701 IE = 1, NELE

A = SIGELE(IE,IJ)

IF (A .LT. 1.E-50) GOTO 701

IEG = NGRP + IE

SUM2 = 0.0

DO 702 IL = 1, NPRO

SUM1 = 0.0

DO 703 IR = 1, NREG

SUM1 = SUM1 + TRINT(IR,IEG,IL,IJ,II,IG,IP)

703

CONTINUE

SUM2 = SUM2 + SUM1 * EQUIL(IEG,IL)

702

CONTINUE

SUM5 = SUM5 + SUM2 * A

701

CONTINUE

GOTO 799

C

720

CONTINUE

IE = IG - NGRP

A = SIGELE(IE,IJ)

IF (A.LT. 1.E-50) GOTO 799

DO 721 IM = 1, NPRO

SUM1 = 0.0

```

DO 722 IR = 1, NREG
SUM1 = SUM1 + TRINT(IR, IG, IP, IJ, IM, IJ, II)
722 CONTINUE
SUM5 = SUM5 + SUM1 * EQUIL(IJ, IM)
721 CONTINUE
SUM5 = SUM5 * A
GOTO 799

```

C

```

750 CONTINUE
IE = IJ - NGRP
IF ( IG .GT. NGRP ) GOTO 775
A = SIGELE(IE, IG)
IF ( A .LT. 1.E-50 ) GOTO 799
DO 751 IM = 1, NPRO
SUM1 = 0.0
DO 752 IR = 1, NREG
SUM1 = SUM1 + TRINT(IR, IG, IP, IJ, IM, IJ, II)
752 CONTINUE
SUM5 = SUM5 - SUM1 * EQUIL(IJ, IM)
751 CONTINUE
GOTO 799

```

C

775 CONTINUE

C

```

IF ( IJ.NE.IG) GOTO 799
DO 776 IS = 1, NGRP
A = SIGELE(IE, IS)
IF ( A .LT. 1.E-50) GOTO 776
SUM2 = 0.0
DO 777 IL = 1, NPRO
SUM1 = 0.0
DO 778 IR = 1, NREG
SUM1 = SUM1 + TRINT(IR, IS, IL, IJ, II, IG, IP)
778 CONTINUE
SUM2 = SUM2 + SUM1 * EQUIL(IS, IL)
777 CONTINUE
SUM5 = SUM5 - SUM2 * A
776 CONTINUE
GOTO 799

```

C

```

799 CONTINUE
DSF = DSF + SUM5 * MULT
7999 CONTINUE
GDNL = DSF
GOTO 999

```

C

C-----

C

```

      ENTRY SOURC(ITYPE, IEND)
C
C-----
C
      IF ( ITYPE .GT. 2 ) GOTO 999
      IF ( ITYPE .LT. 1 ) GOTO 999
      GOTO (5005,5000), ITYPE
C
C      FORM RATIOS TO COEFF(NGRP,1)
C
5005  CONTINUE
      SUM = COEFF(IEND,1)
      IF ( SUM .EQ. 0 ) GOTO 5000
      IF (NLINER .EQ. 1) GOTO 5000
      DO 5006 IG = 1, IEND
      DO 5007 IP = 1, NPRO
      COEFF(IG,IP) = COEFF(IG,IP) / SUM
5007  CONTINUE
5006  CONTINUE
C
C      NOW SOURCE.....
C
5000  CONTINUE
      SUM = 0.0
      SUM50 = 0.0
      SUM00 = 0.0
      DO 5199 IJ = 1, NEQU
      DO 5200 II = 1, NPRO
      SOUR(IJ,II) = 0.0
      SUM22 = 0.0
      IF ( IJ .GT. NGRP ) GOTO 5200
C
      DO 5201 IK = 1, NGRP
      DO 5202 IR = 1, NREG
      AA1 = COEFF(IJ,II)
      SUM50 = SUM50 + AA1
      & * CNSFIS(IR,IK,IJ) * SIINT(IR,IJ,II)
      SUM20 = 0.0
      SUM2 = 0.0
C
      DO 5203 IP = 1, NPRO
      A = DOINT(IR,IK,IP,IJ,II)
      SUM2 = SUM2 + COEFF(IK,IP) * A
5203  CONTINUE
C
      IF ( NADJ .EQ. 0 )
      & SOUR(IJ,II) = SOUR(IJ,II) + SUM2 * CNSFIS(IR,IJ,IK)
      IF ( NADJ .EQ. 1 )

```

```

      & SOUR(IJ,II) = SOUR(IJ,II) + SUM2 * CNSFIS(IR,IK,IJ)
C
5202 CONTINUE
5201 CONTINUE
      SOUR(IJ,II) = SOUR(IJ,II) * DLAM
5200 CONTINUE
5199 CONTINUE
      GDNL = SUM50
      GOTO 999
C
C-----
C
      ENTRY POW(IDUM)
C
C-----
C
C      POW MULTIPLIES THE COEFF OF THE FLUXES SO THAT THE
C      CORRECT POWER LEVEL IS ACHIEVED.
C
      SUM = 0.
      DO 610 IR = 1, NREG
      DO 620 IG = 1, NGRP
      SUM1 = 0.
      DO 630 IH = 1, NPRO
      SUM1 = SUM1 + COEFF(IG,IH) * SIINT(IR,IG,IH)
630 CONTINUE
      IF ( NADJ .EQ. 0 )
& SUM = SUM + SUM1 * SIGFIS(IR,IG)
      IF ( NADJ .EQ. 1 )
& SUM = SUM + SUM1
620 CONTINUE
610 CONTINUE
C
      IF (NLINER.EQ.1) GOTO 664
C
      IF ( NADJ .EQ. 0 )
& POWLE = POWER / 3.0442E-17
      IF ( NADJ .EQ. 1 )
& POWLE = DIRNUT
C
      IF ( SUM .EQ. 0.0 ) GOTO 601
      MULT = POWLE / SUM
      PMULT = 1.0
      GOTO 699
664 CONTINUE
      GDNL=SUM*3.0442E-17
      GOTO 699
601 CONTINUE

```

```

IER = 201
WRITE(NWE,6001)
6001  FORMAT(/, ' POW(F):  NO POWER BEING PRODUCED' )
      WRITE(NWE,*) COEFF
      WRITE(NWE,*) SIGFIS
      GOTO 699
699   CONTINUE
      GDNL = MULT
      GOTO 999

```

C

C-----

C

```

      ENTRY GDNLIN(IDUM)

```

C

C-----

C

```

      SUM = 0.0
      DO 3111 IJ = 1, NEQU
      DO 3112 IG = 1, NEQU
      DO 3113 II = 1, NPRO
      DO 3114 IP = 1, NPRO

```

C

```

      DLIN(IJ,II,IG,IP) = 0.0

```

C

```

      DO 3115 IR = 1, NREG
      IF ( NADJ .EQ. 0 )
& A = SIGOUT(IR,IJ,IG) - CNSFIS(IR,IJ,IG)/KEFF
      IF ( NADJ .EQ. 1 )
& A = SIGOUT(IR,IG,IJ) - CNSFIS(IR,IG,IJ)/KEFF
      IF ( ABS(A) .LT. 1.E-20 ) GOTO 3115
      DLIN(IJ,II,IG,IP) = DLIN(IJ,II,IG,IP)
&      + A * DOINT(IR,IG,IP,IJ,II)

```

```

3115  CONTINUE

```

```

      LINS(IJ,II,IG,IP) = DLIN(IJ,II,IG,IP)

```

```

3114  CONTINUE

```

```

3113  CONTINUE

```

```

3112  CONTINUE

```

```

3111  CONTINUE

```

C

C

```

      DIFFUSION AND TIME PART

```

C

```

      DO 3116 IJ = 1, NEQU
      DO 3117 IR = 1, NREG
      IF ( IJ .GT. NGRP ) GOTO 3171
      A = DIFFUS( IR,IG )
      IF ( ABS(A) .LT. 1.E-30 ) GOTO 3117
      DO 3118 II = 1, NPRO
      DO 3119 IP = 1, NPRO

```

```

      DLIN (IJ,II,IJ,IP) = DLIN(IJ,II,IJ,IP)
& + A * DEINT(IR,IJ,II,IJ,IP)
C
3119 CONTINUE
3118 CONTINUE
      GOTO 3117
C
3171 CONTINUE
C
      IF ( DELTI .LE. 1.E-50) GOTO 3117
      DO 3172 II = 1, NPRO
      DO 3173 IP = 1, NPRO
      DLIN(IJ,II,IJ,IP) = DLIN(IJ,II,IJ,IP)
& -2.0 / DELTI * DOINT(IR,IJ,II,IJ,IP)
3173 CONTINUE
3172 CONTINUE
C
3117 CONTINUE
3116 CONTINUE
C
      DO 88341 IJ = 1, NGRP
      DO 88341 IK = 1, NGRP
      DO 88341 IM = 1, NPRO
      DO 88341 II = 1, NPRO
      SUM = SUM + DLIN(IJ,IM,IK,II)
88341 CONTINUE
      GOTO 999
C
C-----
C
      ENTRY STOLIN(I1)
C
C-----
C
      GOTO ( 801,802,802,802,865), I1
C
801 CONTINUE
C
      DO 871 IG = 1, NEQU
      EQUTOT(IG) = AVETOT(IG)
      DO 872 IR = 1, NREG
      EQAVE(IR,IG) = AVERA(IR,IG)
872 CONTINUE
871 CONTINUE
C
      DO 811 IG = 1, NEQU
      DO 812 IP = 1, NPRO
      EQUIL(IG,IP) = COEFF(IG,IP) * MULT

```



```
812 CONTINUE
811 CONTINUE
    KEQUI = KEFF
    LAMEQU = DLAM
    GDNL = 0.0
    GOTO 999
```

C

```
802 CONTINUE
    DO 813 IG = 1, NEQU
    DO 814 IP = 1, NPRO
        IF ( I1 .EQ. 2 ) COEFF(IG,IP) = 1.E-5
        IF ( I1 .EQ. 3 ) COEFF(IG,IP) = EQUIL(IG,IP)
        IF ( I1 .LE. 3 ) KEFF = KEQUI
        IF ( I1 .LE. 3 ) DLAM = LAMEQU
        IF ( I1 .EQ. 4 ) COEFF(IG,IP) = COEFF(IG,IP)
&                                     + EQUIL(IG,IP)
```

```
814 CONTINUE
813 CONTINUE
    GOTO 999
```

C

```
865 CONTINUE
    DO 866 IG = 1, NEQU
    DO 867 IP = 1, NPRO
        COEFF(IG,IP) = COEFF(IG,IP) *MULT - EQUIL(IG,IP)
867 CONTINUE
866 CONTINUE
    MULT = 1.0
    KEFF = KEQUI
    DLAM = LAMEQU
    GOTO 999
```

C

C-----

C-----

C

```
999 CONTINUE
    RETURN
    END
```

Appendix F

XORA Output for Sample Input

F.1 Sample Output

This appendix contains the output for the sample input given in appendix D.

```

XX   XX   0000000   RRRRRR   AA
XX  XX   00   00   RR  RR   AA  AA
  XXXX   00   00   RRRRRR  AAAAAAAA
XX  XX   00   00   RR  RR   AA  AA
XX   XX   0000000   RR  RR   AA  AA

```

XENON OSCILLATIONS - A RESIDUAL APPROACH

ONE-DIMENSIONAL MODEL

JUNE 1981

N3G2R3PC - NONLINEAR, 3 GROUP, 2 REGION, 3 PROFILE
DATASET C

```

-----
INPUT INFORMATION
-----

```

```

NUMBER OF REGIONS:      2
NUMBER OF ENERGY GROUPS: 3
NUMBER OF ISOTOPES:    2

```

PROFILE EXPANSIONS

```

# RADIAL:  1      # AXIAL:  3      # AZIMUTHAL: 1      # TOTAL:  3

```

THERMAL POWER LEVEL: 2568.000 MEGAWATTS

GROUP	CHI	NU
----	---	---
1	1.000	2.673
2	0.0	2.683
3	0.0	2.565

FOR REGION NUMBER: 1

RADIUS		AXIAL		AZIMUTHAL	
INSIDE	OUTSIDE	BOTTOM	TOP	START	ENDING
0.	163.500	0.0	183.000	0.0	360.000

GROUP	DIFFUSION COEFFICIENT	ABSORPTION X-SECTION	FISSION X-SECTION	TEMP. COEFF. REACTIVITY
1	-1.088D+00	9.216D-03	2.003D-03	0.0
2	-6.692D-01	6.939D-02	3.202D-02	0.0
3	-4.327D-01	1.281D-01	6.947D-02	0.0

THE SCATTERING MATRIX
SEE MANUAL FOR INTERPERATATION

GROUP	1	2	3	4	5
1	0.0	0.0	0.0	0.0	0.0
2	1.675D-02	0.0	0.0	0.0	0.0
3	0.0	1.019D-01	0.0	0.0	0.0
4	6.100D-02	6.100D-02	6.100D-02	-2.870D-05	0.0
5	3.000D-03	3.000D-03	3.000D-03	2.870D-05	-2.090D-05

FOR REGION NUMBER: 2

RADIUS		AXIAL		AZIMUTHAL	
INSIDE	OUTSIDE	BOTTOM	TOP	START	ENDING
0.	163.500	183.000	366.000	0.0	360.000

GROUP	DIFFUSION COEFFICIENT	ABSORPTION X-SECTION	FISSION X-SECTION	TEMP. COEFF. REACTIVITY
1	-1.088D+00	9.216D-03	2.003D-03	0.0
2	-6.692D-01	6.939D-02	3.202D-02	0.0
3	-4.327D-01	1.281D-01	6.947D-02	0.0

THE SCATTERING MATRIX
SEE MANUAL FOR INTERPERATATION

GROUP	1	2	3	4	5
1	0.0	0.0	0.0	0.0	0.0
2	1.675D-02	0.0	0.0	0.0	0.0
3	0.0	1.019D-01	0.0	0.0	0.0
4	6.100D-02	6.100D-02	6.100D-02	-2.870D-05	0.0
5	3.000D-03	3.000D-03	3.000D-03	2.870D-05	-2.090D-05

GROUP	ABSORPTION CROSS SECTIONS FOR	
	1-ISOTOPE	2-ISOTOPE
1	0.0	0.0
2	0.0	4.431D-19
3	0.0	2.483D-18

 END OF INPUT DATA

REGION	VOLUME
1	1.537D+07
2	1.537D+07

TIME: 0.0 HOURS

KEFF: 1.0326276

 REGIONS 1 THRU 2

REGION GROUP	1	2
1	2.670D+14	2.677D+14
2	2.595D+13	2.602D+13
3	1.979D+13	1.985D+13
ISOTOPE		
4	5.826D+15	5.841D+15
5	1.958D+15	1.959D+15

ABSORPTION RATES

 TOTAL AND REGIONS 1 THRU 2

REGION GROUP	TOTAL	1	2
1	2.464D+12	2.461D+12	2.467D+12
2	1.803D+12	1.801D+12	1.806D+12
3	2.539D+12	2.535D+12	2.542D+12
TOTAL	6.806D+12	6.797D+12	6.815D+12

FISSION RATES

TOTAL AND REGIONS 1 THRU 2

REGION GROUP	TOTAL	1	2
1	5.354D+11	5.347D+11	5.361D+11
2	8.322D+11	8.311D+11	8.333D+11
3	1.377D+12	1.375D+12	1.379D+12
TOTAL	2.744D+12	2.741D+12	2.748D+12

TEMPERATURE FEEDBACK ABSORPTION

TOTAL AND REGIONS 1 THRU 2

REGION GROUP	TOTAL	1	2
1	0.0	0.0	0.0
2	0.0	0.0	0.0
3	0.0	0.0	0.0
TOTAL	0.0	0.0	0.0

ABSORPTIONS BY ELEMENT NUMBER 1

TOTAL AND REGIONS 1 THRU 2

REGION GROUP	TOTAL	1	2
1	0.0	0.0	0.0
2	0.0	0.0	0.0
3	0.0	0.0	0.0
TOTAL	0.0	0.0	0.0

ABSORPTIONS BY ELEMENT NUMBER 2

TOTAL AND REGIONS 1 THRU 2

REGION GROUP	TOTAL	1	2
1	0.0	0.0	0.0
2	2.528D+10	2.524D+10	2.531D+10
3	1.080D+11	1.078D+11	1.081D+11
TOTAL	1.332D+11	1.331D+11	1.334D+11

ADJOINT SYSTEM

TIME: 0.0 HOURS

KEFF: 1.0598523

REGIONS 1 THRU 2

REGION GROUP	1	2
1	8.782D+13	8.783D+13
2	1.101D+14	1.101D+14
3	1.152D+14	1.153D+14

ABSORPTION RATES

TOTAL AND REGIONS 1 THRU 2

REGION GROUP	TOTAL	1	2
1	8.094D+11	8.093D+11	8.095D+11
2	7.639D+12	7.638D+12	7.639D+12
3	1.476D+13	1.476D+13	1.476D+13
TOTAL	2.321D+13	2.321D+13	2.321D+13

FISSION RATES

TOTAL AND REGIONS 1 THRU 2

REGION GROUP	TOTAL	1	2
1	1.759D+11	1.759D+11	1.759D+11
2	3.525D+12	3.525D+12	3.525D+12
3	8.006D+12	8.005D+12	8.006D+12
TOTAL	1.171D+13	1.171D+13	1.171D+13

TEMPERATURE FEEDBACK ABSORPTION

TOTAL AND REGIONS 1 THRU 2

REGION GROUP	TOTAL	1	2
1	0.0	0.0	0.0
2	0.0	0.0	0.0
3	0.0	0.0	0.0
TOTAL	0.0	0.0	0.0

DIRECT TIME DEPENDENT SYSTEM

PERTURB WITH SIGMA-ABSORPTION OF REGION 1 = 0.25%

TIME: 0.2500 HOURS

KEFF: 1.0321844

REGIONS 1 THRU 2

REGION GROUP	1	2
1	2.603D+14	2.744D+14
2	2.530D+13	2.667D+13
3	1.930D+13	2.034D+13
ISOTOPE		
4	5.824D+15	5.843D+15
5	1.960D+15	1.958D+15

TIME: 0.5000 HOURS

KEFF: 1.0321856

REGIONS 1 THRU 2

REGION GROUP	1	2
1	2.596D+14	2.751D+14
2	2.524D+13	2.674D+13
3	1.925D+13	2.039D+13
ISOTOPE		
4	5.820D+15	5.846D+15
5	1.962D+15	1.956D+15

TIME: 0.7500 HOURS

KEFF: 1.0321872

REGIONS 1 THRU 2

REGION GROUP	1	2
1	2.590D+14	2.757D+14
2	2.517D+13	2.680D+13
3	1.920D+13	2.044D+13
ISOTOPE		
4	5.816D+15	5.851D+15
5	1.964D+15	1.953D+15

TIME: 1.0000 HOURS

KEFF: 1.0321889

REGIONS 1 THRU 2

REGION GROUP	1	2
1	2.583D+14	2.764D+14
2	2.511D+13	2.687D+13
3	1.914D+13	2.050D+13
ISOTOPE		
4	5.811D+15	5.855D+15
5	1.967D+15	1.951D+15

TIME: 1.2500 HOURS

KEFF: 1.0321919

REGIONS 1 THRU 2

REGION GROUP	1	2
1	2.569D+14	2.778D+14
2	2.497D+13	2.700D+13
3	1.904D+13	2.060D+13
ISOTOPE		
4	5.806D+15	5.860D+15
5	1.969D+15	1.948D+15

TIME: 1.5000 HOURS

KEFF: 1.0321940

REGIONS 1 THRU 2

REGION GROUP	1	2
1	2.563D+14	2.784D+14
2	2.492D+13	2.706D+13
3	1.900D+13	2.064D+13
ISOTOPE		
4	5.801D+15	5.865D+15
5	1.972D+15	1.946D+15

TIME: 1.7500 HOURS

KEFF: 1.0321961

REGIONS 1 THRU 2

REGION GROUP	1	2
1	2.557D+14	2.790D+14
2	2.485D+13	2.712D+13
3	1.895D+13	2.069D+13
ISOTOPE		
4	5.796D+15	5.871D+15
5	1.975D+15	1.943D+15

TIME: 2.0000 HOURS

KEFF: 1.0321983

REGIONS 1 THRU 2

REGION GROUP	1	2
1	2.550D+14	2.797D+14
2	2.479D+13	2.719D+13
3	1.890D+13	2.074D+13
ISOTOPE		
4	5.790D+15	5.876D+15
5	1.977D+15	1.941D+15

TIME: 2.2500 HOURS

KEFF: 1.0322006

REGIONS 1 THRU 2

REGION GROUP	1	2
1	2.543D+14	2.804D+14
2	2.472D+13	2.726D+13
3	1.884D+13	2.080D+13
ISOTOPE		
4	5.784D+15	5.882D+15
5	1.980D+15	1.939D+15

RETURN TO OLD VALUE OF SIGMA-ABSORP.

TIME: 2.5000 HOURS

KEFF: 1.0326339

REGIONS 1 THRU 2

REGION GROUP	1	2
1	2.573D+14	2.774D+14
2	2.501D+13	2.697D+13
3	1.906D+13	2.058D+13
ISOTOPE		
4	5.779D+15	5.888D+15
5	1.981D+15	1.937D+15

TIME: 2.7500 HOURS

KEFF: 1.0326336

REGIONS 1 THRU 2

REGION GROUP	1	2
1	2.578D+14	2.769D+14
2	2.506D+13	2.692D+13
3	1.910D+13	2.054D+13
ISOTOPE		
4	5.775D+15	5.892D+15
5	1.982D+15	1.936D+15

TIME: 3.0000 HOURS

KEFF: 1.0326333

REGIONS 1 THRU 2

REGION GROUP	1	2
1	2.582D+14	2.765D+14
2	2.509D+13	2.688D+13
3	1.913D+13	2.051D+13
ISOTOPE		
4	5.771D+15	5.896D+15
5	1.983D+15	1.935D+15

**The vita has been removed from
the scanned document**

A NONLINEAR DIFFUSION THEORY MODEL FOR
XENON-INDUCED FLUX OSCILLATIONS

by

John D. Teachman

(ABSTRACT)

A nonlinear model is developed for the xenon induced flux oscillation problem that occurs in nuclear power plants. The model is based on Galerkins's method of weighted residuals applied to multigroup diffusion theory. A similar linear model is developed by the same methods in order to consider the effects of the nonlinearities of the system. The effects of multi- and single-energy group considerations are also examined. Finally the effects of various number of basis functions used to approximate the flux, iodine, and xenon concentrations is determined.

A partial listing of the computer program XORA, developed from the nonlinear and linear models, is given along with representative input and output from this program.